



**UNIVERSITA' DI CAMERINO**

**Dipartimento di Biologia Molecolare,  
Cellulare e Animale**

---

**CARATTERIZZAZIONE ED ATTIVITÀ DI ESTRATTI  
VEGETALI AD ELEVATO CONTENUTO DI  
POLIFENOLI**

*PhD thesis in Biology*

PhD student

**LUCA SPARAPANI**

Tutor

**MAURO ANGELETTI**

---

2003-2006

# 1 Introduction

## 1.1 Polyphenols

Polyphenols are a class of natural chemical substances that can be found in many vegetables. Their main chemical characteristic is the presence of multiple phenolic groups. Among them there are other several subclasses like flavonoids.

Flavonoids are important secondary metabolites that can be also found in plants. Flavonoids are based around a phenylbenzopyrone structure [fig.1]

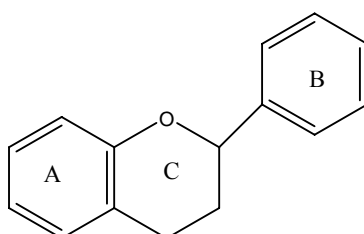


Fig. 1 phenylbenzopyrone structure

In general plants alone possess the biosynthetic ability[1]. Flavonoid were found also in primitive plant species like green algae[2] and they survived through evolution.

Flavonoids can be divided in several subclasses depending on their substituents. Moreover flavonoids have other substitution patterns with addition hydroxyl, methyl, methoxyl and glycosil groups.

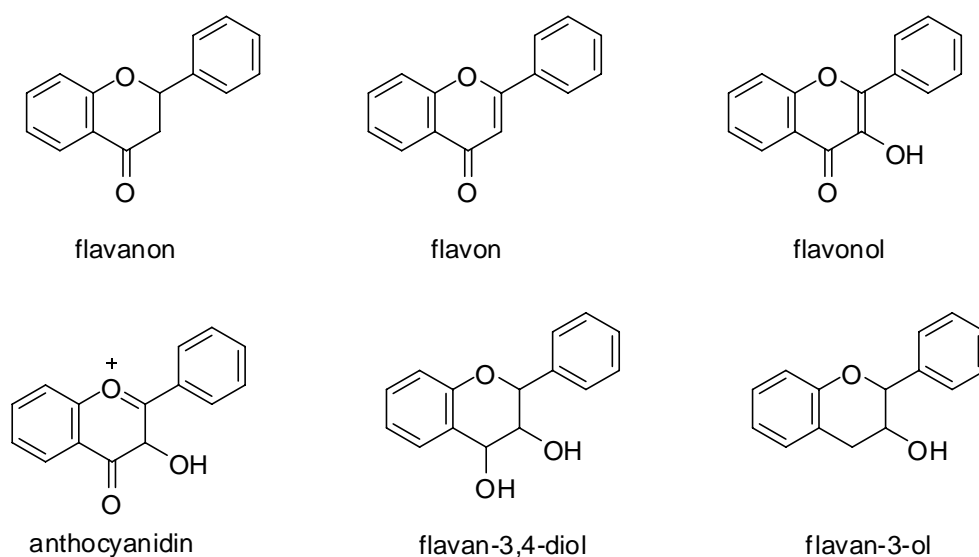
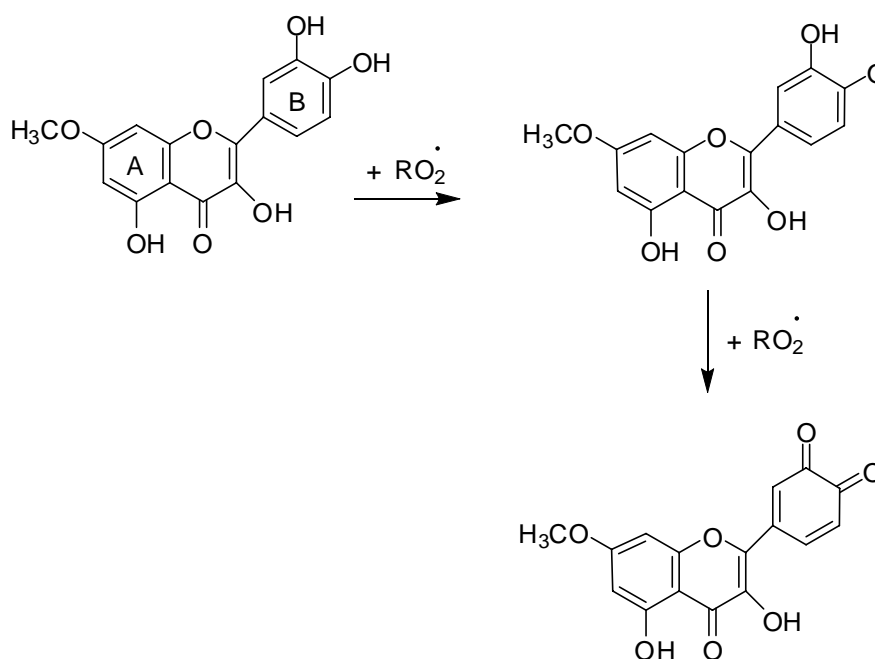


Fig. 2 : structures of flavonoids classes

The main activity of flavonoids is as antioxidant, but they have also protective function versus physiological regulatory mechanisms [3]. In plants flavonoids can be found in several components, like leaves[4], seeds[5], stems and roots[3].

Flavonoids are also responsible of several sensorial aspects: they are found as pigments in several plant components [6], and are responsible of astringency [7] and bitterness [8]. Flavonoids are also responsible of browning in fruit [9].

The antioxidant activity of flavonoids is comparable to that of other synthetic antioxidants like BHT and BHA. It has been postulated[10] that the mechanism of the peroxy radical reaction involves a consecutive two-electron mechanism with 3',4'- and 2',5'-dihydroxyflavonols to yield corresponding quinones. The first one-electron oxidation produces the flavonoid phenoxyl radical, which subsequently scavenges another peroxy radical:



*Fig. 3: mechanism of the peroxy radical reaction*

One of the most important sources of flavonoids are red grape seeds[11]. In grape seeds flavonoids are mainly present as proanthocyanidines. Proanthocyanidines are condensed flavonoids responsible of red colouring in various berries and have protecting activities. They exhibit an higher antioxidant activity compared to other monomeric flavonoid ( i.e. catechin, epigallocatechin gallate). Grape Seed Extract (GSE) is one of the most used nutraceutical supplement of antioxidants in the market and the consumption estimated year consumption is 1 million kg. The great success of GSE is probably due to the so called “French Paradox”, where a normal consumption of red wine leads also to a low rate of cardio-vascular diseases;

even if this paradox has not been confirmed several studies have been conducted on possible benefits of GSE on human health.

The polyphenol content of seeds may range from 1% to 8% by weight [12] depending from several aspects[13] like the cultivar, the climatic conditions from year to year, the effect of geographic origin of grapes, soil chemistry and fertilization.

The flavonoid composition of white grapes is different from that of red grapes[12] and are richer in catechins and their polymeric forms. White grape seeds are used for the production of one of the most sold GSE (Leucoselect, Indena, Milan), while other GSE producers use only red grape seeds.

## ***1.2 GSE and health***

### **1.2.1 Effects on myocardium and the cardiovascular system**

Free radicals play an important role in myocardium pathogenesis, such as ischemia and reperfusion. Since grape seeds extract exerts a great power in free radical's disruption, some studies could also prove its effectiveness within these related fields. Instead, cardiovascular diseases are associated to modifications of fatty acids metabolism and to an extreme LDL lipidic peroxidation. These oxidation products are also involved in the thromboxane formation, which first of all leads to an increase in the platelet aggregation, secondly to artery obstruction and finally to thrombosis [14]. Possible accumulation of lipidic oxidation products coming from LDL, may be attributed to the low antioxidants contents in plasma.

It clearly results (see paragraph 3.4) how polyphenols, originated from grape seeds by inhibiting LDL oxidation, may reduce the cardio pathologies risk.

#### ***1.2.1.1 Protection against reperfusion and myocardium ischemia***

The GSE protective effect was tested during post ischemic reperfusion and after an ischemic cardiac arrest on laboratory mice [15, 16]. Mice were divided into two separate groups: to one group GSE was given, while for the second group, just water was supplied. After three weeks, on rats hearts a global ischemia was induced for 30 minutes, following a 2 hours reperfusion. The left ventricle functions were monitored continuously and both creatin kinase (CK, as an indicator of necrosis and of tissues inflammation) and malondialdehyde (MDA, as an oxidative stress indicator) was estimated. Besides, the entity of heart failure was measured through TTC.

From the analyses, it was possible to verify a high cardiac protecting activity of GSE: better post-ischemic functions of the left ventricle, a reduced CK release and a minor formation of MDA in coronary effluents, by comparison with the control. In addition, the myocardium heart failure entity of the group which received GSE, was almost 25% lower than the control.

#### ***1.2.1.2 The effect on platelet aggregation***

Grape products, rich in polyphenols, are responsible for the platelet aggregation (PA) inhibition, a risk factor of coronaries. *In vitro* studies on human platelets and *ex vivo* research on dog platelets have been performed. More precisely, the extract effect was tested on collagen-induced whole blood PA [17]. In these studies, an interesting synergy between seeds extract and grape skins was highlighted. Furthermore, investigations done by Chang and Maffei Facino have hypothesized that GSE mechanism of action is related to the inhibitory effect that is exerted on B2 thromboxan biosynthesis [18, 19].

#### ***1.2.1.3 Effects on micro circulation***

Grape seeds derived procyanidines, have demonstrated to show effects on micro circulation, by a capillary strengthening [20, 21]. These data were obtained via double-blind analyses. More accurately, researchers have analyzed the vascular permeability both of brain and heart muscle capillaries. Their normal permeability grade was easily increased in pathological inflammation conditions or in case of diabetes. In laboratory, these pathologies were reproduced through collagenase injections. Animals pre-treated with procyanidolic oligomers, have considerably reduced the capillary permeability increase, induced by collagenase injection, with a final effect of microcirculation reinforcement.

Further double blind studies done on patients affected by peripheral venous insufficiency have proved the GSE efficacy in the treatment of these pathologies [22].

#### ***1.2.1.4 Effects on blood pressure on hypertensive patients***

Research has been done on hypertensive rats feed with GSE [23]. After three weeks of treatment it has been evidenced a decrease in the systolic pressure, in comparison with controls. In this study it has been shown the greater and non synergistic effectiveness of the GSE with respect to other antioxidant species (chrome and zinc), which act positively in this kind of pathology.

## 1.2.2 Cytotoxicity

### 1.2.2.1 Different toxicity on normal cells as regards malignant cell

The GSE cytotoxicity has been tested on carcinogenic human cells cultures, including active cells in breast cancer, in gastric adenocarcinoma and in lung cancer. This has been tested via morphological analysis and cytotoxic test of MTT( 3-(4,5-Dimethylthiazol-2-yl)-2,5-diphenyltetrazolium bromide). These effects were compared with two normal cells, comprising human gastric mucous membrane and macrophages cells. The GSE has demonstrated a selective toxicity against the examined cancerous cells, whereas at the same concentration, positive effects on normal cells growth were observed [24] .

### 1.2.2.2 Protection against citotoxicity induced by chemotherapeutical agents.

The anticancer chemotherapeutical agents are very effective, both *in vitro* and *in vivo*, in the reduction of cancerous cells growth; unfortunately the inconvenience is their toxicity as regards normal cells.

As an example, Idarubicin or the 4-hydroxyperoxycyclofoafammide (4-HC) are very effective chemotherapeutic agents, capable of inducing apoptosis to target cells. Healthy cells have been treated *in vitro* with such medicines, with or without GSE. Results have shown a decrease of their inhibitory effect on growth (using MTT assay) and of their cytotoxicity in cells treated with GSE. Besides, from flux cytometric analysis, a greater decrease by 50% has been found on the number of cells undergoing apoptosis [25].

The Doxorubicin is another anticancer medicine, whose application is strongly limited by its elevated cardiotoxicity. The principal *in vivo* target of the Doxorubicin is DNA. For this reason studies have been done on GSE possibility of protecting DNA from Doxorubicin induced damages, owing to its antioxidant properties, therefore preventing cardiotoxicity. Laboratory guinea pigs were fed with GSE and subsequently Doxorubicin was supplied. Hystopathologic analysis and investigations on DNA performed on guinea pigs heart have shown a protection of GSE towards damages caused by Doxorubicin, thorough a decrease of apoptosis and cellular necrosis, also preventing DNA damages. Such effect is almost equivalent to that of the 3-amminobenzammide (3-AB), a promising anticancer medicine, which inhibits DNA damages significantly.

Studies on the probable mechanism that takes part in the protection of GSE towards cellular damages induced by chemotherapeutic agents have shown mediation, due to alterations in some genes expression. More precisely, GSE increases the expression of the antioxidant gene bcl-2 and decreases the expression of the gene which induces the cancer c-myc and of the p53 gene, responsible of the apoptosis regulation [25].

### ***1.2.2.3 Anti-ornithine decarboxylase activities in animals***

Researchers working in institutes of research committed with cancer at Kansas State University have found that when laboratory animals are exposed to a variety of chemical carcinogenic agents, the production of a skin cancer type was stimulated. One of the markers of this cancer is the ornithine decarboxylase. It was observed that when the synthesis of this enzyme is chemically promoted, such event is responsible of the development of skin cancer in animals. When animals are fed with of GSE supplements, an inhibition of the ornithine decarboxylase formation was found. This prevents the formation of cancer in animals, even when they are deliberately exposed to chemical carcinogenic agents [26].

### **1.2.3 Protection against inflammation and allergy**

The polyphenols activity deriving from grapes seeds, expounds even on enzymatic systems, responsible for the production of free radicals, associated with inflammatory reactions. Furthermore, they operate during the synthesis and the release of any substances that promote inflammations and the onset of allergies, as for example the histamine [27-29].

The proanthocyanidines even inhibit the formation of hyaluronidase, an enzyme acting against several tissues during inflammatory processes. Its action is correlated to the antihistaminic effect and to the ability of strengthening the cell membranes of the basophile plants and the macrophages, containing allergens, hence preventing the hypersensibilization to polluting agents and to food allergens [30].

Other studies confirming the GSE anti inflammatory action (against arthritises, etc.) have identified a mechanism that shows the active proanthocyanidines radicals as scavenger of oxygen, as protectors against the lipidic peroxidation of the cell membranes and as promoter of the inhibition of the inflammatory cytokines formation. [31].

## 1.2.4 Antioxidant activity

The antioxidant activity of a system is always relative to the mean in which the system operates. It's widely known the antioxidant property of vitamins C and E, which are supplemented as such, in several commercial supplements. In nutraceutical products, the presence of both is justified by the fact that a combination of the two represents a more powerful antioxidant system than the one observed when each one is taken separately.

In 1960, as a consequence of this effect, Richard Passwater, Ph.D., coined the new term "antioxidant synergism". In "All about antioxidants" (Avery Publishing, 1998) he stated the existence of a synergy when the system as a whole has a better effect than the total of the effects which derives from the singular parts that make it up.

The antioxidant activity of vitamin C and E finds its expression in different matrix; in fact, while vitamin C operates in aqueous systems, hence on water soluble molecules, vitamin E is mainly present in cellular membranes lipids and it's active against LDL cholesterol oxidation.

The great advantage of GSE lies on the possibility of expressing both its own antioxidant activity in aqueous matrix, owing to its hydrophilic component at the lowest molecular weight, and also in lipidic matrix, thanks to lipophilic component at the highest molecular weight [32].

### 1.2.4.1 Antioxidant activity, higher than vitamins C and E

The antioxidant activity of a system is measured in relation to its ability of disrupting free radicals, responsible of damages (more or less permanent) to those biological systems in which they are formed.

*In vitro* analyses on the free radical scavenging ability (RSA) were performed by Bagchi and co-workers [33]. They have discovered an RSA of 84 and 98% higher than that of vitamin E, versus the formation of super oxides anions and hydroxyl radicals respectively. In comparison with vitamin C, the grape seeds extract afforded RSA values of 439 and 575% greater. Additional *in vitro* studies, which were reported in the literature [18, 34-36] validate the hypothesis of a better GSE antioxidant potency than that of the well-known vitamins C and E. It's worth mentioning that, despite *in vitro* studies give an indication of the potential product's efficacy, they do not necessarily reflect the actual antioxidant power in biological systems. However, studies done on animals by Bagchi D. [33] and on human cellular cultures, carried out by Bagchi M. [37], have demonstrated that the GSE antioxidant activity is significantly higher than that of vitamins C and E, even in biological systems. With regards to



analyses on human cells, the experiment was done on oral keratinocytes, treated with tobacco's extract. In fact, this extract causes oxidative damages and scheduled cell death (apoptosis). In this case, the pre-treatment with GSE reduces cellular apoptosis to about 85%, while a combination of vitamin C and E, reduces it to 46% only.

### **1.2.5 Antioxidant effect on vitamin E**

As a consequence of GSE antioxidant activity, in comparison with vitamins C and E, some researchers have hypothesized a grape seeds extract function, which may allow vitamins to become more bioavailable during their recycling phase.

Maffei Facino and collaborators [38] found a positive match, investigating the effect of procyanidines derived from grape seeds both on phosphatidylcholine liposomes (homogeneous system) and also on red corpuscles (heterogeneous system). In either case, a decrease of vitamin E reduction content, due to the oxidative processes, was observed. In fact, phosphatidylcholine liposomes, owing to the presence of hydroxyl radicals, undergo a peroxidation stage; on the contrary, in the case of red corpuscles, the oxidative stress was induced by the system exposure to UVB rays.

As an alternative, GSE was given orally to some healthy volunteers. By analyzing their blood samples, taken at the beginning, at the end and seven days after the administration period, Simonetti and his co-workers [39] could verify a significant increase of vitamin E in red corpuscles membranes, along with a reduction in membrane lipidic peroxidation correlated, in a linear manner, to the vitamin E concentration in the membrane itself.

#### **1.2.5.1 Synergic effect with vitamins C and E**

Vinson J [40, 41] has optimized a set of *in vitro* tests, in order to investigate the synergic activity among vitamins C, E and the grape seeds extract. The employed *in vitro* models, simulate the initial stage of arteriosclerosis. The procedure provides that the measurement of LDL (low-density lipoprotein) and VLDL (very low-density protein) oxidation inhibition by antioxidant agents. Vitamin C, vitamin E and grape seeds extract were tested separately, to establish the basal effect at a wide concentration range. These effects were added up, in order to provide "The Individual Inhibition Amount", which was subsequently compared to "The Actual Mixture Inhibition".

The Actual Mixture Inhibition subtracted to the Individual Inhibition Amount, carried to 100, yields the synergy percentage. This set of *in vitro* tests, has allowed Dr. Vinson to afford

the maximum synergism concentrations among the oxidizing species. Furthermore, he has observed a strong synergism between grape seeds extract and vitamin C, as well as between GSE and vitamin E.

### ***1.2.5.2 Antioxidant effect on LDL and VLDL***

By now, the antioxidant effect of GSE towards LDL and VLDL has been thoroughly elucidated. In fact, these type of data may be obtained from simple investigations on the GSE antioxidant activity, carried *in vitro* and in lypophilic phase [35]. Furthermore, the activity on LDL and VLDL is the basis of an assay, optimized by Vinson [40, 41], who explored the extract's synergic activity with vitamins C and E (see paragraph 3.3).

*In vivo* studies on hypercholesterolemic were done by Talpur N. A. [23], who administrated the grape seeds extract in combination with polycotinate chrome (Cr) (ChromeMate). With regards to the control (placebo bid and chromium only), a significant decrease in total cholesterol as a consequence of a net reduction of LDL levels (placebo effect -3%, Cr -14%, Cr+GSE -20%), was detected. On the contrary, HDL values were not subjected to considerable variations.

## **1.2.6 Toxicity studies on grape seeds extracts (GSE)**

Several toxicological studies on different grape seeds extract sources and on different administration modes were carried out.

### ***1.2.6.1 Oral Administration***

Studies performed by Bombardelli and Morazzoni [42] demonstrated an LD<sub>50</sub> (median lethal dose) value equal to 4 g/Kg of body mass. In addition, it was evinced that a daily dose of 60 mg/Kg for a time period of 6 months in mice and 12 months in dogs, did not cause any toxic effect on treated animals. YamaKoshi J. and coworkers [43] afforded LD<sub>50</sub> values even higher than 4 g/kg. They investigated the GSE mutagenic action through a reverse mutation test, a chromosome decay test, micronuclei test and found no mutagenic activity relatively to the GSE.

Studies by Bagchi D. and collaborators [44] reported an increment of LD<sub>50</sub> value up to 5g/kg body mass when orally administered in both male and female albino rats, via gastric intubation.

### ***1.2.6.2 Studies of acute epidermic toxicity***

Bagchi D. and co-workers [44] have epidermically administered a 2 g/kg body mass dose to five male white rats and 5 female ones. A 24 hours exposure using semi-occlusive bandages, induced exclusively a slight erythema along with a moderate desquamation in all treated subjects. Such effects later disappeared within 12 days or even earlier.

Therefore, in case of a 24 hours administration on unwounded skin, the LD<sub>50</sub> value was estimated to be higher than 2 g/kg body mass. Moreover, a 2 g/kg dosage resulted as the NOEL (no-observed effect-level) value in case of a systemic toxicity.

### ***1.2.6.3 Studies of primary epidermis irritation***

A single 0.5 g dose of GSE was applied on New Zealander white rabbits healthy skin for an exposure period of 4 hours, under semi-occlusive bandages. The application sites were evaluated according to Draize methodology after 30-60 minutes, then after 24, 48, 72 hours from the bandages removal and subsequently once a day until the 12th day, in case of a persistent irritation. The primary irritation index was estimated to be 2.7, which counts GSE in the class of moderately irritant substances [44].

### ***1.2.6.4 Primary irritation on albini rabbits eyes***

Bagchi D. and co-workers [44] have given an 85 mg single dose of GSE by injection directly in the right eyes inferior conjunctival sac of 6 rabbits. The eyelids were closed for approximately 1 s and right after they were released. In accordance with Draize methodology, the ocular reactions were examined. The highest value was 16.7, reached at 24hrs from the instillation. The encountered irritation is completely reversible within fourteen days.

## **1.2.7 Use as food preservative**

All foods and drinks undergo gradual changes during their preservation. Setting aside the degradation caused by microorganisms, the typical causes of rancidity is ascribed to the presence of oxygen and products derived from molecules chemical oxidation. The selfoxidation process entails different steps and the rancidity development involves a chain mechanism, driven by the presence of free radicals. Furthermore, the quality of the lipids, deteriorates in conditions of oxidation promoted by light and temperature. For this reasons,

most of the time manufactured products have food preservatives added. Preservatives commercially in use are benzoates, sorbates and synthetic antioxidants, such as BHT and BHA. In the optics of improving the quality and the products maintenance, without resorting to synthetic chemical substances, the scientific research is committed to the discovery of powerful and safe preservatives of a natural origin. A particular attention has been focused on natural extracts, obtained without the introduction of chemical solvents.

Owing to the ability of the GSE to act as scavenger of peroxy radicals and as a strong antioxidant, studies were focused on their effectiveness as "food preservatives". In this way food added with GSE should not to be subsequently added with preservative, with the aim of maintaining the product's integrity over a time period (BHA, BHT), as well as to have a strong nutritional value, given by the presence of polyphenols and their various biological activities.

Investigations conducted on a commercial product and published over the internet, showed that the GSE possess a greater activity than that of BHT and BHA. Studies were performed by analysing the quantity of hexanale developed from the food in a certain period of time, comparing the obtained value with the one afforded from rancid food.

### ***1.3 Interaction polyphenols-thrombin***

#### **1.3.1 Thrombin**

Thrombin is a plasma constituent that has several activities: promoters the conversion of fibrinogen into fibrin and of factox XIII into factor XIIIa [45], by stabilizing the fibrin polymers; it promotes the piastrinic aggregation, by activating the receptors of activated protease (PARs) [46], and also of the cancer growth, the arteriosclerosis and inflammatory processes, the mioblast survival, the neutrophilic survival, the apoptosis/survival of the neurons in glyal cells; moreover the thrombin is able to promote the chemiotaxy of monocites through a non proteolytic mechanism.

#### **1.3.2 Molecular structure**

Thrombin is a serin protease glicosilated from the family of tripsins. Like all the other enzymes of the tripsin family, it has a catalytic triads ( Asp102, His57, Ser195) and the two amminoacid Asp189 and Glu192 ( charged residues with an important role in the recognize and binding of the substrates and inhibitors), fundamentally inside of the active site.

The human thrombin can exist in three forms:  $\alpha$ ,  $\beta$  e  $\gamma$ , even if *in vivo* this last structure has never been demonstrated. By means of proteolytic fragmentation or tryptic, the  $\beta$  and  $\gamma$  forms are generated and they maintain the same primary structure and the same active site of the  $\alpha$  form, with the exception of more chains not covalently bonded.

The  $\alpha$ -thrombin is a molecule of 36.6 kDa with an isoelectric point of 7.0-7.6 and is formed by two chains: the A chain (4,6 kDa) of about 36 residues and the B chain (32 kDa) of 259 residues, containing the catalytic site, and linked together by a disulphure bridge [47]. This molecule can be described like an ellipsoid with 45x45x50 Å dimensions. Its A and B chains are organized in separate domains but they form an unic continuous body with a non continuous surface. Like the other serine protease trypsin-like, it is formed by two similar domains, barrel like, constituted by six linked  $\beta$ -sheets and from various other random-coil structures and  $\alpha$ -helix on the surface. The catalytical residues are localized between the junctions of this two barrel structures, with the discontinuity of the active site on the surface. The characteristic of this discontinuity and the presence of two extroflexions able to block the active site (produced by aminoacid Trp60d and Glu192) play an important role in the selection of substrates and macromolecular inhibitors [48, 49].

It is possible to observe wide zones of charged residues . mainly positive, in the surroundings of the  $\alpha$ -helix C-terminal of the B chain and on the surface of the segment 67-80. Such residues are involved in the electrostatic interactions, fundamental for the stabilization of the A chain, for the cohesion of the two chains and for the composition of the two binding sites[50].

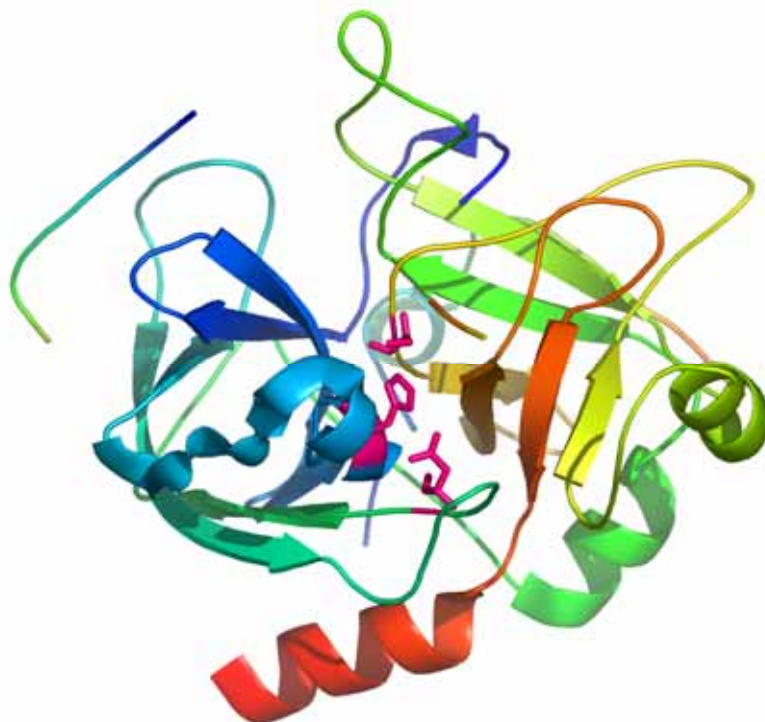


Fig. 4: Representation of the molecular structure of the  $\alpha$ -human thrombin

Functional studies have evidenced that the thrombin is an allosteric enzyme that exists in two different conformations in rapid equilibrium: the *slow* form and the *fast* form [51]. The *slow* form plays an important anti-coagulant role, by interacting with the thrombomodulin, activate the protein C generating a strong inhibitor of the coagulation that inhibits the factor Va and VIIIa; instead the *fast* form gives to the thrombin the characteristic role of procoagulant agent. The transition *slow-fast* is induced by the binding with  $\text{Na}^+$ , that binds to the molecule in a site near to Asp189, at more than 15 Å from the catalytic triads, inside of a cylindrical cavity formed by three antiparallel  $\beta$ -strands of the chain B. This shows an octahedral coordination that involves the amino acid Tyr184, Arg221, Lys224 and three water molecules [52]. In physiological conditions of concentration of  $\text{Na}^+$ , pH and temperature, the two forms are present in similar concentrations and they help in maintaining the equilibrium between the pro and anti coagulant activities.

### 1.3.3 Reaction mechanism.

In figure 16 is evidenced the mechanism of general reaction of the serine protease [53]. In bold are evidenced the amino acid of the catalytic triads. Ser195 is activated by nucleophilic attack from His57 at the carbonyl of the scissile binding. The acylation (a) proceeds through

the formation of an tetrahedral intermediate, stabilized by the interactions between the oxygen atom negatively charged of the substrate and the aminoacid 193-195 of the protease chain. The deacilation proceeds through addition of water (b); R and R<sup>1</sup> indicate the fragments that are found upwards and downwards respectively.

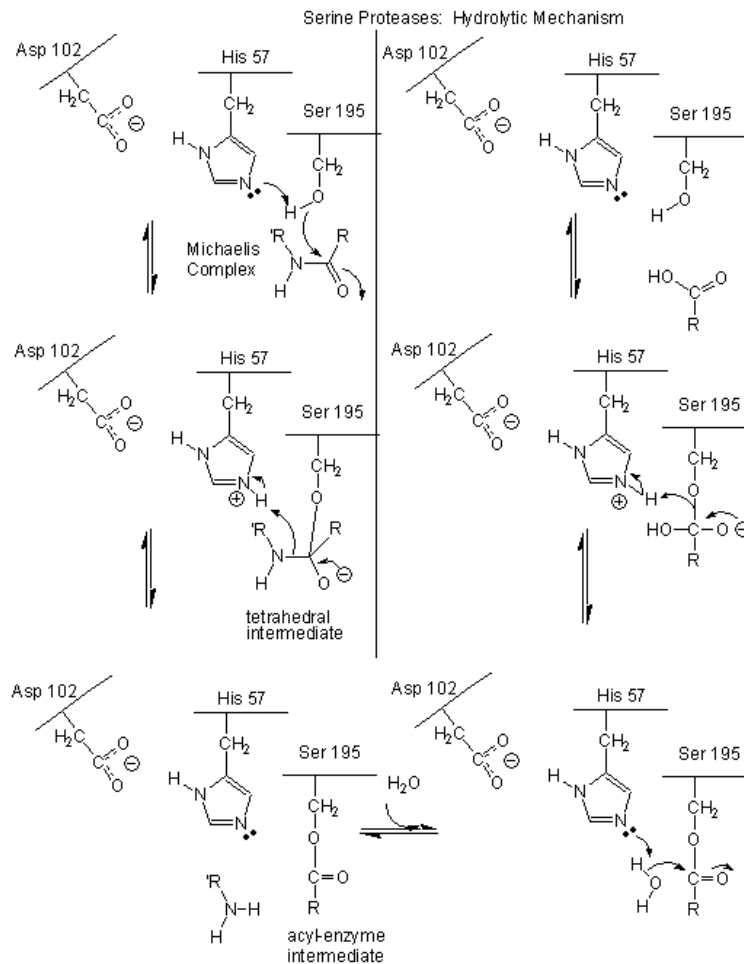


Fig. 5: Reaction mechanism of the serine protease

### 1.3.4 The coagulatory process

After a vascular damage, the thrombin plays an important role in the process of coagulatory cascade. This process has in its principal phase the activation of the factor X in Xa factor and my develop through two different ways: the internal and external way. The internal way needs that the activation of the X factor begins when, after a damage in blood vessel, the blood came in contact with different surfaces from the vascular endothelium (collagen, basal membranes) provoking the activation of precalliecin in calliecin and factor XII in factor XIIa. This last provokes the conversion of factor XI in Factor XIa, that, in association with

calcium ion, phospholipids and factor VII (antithrombin) determines the activation of factor X. The external way instead, is more rapid and begins as a consequence of a vascular or tissue damage and a release of a membrane glycoprotein (tissue factor) that in association with the factor XII, present in blood, cause the activation of the factor X [54]. The factor Xa (a serine-protease) forms a complex, known as prothrombinase, with the factor Va in presence of calcium ions and phospholipids [55]. Is this complex that determine the conversion of prothrombin (the inactive zymogen synthesized in liver and present in plasma) in thrombin.

This process needs the hydrolysis of two internal peptidic bonds (Arg271-Thr and Arg320-Ile) that reduces the molecular weight of the precursor from 71,6 to 36,6 kDa, while the second determine the formation of the active thrombin.

The calcium ions necessary for the conversion prothrombin-thrombin and for the increase of affinity of prothrombin for the superficial phospholipids of endothelial cells, binds to some residues of  $\gamma$ -carboxyglutamic acid present in the C-terminal of prothrombin and to carboxylates by a carboxylase-vitamin K dependent.

Once formed, thrombin catalyze the process of formation of fibrin coagulum from fibrinogen. In this process four peptidic Arg-Gly bonds are broken in the N-terminal region of the fibrinogen with consequent release of fibrin-peptides and a monomer of fibrin [56] so it could not undergo self-activation. The monomers polymerize linearly in order to give origin to an insoluble coagulum that is made even more stable by further covalent bonds (covalent cross-linking) made by the intervention of the factor XIIIa [57] and by incorporation of fibrin, blood cells and thrombin [58].

### **1.3.5 Thrombin inhibitors**

The most important physiological thrombin inhibitor is without doubts the antithrombin [59, 60], this molecule (or also called antithrombin III) is a polypeptide glycosylated at single chain, with a mass of almost 68 kDa. This protein belongs to the serpins family, inhibitors of protease to whom belongs the  $\alpha$ -antitrypsin.

The antithrombin is synthesized in the liver and circulates in a plasma concentration of approximate of 2,6  $\mu$ M. This inhibits the factors of the activated coagulation of the internal way and common way, comprehending the thrombin, the Xa, IXa, XIa and XIIa factors and the kallikrein; it has however a low activity or none in comparisons with the VIIa factor. The antithrombin is a "suicidal inhibitor" for this protease; the inhibition in fact happens when the



protease attaches an Arg-Ser specific peptidic bond in the reactive site of the antithrombin and is trapped like a stable complex 1:1.

Some inhibitors of the thrombin exploit the potentialities of the antithrombin, so they behave their inhibitory activity by binding themselves to this molecule. Among this group of inhibitors, defined antithrombin-dependent, the more remarkable and effective is heparin, or the heparins with low molecular weight (LMWH). However, the complex heparin-antithrombin are weak inhibitors for the binded thrombin over surfaces, maybe due to the difficulty of formation of the ternary complex [61], and this event represents a pharmacokinetic limit [62].

The more powerful “direct” inhibitors of the thrombin, are those that do not require the antithrombin as cofactor, for example like the irudin, the melagratin and the [62] argatroban. The irudin is a powerful and specific inhibitor of the thrombin initially found in the salivary glands of the medicinal leech. This peptide of 65 or 66 amino acids, possesses a dominant N-terminal with globular form that interacts with the active site of the thrombin, while the dominant C-terminal binds the exosite 1. The irudin binds the thrombin with high affinity forming a reversible complex with 1:1 stoichiometry

Some derived of this molecule are the lepirudin, the desirudin and the bivalirudin. The melagratin is a dipeptide that mimics the portion of fibrinopeptide A that interacts with the active site of thrombin. While the melagratin is badly adsorbed by gastrointestinal tract, the ximelagratin, one of its derivatives, is well absorbed and doesn't show any interaction with food or other medicinals. The argatroban is a small synthetic molecule (MW=526,66) that acts like competitive inhibitor for thrombin. It's a derivative of arginin and interacts only with the active site of thrombin. The argatroban is metabolized in liver with a process that generates at least three active intermediates.

## ***1.4 Interaction Polyphenols-Plasmin/Plasminogen***

### **1.4.1 The system Plasmin/Plasminogen**

The system Plasmin/plasminogen (PPS) [63] is a proteolytic system that is involved in many physiological and pathological processes. It includes a series of components, characterized by a different structure and biological activity.

The Plasmin is a serine protease [64] with an high specificity and is capable to activate od degradate the coagulation components of the methabolism of kinine and the omplementary system. Even if the Plasmin can be inhibited by a various number of plasmatic inhibitors *in vitro*, the regulation of Plasmin *in vivo* is belived to be made through the interaction with the l' $\alpha$ 2-antiplasmine, and in a diminished manner, with the  $\alpha$ 2-macroglobulin [65].

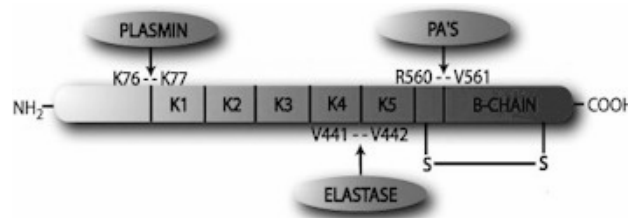


Fig. 6 Representation of the primary structure of plasmin.

The Plasminogen is converted into Plasmin, an active serine protease, by hydrolysis of the peptide binding Arg560-val561 producing an heavy NH<sub>2</sub>-terminal (A) and a light chain COOH-terminal (B) binded by two disulphure bonds. This conversion is catalyzed by a variety of physiological and pathological activators, including the plasminogen urinary activator uPA, the tissutal plasminogen activator tPA, the streptokinase, the kallikrein and the factors IXa and XIIIa [66]. The light chain COOH-terminal (MW=26kDa) contains the catalytic triads and the active site versus the streptokinase. The heavy chain NH<sub>2</sub>-terminal is included in an 12-63 kDa range, depending from the Plasminogen kind from wich has origin. In absence of inhibitors, the Plasmin cuts from the Plasminogen itself the N-terminal Glu<sup>1</sup>-Lys76plasmin in order to give the form Lys77-plasmin, that has an higher affinity for the fibrin of the Glu<sup>1</sup>-plasmin form. The heavy chain Lys-Plasminogen contains 5 homologue internal regions binded by disulphure bridges known as kringle. The regions from kringle1 to kringle4 contain binding sites for the  $\omega$ -aminocarbossilic acid and for the fibrine. Moreover exists also the form Val<sup>442</sup>-plasmin produced by hydrolysis of elastase[67].

#### **1.4.1.1 Role of the system PA-Plasmin in angiogenesis**

The plasmin is a wide spectrum protease belonging to the family of tripsins; it is belived that it can easily hydrolyze both directly and indirectly, through the activation of particular pro-MMP, various extra cellular proteins, the most important of it is fibrin. The uPA and the tPA, the main activators of Plasminogen, are the products of two different that are regulated

independently by different factors, like hormones and cytokines. Like for Plasmin, uPA and tPA are serin protease belonging to the family of tripsin, but differently from plasmin, they present a less specificity for the substrate, the Plasminogen. The uPA ( or more prcisly, its inactive precusros pro-uPA) is secreted like a soluble protein and bings with high agginity to a specific receptor binded on the cellular surface with an anchor GPI (receptor uPA, or uPAR), present in many cells, like epithelial cells. The Plasminogen and the plasmin bind togheter with plasmatic membranes, and the co-localization of the uPA and of Plasminogen on the cellular surface increments the grade of activation of Plasminogen and the consequent proteolysis plasmin-dependnet. The existence of more specifical physiological inhibitors of plasmin ( $\alpha_2$ -antiplasmin) and of PA (PAI1 and PAi-2) gives more points of regulations to this process. The specificity, the activity and the localization of the seine protease can be regulated by ECM and other glycoproteins[66, 68]. For what regards the stydies of localization, essentially uPA, uPAR and PAI-1 are not expressed in the quiescent endothelium. In different terms, the tPA was found int the quiescent endothelium of a small amount of arterioles, venules and vasa vasorum of normal human tissues. In contrast, uPA, uPAR and PAI-1 are expressed durin the angiogenic process *in vivo* with different modalities. uPA and uPAR seem to be expressed in the endothelial cells, depending on the situation, while PAI-1 is expressed both in endothelial cells and non-endothelial cells. (stromal and endothelial), where is believed to act with an important role in the maintaining of integrity of the matrix [69, 70].

Very few is known about the expression of tPA durino angiogenesis. These observation *in vivo* are widely supported by results obtained *in vitro*. That grown endothelial cells were able to produce uPA, uPAR,tPA and PAI-1 was already known, and their regulation from bFGF and VEGF wan widely studied [69]. It must be evidenced that endothelial cells with human origin respond more slowly related with similar cells from bovine towards the induction of PA from bFGF and VEGF. The reason of this reduced response can be correlated to the chronical stimulation of this cells from components of the endothelial growth (FGF and probably VEGF) used in cells culture. The response to VEGF seems to be dependent from the vascular bed from where they are isolated. So VEGF induces uPA and tpA in endothelial cells derived from capillaries but not in cells derived from aorta [71, 72].

This distinction may have several implications in the regulation of angiogenesis, that normally is believed to be dependent from already existing vessels in the microcirculatory system. It was reported that the ipoxy, one of the most important stimuli in angiogenesis, can increment uPAR [73] and PAI-1 [74] in endhotelial cells. The angiogenesis determines the

formation of new blood vessels in the circulatory system. A comparable process called lymphoangiogenesis, is responsible of the formation of new vessels in lymphatic system. The lymphoangiogenesis is traditionally eclipsed by the major attention dedicated to angiogenesis. This is partially due to the lack in the identification of lymphoangiogenesis factors as markers capable to distinguish the blood from the lymphatic vascular endothelial. This situation is rapidly evolving following the discover of the first lymphoangiogenic factors ( VEGF-C and D) and of some other specific markers of lymphatic endothelium [75]. In adult tissues, new lymphatic capillaries are developed as extension of previously existing and at the same time new capillaries are created by pre-existing microvascular system during angiogenesis. Even if we know little of the mechanism regarding the lymphoangiogenesis, it was demonstrated that VEGF, VEGF-C e bFGF are able to stimulate uPA, uPAR, tPA e PAI-1 in endothelial cells of the biggest lymphatic vessels [76-79]. The relevance for the lymphoangiogenesis *in vivo* of this *in vitro* data has to be clarified. The production of mice without the system PA-plasmin have given an opportunity in order to elucidate the role of single componensts of this particular system durin angiogeneisi *in vivo*. Previous studies, both *in vivo* and *in vitro*, have evidenced the crucial role of the PA-plasmin during angiogenesis. Unexpectedly it was found that the embional and post-born development it was not influenced by this system, at least in the casof the phenotype associated with angiogenesis [69]. One study conducted on the healing of wounds of mice deprived of plasminogen have definitely clarified the role of the system PA-plasmin during the migration of cheratinocites *in vivo* [80]. In every case, even if the migration of cheratinocites was rapidly altered, the wasn't no qualitative difference in the granulation tissue (infiltration of inflammatory cells , fibroblast migration and neo-vascularization) between wild-type mice and without plasminogen; this has suggested that in this case the angiogenesis is not PA-plasmin dependent. Moreover the expression of six MMP, like for example MMP-1,-3 and -9 MMP-2, was not influenced in mice without plasminogen. This results have indicated that even if the cheratinocites migration is plasmin dependent, the execution if the genetic program that controls the migration is plasmin independent. Even if the angiogenesis associated to growth and to the cure of wounds, seems not to be influenced in mice without uPA, uPAR, tPA, PAI-1 and plasminogen, sevrclal studies *in vivo* have evidenced the necessity of this system during angiogenesis associated to other process. For example, the cancer angiogenesis ( vascular density) is inhibited in mice without thymus using human carcinogenic cellular lines PC-3, transfused with human PAI-1 [81]. Even if this study shows a role of PA in the tumarl angiogenesis, it hasn't given andy meccanicistic informations. More detailed informations were given in a heart attack of the

myocardium, where the new myocardium vascularization was seriously altered in mice destitute of uPA [82].

Since this kind of phenotype can't be saved by adding of exogenous VEGF, and since endothelial cells and the smooth musculature express uPA during the revascularization, it was demonstrated that a defect in the angiogenesis is due to the altered invasion of endothelial cells. In particular, if assayed in the corena of rabbits or in chicken CAM, the uPA itself has demonstrated a pro-angiogenic effect [83-85]. In CAM, this event can be attributed to the relay of bFGF engoenous [85].

#### ***1.4.1.2 The interaction uPA-uPAR is requested for angiogenesis.***

The importance of the interaction between uPA and uPAR dring angiogenesis is shown in different systems *in vivo*. The angiogenesis induced by bFGF in atrigel by subcutaneous injection was inhibited by a fusion protein that consist in a ammino termina fragment of the specific uPA for the receptor and the Fc portion of the human IgG, that acts as high affinity antagonist for the uPAR [86] At the same way , cancer models on synergic rats and XENOGRAFT, the amino-terminal fragment diffused by adenoviruses was able o inhibit the cancer angiogenesis [87]. In an analogous model of rats immunocompetent of cancer cells transfused with human mutant uPA, that allows the conservation of the binding with the receptor but not the proteolytic activity, the microvasal density was diminished [88]. The cancer angiogenesis in different murin models was inhibited by an octa-peptide deriving froma region of the uPA not binding for the receptor [89, 90]. This studies have defined a new epitope in uPA involved in the interaction uPA-uPAR.

#### ***1.4.1.3 PAI-1 is necessary for the angiogenesis.***

Studies of localization have shown that PAI-1 is highly expressed in endothelial cells in a series of cancer types [69]. Studies on mice that do not express PAI-1 have revealed an absolute necessity of PAI-1 in the induced cancer angiogenesis.

In a model, cancer and stromal cells are separated by interposition of a collagen gel of type 1, that allows the evaluation of added esogen cancer cells and invasive guest stromal cells [91, 92]. The absence of PAI-1 ( but not of uPA, uPAR or tPA) in the guest may alter significatively the invasion of cancer cells and the neo-vascularization guest-derived. The inversion of this phenotype is realized from mice that do not express PAI-1 to which was distributed human PAI-1 as adenovirus. In wild-type mice, the expression of PAI-1 in stroma

can be localized in endothelial cells and not endothelial. Surprisingly, even if uPA is localized in blood vessels formed in wild-type mice, uPA was substituted by tPA in mice that do not express uPA, demonstrating the capacity of compensation between the PA's. The request of PAI-1 ( but not of uPA) during the cancer angiogenesis was demonstrated in a model of fibrosarcoma in the genetic inactivation of mice [93]. The corneal angiogenesis induced by bFGF is simply blocked by PAI-1 but not in mice where is not expressed uPA- Two possible mechanisms can explain the reason why pAI-1 is essential during angiogenesis. In the first by protection of ECM against excessive degradation, PAI-1 provides to the maintaining of the structure of the matrix requested for the endothelial cells migration and for the formation of tubules [94]. In the second mechanism a complex series of interactions between PAI-1, uPAR and the vitronectine was described [95-97]. Alterations of the expression and the activity of PAI-1 can alter the adhesive, migration and growth properties of endothelial cells, that subsequently may be able to regulate angiogenesis. In order to redirect directly this issue, adenovirus was used to distribute the mutant forms of PAI-1 to mice that do not express PAI-1. The mutants of PAI-1 either bind normally the vitronectine but do not inhibit uPA or tPA, or they inhibit normally the PAs but they do not bind relevantly to vitronectine. The angiogenesis is restored by mutants of PAI-1 that maintain the inhibitory effects for PA but not for mutants that bind to vitronectine but do not inhibit the PA, demonstrating that the necessity for PAI.1 in this model is due to the inhibition of excessive proteolysis rather the inhibition of cellular adhesions to vitronectin. In a different study was reposted that the addition of exogenous PAI-1 have induced the angiogenesis induced by bFGF in Cam [98]. By he use of diversion-mutants of PAI-1, this activity can be attributed to both anti-proteasic activity of the PAI-1 ant to its capacity of binding to vitronectine.

#### ***1.4.1.4 Role of the tPA in the angiogenesis***

Few informations are available on the role of tPA in the angiogenesis. In vivo the antigen for tPA is localized in the microvascular endothelium [99], hat as revealed in morphological studies, is the region of the vascular bed where new blood vessels are formed during angiogenesis. The presence of tPA in the angiogenic endothelium has to be described yet. In vitro, tPA is implicated in the formation of capillaries tubules on matrix of collagen of type 1 and Matrigel [100-104]. The necessity of tPA in the migration of endothelial cells *in vitro* was studied with different results [105, 106]. Surprisingly, the combination of bFGF abd VEGF have induced the activation of tPA mRNA and of the enzyme in synergic way in

coltures of endothelial cells [72]. Analysis of immunofluorescence have revealed that cells associated to tPA was co-localized with the von Willebrand factor, a marker of Weibel-Oalade bodies, that are mantaining grains specific for epithelial cells. A combination of bFGF and VEGF have raised the number of positive tPA cells like for the number of tPA grains positive for the cell.

The angiostatin, an endogenous inhibitor for the angiogenesis, have shown to be able to inhibit the activation of plasminogen catalyzed by tPA in endohelial cells [107]. At the moment is possible only to suggest possible functions of tPA in the Weibel-Palade bodies in the contest of angiogenesis. An important role can be the protection of blood vessels formed after thrombotic occlusion. The stagnant blood in the formation of “close roads” of new blood vessels can be easily subject of coagulation, due to potential exposition of blood to ECM ( and in particular to collagen), and to the blood coagulation activatd can be removed less easily. In order to overcome to this problem , the thrombin generated locally can be resulting in an acute release of tPA by the Weibel-Pallade bodies [108, 109], that can result in a removal of fibrin deposits. It is interesting to notice that the secretion of MMP-1 and MMP2, but not of TIMP-2, can be realized through a post-traslational mechanism in endothelial cells [110]. The MMP are regulated at different levels: in endothelial cells, the stimulation of MMP can happened during secretion., giving a mechanism for the rapid mobilization of the initial phase of angiogenesis. It has to be cleared if this enzymes, like tPA, are localized in the Weibel-Palade bodies. The intracellular accumulation of MMP-9 in the secretive vescicles as response to ester of forbolo was reported [111].

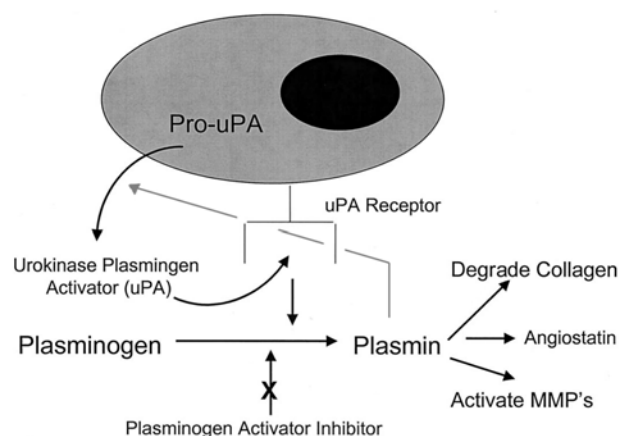
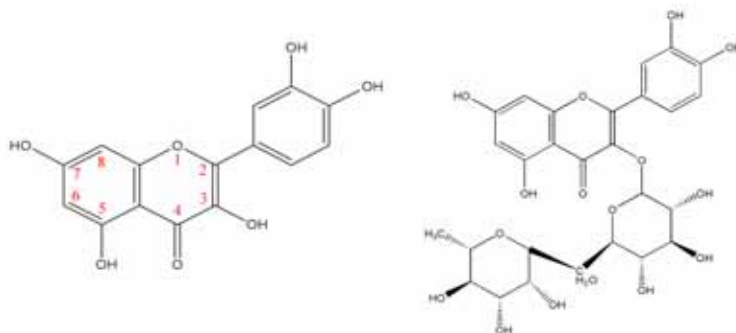


Fig. 7: The system plasmin/plasminogen in colon cancer

In this work we have tried to study and characterize from a kinetic and thermodynamic point of view the interaction of plasminogen and plasmin with two flavonoids ( quercetin and rutin) by utilization of SPR Biosensor, spectrophotometric and fluorimetric assays coupled with procedures of molecular modeling.



*Fig. 8 : Molecular structure of quercetin and rutin*

Quercetin is one of the most common and present flavonoid, and can be assimilated through fruits and vegetables with an approximate consumption of 16 mg/die [112]. It was shown that quercetin has a mutagenic and antimutagenic function, and is considered as inhibitor of carcinogeni effects and as potential chemopreventive agent versus cancer [113-115]. Further studies were pointed to the determination of the effective dosage and the relative toxicity, in order to evaluate the possible utilization in the prevention in the formation of malignant human pathologies. Rutin is a glycosilated form of quercetin (quercetin-3-rutinoside) and is hydrolized in liver [116].

Quercetin was found to be abundant in onions (284-486 mg/kg), broccoli ( 30 mg/kg), lettuce (15 mg/kg), tomatoes ( 8 mg/kg). In fruits quercetin was found to be present at a medium concentration of 15 mg/kg. In a similar study it was determined the concentration of quercetin in tea infusions, grape juices and wine.

This compounds are essentially known as natural antioxidants [117], and they exhibit a protective action towards the oxidation of membrane phospholipids [118], nucleic acids [119] and proteins [120].

It was also recently reported that this kind of molecules can act as specific binding/ effectors of a series of macromolecules involved in relevant physiological processes [121-123] and in particular, they can modulate the enzymatic activity of elastase [124], a serine protease belonging, like plasmin, to the family of tripsin-like family.



## 1.5 Interactioun polyphenols-DHFR

### 1.5.1 The dihydrofolate reductase: function and structure.

The dihydrofolate reductase ( DHFR, EC 1.5.1.3.) is an ubiquitous enzyme NADPH-dependent that catalyze the reduction of 7,8-dihydrofolate ( $H_2F$ ) to 5,6,7,8,-tetrahydrofolate ( $H_4F$ ). At acidic pH it catalyze the reduction of folate to tetrahydrofolate involving two equivalents of NADPH.

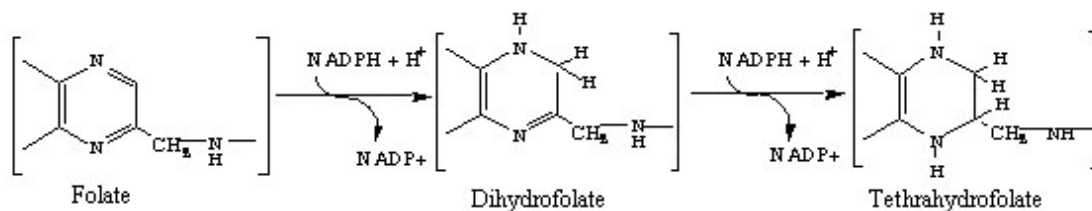


Fig. 9: Reactions catalyzed by DHFR

This enzyme is fundamental in the maintaining the quantity of intracellular  $H_4F$  and its derivatives, involve in the transfer of monocarbonic units in several methabolic processes like the biosynthesis of purines, of timidilate and several aminoacids:

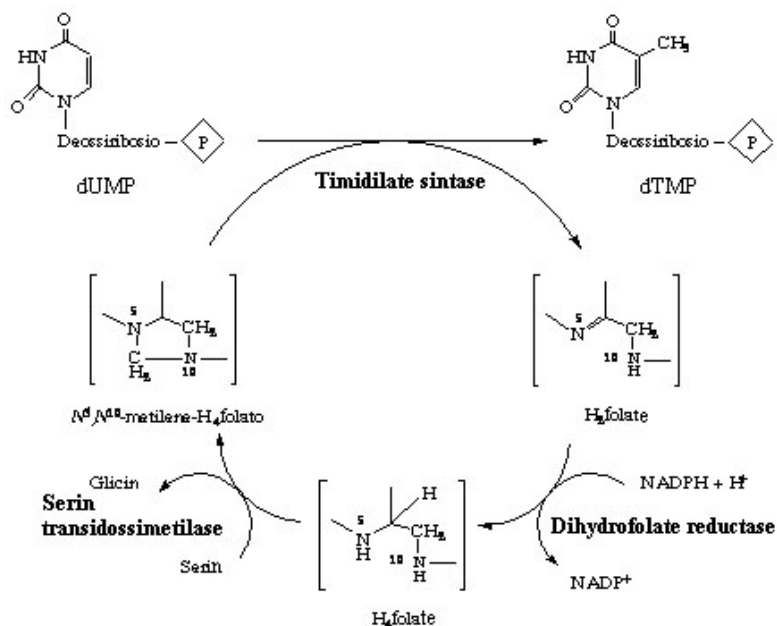


Fig. 10: Role of the DHFR in the biosynthesis of nucleotides

In figure 36 is reported a critical reaction associated with the activity of DHFR: the conversion of 2-deossiuridilate to deossitimidilate, used for the synthesis of DNA. The intervention of DHRF in metabolic connected with the synthesis of DNA gave to the scientific community great interest towards this enzyme since the half of the fifties, when was discovered the anticancer activity from one of the most powerfull inhibitor of the DHFR, the

metotrexate. It's an analogous of folate that present a a costant of equilibrium of association for the enzyme of an order of  $10^{10} \text{ M}^{-1}$ .

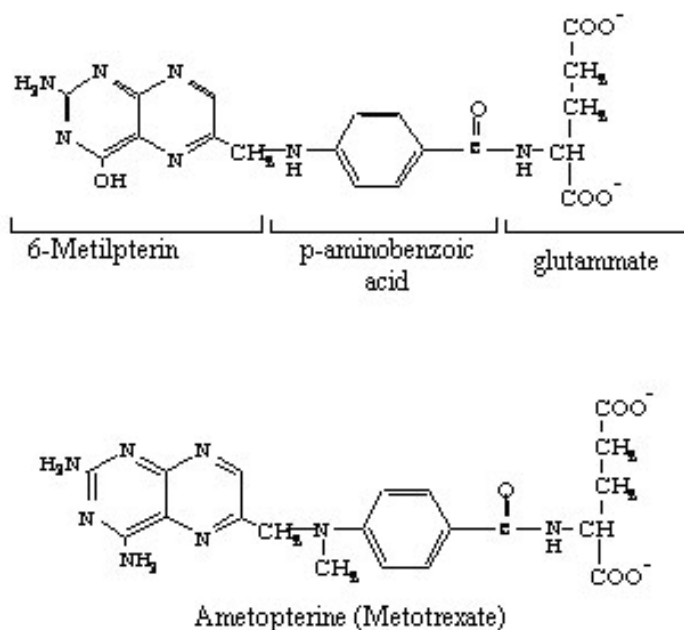


Fig. 11: Structure of Folate and Metotrexate

### 1.5.1.1 Mechanism of reaction:

Recent studies on DHFR [125] have evidenced an intrinsic structural flexibility of the protein that allows to overcome to the rigidity request imposed by the formation of a reactive complex, with the capacity of discriminating between substrate and product of reaction through the fine modulation ligand-dependent.

The reaction catalyzed by DHFR from *E. Coli* involves the formation of a ternary complex DHFR:NADPH:H<sub>2</sub>F by which happens the transfer of the hydrogen pro<sub>R</sub> from the cofactor NADPH at the C6 carbon of the pteridinic ring of the dihydrofolate with consequent protonation of the nitrogen N5 of the substrate. The reaction is strongly pH dependent and is characterized by a pKa of 6.5 and a transfer rate velocity for hydride of  $950 \text{ s}^{-1}$  [126]

The correct positioning of the substrate relative to NADPH, inside of the binding site, constitute a critical factor in determining the reaction velocity, as the right orientation of the side chain of Asp27 that represent the chemically significative residue for the formation of transition state.

The proposed reaction mechanism request infact to it has to be established a network of hydrogen bonds inside of the active site of the enzyme, involving the Trp22, Thr113 and a molecule of water [127].

Muthagenesis specific-site studies [128-131] have demonstred that sustituions of Trp22 and Thr113 are able to determine a diminution on the affinity for the substrate without affecting the transfer-rate velocity of hydride from NADPH to DHFR. From this results is possible to attribute the most significant role, in the mechanism of catalysis of DHFR, to Asp27, while the already cited residue responsible of the formation of hydrogen bonds inside the pteridinic ring of DHFR, and some hydrophobic residues (Leu28, Phe31,Ile50 and Leu54) that are found to be in contact with the substrate, seems to have a marginal role in the transfer process of hydride, but fundamentally in the correct positioning of the DHRF respect to NADPH and asp27. Based on crystallographic studies, NMR spectroscopy and Raman [130] is possible to describe the reaction mechanism based on a cheto-enolyic tautomery induced by the presence of a carboxylic group of Asp27. After the binding of the substrate, the concomitant expulsion of molecules of water from he catalytic site brings to a lowering of the dielectric constant of the surrounding of the carboxylate residue of Asp27 and a consequent rising of the pKa. The carboxylic oxygen after this shift of pKa, in proximity of the N3 hydrogen of the pteridinic ring, promotes the formation of the enolic tautomer inducing an electronic shift towards N3 and allowing the protonic transfer from a molecule of water to O4. This enolic intermediate results favourable in the hydride transfer from NADPH to c6 of dihydrofolate and at the same time allows to stabilize the negative charge of the COO- group of the Asp27 inside of the hydrophobic pocket. Subsequently to the transfer of hydride a proton is released from the enolic O4 to the pteridinic N5 leading to the formation of H4F and to the restoration of the negative charge on the carboxyle of Asp27. An important process based on the catalytic mechanism results to be the variation of the dielectric constant inside of the active site that derives from the expulsion of water molecules after the binding of the substrate. Substitution of hydrophobic residues, involved in the catalytic site, with more polar side chains that are able to determine an higher accessibility to solvent, have shown a negative effect on the affinity for the substrate and on the kinetic transfer constant of hydride [132]. Finally it's possible to indicate that there is a concerted kinetic mechanism that request the coupling of precise steric and chemical-physic factors; the correct aligning of the substrate respect to the cofactor and the Asp27, assisted by the presence of hydrophobic surfaces that are able to block the paraminobenzoic group, inside of the active site, united with the lower dielectric constant in the catalysis region, are able to realize the electronic rearrangement of the

pteridinic ring of the dihydrofolate to be found in the optimal configuration for the hydride transfer.

### ***1.5.1.2 Molecular structure of DHFR.***

The DHFR is a monomeric protein of 17Kda constituted of 159 aminoacids, and its secondary structure presents a big central  $\beta$ -sheet formed by eight  $\beta$  segment ( from  $\beta$ A to  $\beta$ H), four  $\alpha$ -helix and loop structures that connect the different elements of the secondary structure and modulate the conformational changes of the enzyme. In spite of the little dimensions of the protein, two domains can be found that delimitate the hydrophobic pocket involved for the binding site of DHFR: a big subdomain that binds the adenosinic portion of NADPH (adenosine-subdomain) and a subdomain rich of loop structures (loop-subdomain) [126] dominated by three regions highly flexible: the Met-20 loop, the loop that connects the segments  $\beta$ F and  $\beta$ G and the loop between the segments  $\beta$ G and  $\beta$ H.

The space between the two subdomains generates the inlet of the active site where is able to position the cofactor (NADPH) and the substrate ( $H_2F$ ) with an angle of  $45^\circ$  in order to favour the transfer of hydride from C4 of NADPH to C6 of  $H_2F$ . The accessibility of the active site towards ligands is regulated by the conformation of the flexible loop Met-20 that exerts an action of control of the opening/closure of the binding site towards NADPH. The presence of a rich subdomain rich in loop structures makes the DHFR a protein highly flexible. The possible conformations assumed by the enzyme after the concerted movement rotations of the two subdomains and the oscillation of the loop Met20 represent an efficient mechanism of regulation of the catalytic activity of the DHFR.

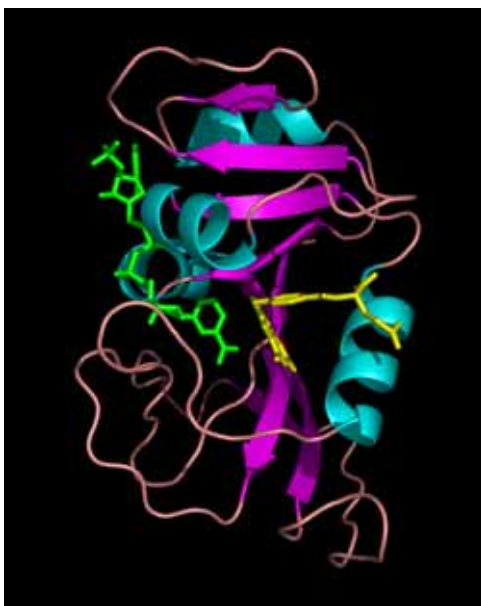


*Fig. 12: Structure of DHFR: ternary complex DHFR:H<sub>2</sub>F(yellow):NADPH(green)*

From crystallographic data [133], all the subdomains of DHRF are stabilized by the presence of hydrophobic clusters: particularly in the major domain we can find a large cluster of hydrophobic formed by six leucine (Leu4, 8, 104, 110, 112, 156), two tyrosines (Tyr100, 128) two phenylalanine (Phe103 and Phe125), two valines (Val93 and Val99), two alanines (Ala6 and Ala107) and Trp133 and Ile2. This group of hydrophobic chains stabilize the interface between the central  $\beta$ -sheet and the helix  $\alpha$ F, while on the other side of the  $\beta$ -sheet (in front of the helix  $\alpha$ B) there is a cluster of minor dimension composed by the side chains of Ile5, Trp30, Met92, Tyr111, Phe137, Tyr151, Phe153 and Ile155. Since this two hydrophobic clusters are linked with the central  $\beta$ -sheet is possible that they are able to act as a single rigid unit [133]. Also in the other subdomain more flexible is present a group of hydrophobic residue (Met42, Trp47, Ile61, Val72 and Trp74) that are able to maintain a constant spatial position during the subdomain movements involved in the catalysis mechanism.

The catalytic turnover of the DHRF involves the conformational changes of the enzyme to which are associated the skid movements of the interface and the  $\alpha$ B and  $\alpha$ C helix (that are able to determine the enlargement of the binding site of the substrate), and the movement of oscillation of the loop Met20, that regulate the entrance and the exit of the cofactor from the catalysis environment. In particular in the Michaelis complex DHFR:NADPH:H<sub>2</sub>F both the active site and the loop Met20 are found to be in a close conformation that determines a high affinity for the substrate and for the reduced cofactor. Once there is an hydride transfer, the socket of the active site opens and the loop Met20 has a conformation that blocks the positioning of the NADP<sup>+</sup> and induces the leaving of the catalytic site with consequent formation of the complex DHFR:H<sub>4</sub>F that presents a low affinity for both ligands and so, for

the saturating concentration of NADPH, provokes the dissociation of the H<sub>4</sub>F in order to form the binary complex DHFR:NADPH where the loop Met20 has the close conformation ready to start a new catalytic cycle. Recent studies have evidenced a wide variety of biological activities of catechin, mainly of EGCG, the most abundant flavonoid component in green tea and various beneficial effects among them the antioxidant activity, antibiotic and antiviral [134-136]. Some authors consider EGCG as a potential anticarcinogenic agent [137]. Green tea extracts have shown *in vitro* to provoke the apoptosis of several cancer cells, like prostate, lymphoma, colon and lungs [137-140].

It has been reported also that EGCG is able to inhibit the cancer invasion and the angiogenesis, two processes necessary for the cancer growth and metastasis [137], even through a mechanism not already cleared. On the basis of the observation that classical antifolate compounds (MTX) have chemical structures similar to some polyphenols [141], it was hypothesized that catechins (and in particular EGCG) are able to inhibit the activity of DHFR.

## ***1.6 Interaction polyphenols- proteasome 20S.***

### **1.6.1 The complex of the multicatalytic protease and the degradation of oxidized proteins.**

#### ***1.6.1.1 The control of the protease through proteic autocompartmentation .***

The proteic degradation is fundamental in the regulation of several physiological processes like the maintaining of homeostasis during continuous reconstruction of cellular structures, both during the development and as response of external stimulations, the removal of misfolded proteins after mutations, oxidative stress or heat, the elimination of regulatory proteins in defined moments (cyclins, transcriptional factors, components of signal transduction paths and the degradation of external antigens and the consequent production of immunocompetent peptides. Since the degradation represents a possible risk, it has to be checked through space and time in order to prevent the removal of proteins not destined to proteolysis. A potential control strategy of the proteic degradation is represented by compartmentalization, defined as the ability to define the proteolytic action to sites that result accessible only to proteins with degradation signals. The prokaryotic cells that do not possess membrane compartments or vesicular transport systems have developed a different

compartmentalization, defined as autocompartmentalization, defined as the formation of a commune architecture where different proteolytic subunits are able to form cylindrical structures where the catalytic sites are confined in the internal cavities (several nanometres of diameter) [142].

The access to the internal compartments is generally limited to unfolded polypeptides, able to pass through narrow pores or entering channels. The target proteins must be able to interact with a system able to bind to them and to be presented to the catalytic site in an unfolded way.

Since protein unfolding and folding are related mechanisms, it is supposed that the unfolding complexes are ATPase ones, partially similar to chaperonins and defined as inverted chaperonins or unfoldases. Since their action requires the hydrolysis of ATP, the protein degradation is an energy-demanding process. The proteolytic autocompartmentalization is common for all life domains: archaeobacteria, eubacteria and eukaryotes. This is a testimony of the importance of one of the evolution principles. Differing from organelles, the autocompartmentalization offers more flexibility: by having appropriate localization signals, such proteolytic complexes can reach different cellular districts where necessary their action.

#### ***1.6.1.2 The proteolytic system ubiquitin-proteasome:***

The turnover of normal and altered proteins is realized principally by a proteolytic system ATP-ubiquitin-dependent, present in nucleus and cytoplasm of eukaryotic cells but also in eubacteria and in archaeobacteria [142-144]. The proteolytic substrates destined to degradation are marked through covalent binding with multiple molecules of a small protein called ubiquitin. This protein is made by 76 amino acids with a molecular weight of 8.5 kDa, and it's highly conserved through evolution. The polyubiquitination happens through the sequential action of three enzymes: an ATP-dependent enzyme ubiquitin dependent (E1), an ubiquitin conjugating enzyme (E2) and ubiquitin ligase (E3).

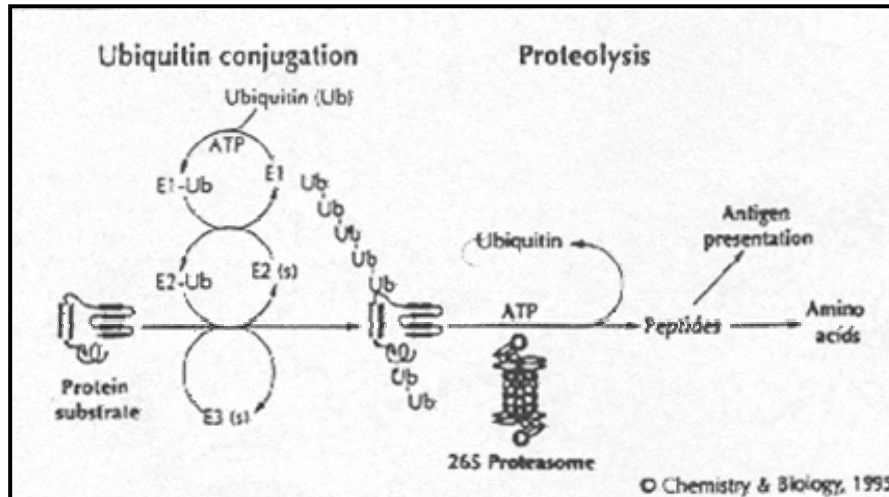


Fig. 13: Schematic representation of the polyubiquitination of a proteic substrate and further recognition and degradation by a part of the multicatalytic protease complex

The three enzymes are able to act simultaneously by realizing a covalent attack to the C-terminal of ubiquitin to the aminic group of a lysine residue of the target protein. Other ubiquitin molecules are able to link to the first by forming a long linear or ramified chain. The polyubiquitinated chains are first recognized and degraded by a part of a proteolytic complex ATP-dependent called proteasome 26. This last is a proteinase of 2000 kDa formed by a catalytic center, the proteasome 20S, with a molecular weight of 700 kDa. The proteasome 20S is a multiproteic structure with a cylindrical structure containing several peptidasic activities and for this reason called also MPC or Multicatalytic Protease Complex.

### 1.6.1.3 The proteasome 20S: the structure

The proteasome of the archibacteria *Thermoplasma Acidophilum* is the prototype for the quaternary structure and the enzyme topology. Its 28 substructures represent two homologous genetic products ( $\alpha$  e  $\beta$ ), each of them present in 14 copies for each proteasomal molecule [142, 145, 146].

The subunits are arranged in order to form four heptameric rings with the  $\alpha$  subunits forming the two external rings and the subunits  $\beta$  forming the internal rings. Together they form a complex with cylindrical shape, with a length of almost 15 nm and diameter of 11 nm, that includes the three internal cavities of 5nm of diameter delimited by four close constrictions.



The central cavity is formed by two adjacent  $\beta$  rings, while the two external cavities are delimited by an  $\beta$  and  $\alpha$  ring.

In the eukaryotes the subunits represent 14 genetic products, seven of them are homologues of the subunit  $\alpha$  of the *Thermoplasma* and the other seven homologues of the  $\beta$  subunits.

The relative positions of the subunits of  $\alpha$  and  $\beta$  type of the eukaryotes are analogous to those of the proteasome in the *Thermoplasma* and each ring contains a complete set of the seven genetic products. So the proteasome is a multimeric dimer with a symmetric axes that passes through the two  $\alpha$  and  $\beta$  ring and their subunit are disposed in order turning the active sites toward the inside surface of the central channel. The ternary structure of the non catalytic structures  $\alpha$  and of the catalytic ones of  $\beta$  type is very similar: every subunit is constituted by a sandwich of five antiparallel  $\beta$  sheets in contact with  $\alpha$  helix

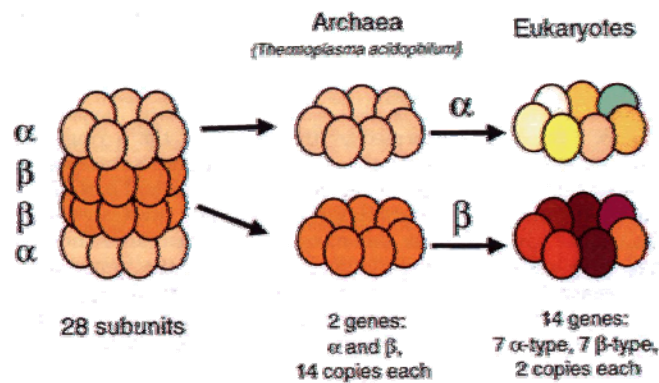


FIG. 1. Structural organization of the proteasome.

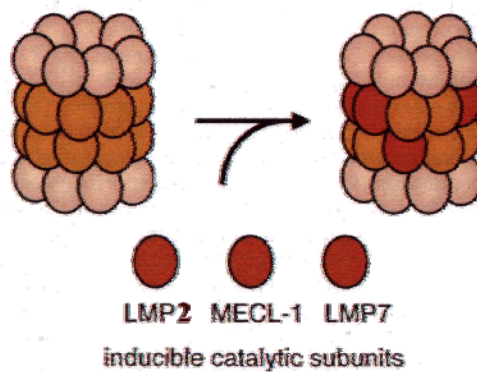


Fig. 14 Structural organization of the proteasome 20S (upper) and schematic representation of the subunit substitution in the immunoproteasome (below)

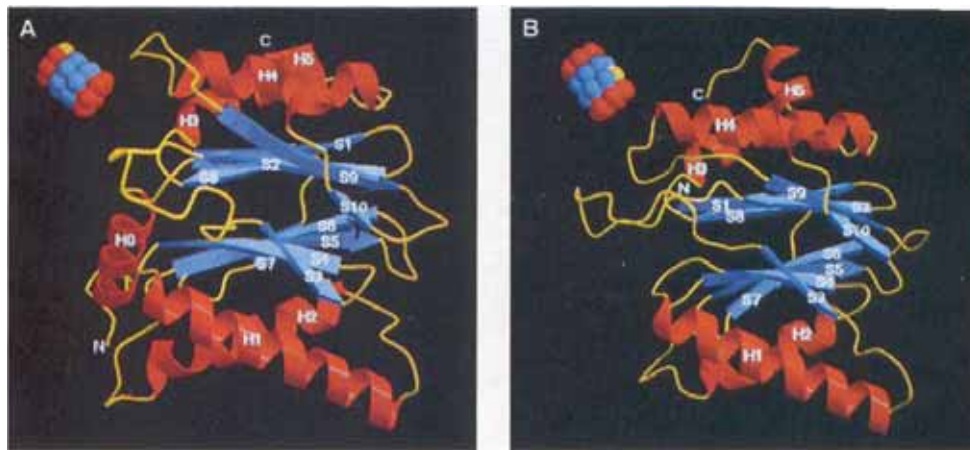


Fig. 15: Ribbons representation of the  $\alpha$  subunits (A); the  $\alpha$  helix are indicated with H, the  $\beta$  sheets with S. The helix HO at the NH<sub>2</sub>-terminal extremity represent the internal side of the proteosomal complex. In the barrel structure in the upper left, orientated in the same way, is indicated with a yellow sphere; (B) represents the  $\beta$  subunit.

The H1 and H2 helix mediate the interaction between the rings  $\alpha$  and  $\beta$  ( $\beta$ -trans- $\alpha$ ) by disposing in an intersecated way; the helix H3 and H4, on the other side, constituted the dominant concats between the two rings  $\beta$  ( $\beta$ -trans $\beta$ ). Hte major difference between the sububits  $\alpha$  and  $\beta$  is the presence of an extention N-terminal on the subunit  $\alpha$  ( $\alpha$ -helix-HO) that crosses the central sandwich.

The N-terminal extention can be found in the upper part of the  $\alpha$  rings, near to the entrance of the antechambers, and can be important for the translocation of the substrates and for the interaction between the proteasome and its regulatory complex. Instead of this N-terminal the  $\beta$ -subunits have a pro-sequence, of differing length, that is removed proteolitically during the assembling of the proteasome making freely accessible the internal cavity. Based on data obtained from crystallographic studies of the proteasome 20S in presence of its peptidic inhibitor it was concluded that the active site of the complex are found in the central chamber, and each subunit ha a fixed position and the interaction of the  $\beta$  subunits seems to be exential for the expression of the proteolytic activity.

The proteasome belongs to the family of the Ntn-idrolase ( N.terminal nucleophil-idrolase): its catalytic center is constituted by a residue of N-terminal treonine present in  $\beta$  subunits that acts as nucleophile and as proton acceptor while other residue (Glu17, Lys33, Asp166) participate to the expression of the photolytic activities [144].

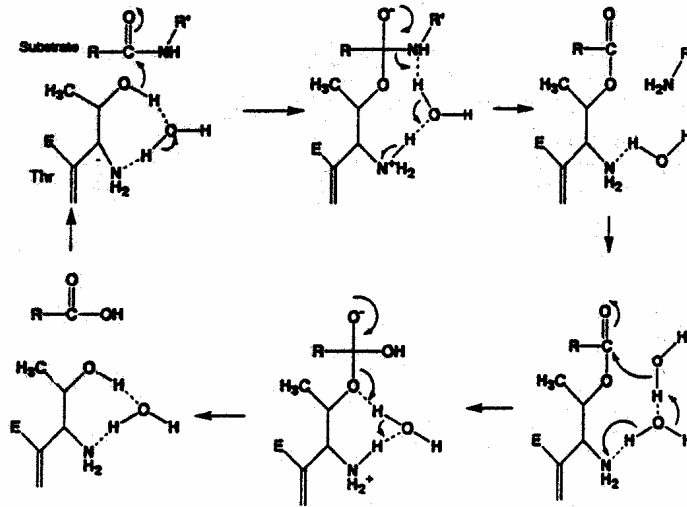


Fig. 16 :Schematic representation of the catalytic mechanism of the proteasome 20S with the residue of threonine that acts as nucleophile and a molecule of water that acts as base

### 1.6.2 Proteasome 20S: the functionality

To the complex 20s of mammals have been attributed five different peptidasic activities, that are distinguishable for the kind of aminoacidic residue involved in the cleaved bond [144, 147, 148].

It's possible to distinguish

- the chymotrypsin-like activity ( ChT-L), that cuts the carboxylic side of aromatic residues
- the trypsin-like activity (T-L), that cuts preferably the carboxylic side of basic aminoacid residues
- the peptidil-glutamyl-peptide idrolasic (PGPH), that cuts preferably the carboxylic side of acidic aminoacidic residues
- the BrAAP (branched chain amino acid preferring) activity
- the SNAAP ( small neutron amino acid preferring) activity

It seems that each of this activity is associated to different  $\beta$  subunits, but the aminoterminal threonin residues have been evidenced only on 4  $\beta$  subunits; so 3 of the 7 subunits doesn't seems to have catalytic sites.

Researches made with irreversible inhibitors have indicated that  $\beta$  subunits called X, Y and Z of mammalian proteasome, were associated respectively with the activity ChT-L, PGPH and T-L, while it is not already clear if the activities BrAAP and SNAAP must be associated to one or more cooperating  $\beta$  subunits. *In vitro* the proteasome is not able to degrade proteic substrates that were already denaturated but it should have at least activation by exposition to heat or by low concentration of SDS or in particular ionic conditions.

The molecular base for this activating effects is not already clear, but probably involves conformational changes in the proteasome (capable of opening the central cavity towards the external side) and/or allosteric modifications of the catalytic site. This mechanism doesn't have a physiological significance but they can mimic the activity promoted by regulatory proteins, even if it is not already clear if the direct activation of 20S by non proteic factors happens in intact cells.

For what regards the physiological role, the complex ubiquitin-proteasome seems to be involved in multiple cellular functions like the growth and the division of cells, the degradation of regulatory cells like proto-oncogenes, the transcriptional factors and cyclins.

It was demonstrated that the system proteasome-ubiquitin regulates the activation of transcriptional factors NF- $\kappa$ B, implicated in the acute and chronic inflammatory response, operating as promoter and process amplifier. In superior eukaryotes the proteasome is involved in the presentation of antigens by the major complex of histocompatibility of class I (MHC I), since it degrades proteins to small peptides of about 7-10 amino acids that once transferred in the endoplasmic ring, are able to bind to MHC I molecules giving rise to a complex that is then transported on the plasmatic membrane and presented to cytotoxic lymphocytes T that precede the cell disruption [149, 150]. On the other side it was observed that in certain pathological states, the cytokines are able to induce structural alteration on the proteasome that gains a more efficiency in the process of antigen presentation. In fact the induction by interferon  $\gamma$  in the cell of superior eukaryotes, lead to the appearance of three additional  $\beta$  subunits catalytically active (LMP2, MECL-1 and LMP7), that substitute respectively the subunit Y, Z and X of the proteasome giving rise to a complex known as immunoproteasome [151, 152]. The immunoproteasome differs from the original one for the quaternary structure and consequently for its structural function, acquiring a capacity of cutting more faster after hydrophobic and ramificated side chains residues and more slowly after acidic residues. Between the functions of the system ubiquitin-proteasome, the degradation of oxidised cellular proteins is of fundamental importance, giving to proteasome itself a primary role in antioxidant defence mechanism, and it seems to be able to act

preferably at the level of hydrophobic residues that more exposed during the structural rearrangement of the oxidised protein. The selective degradation of damaged proteins by oxidation allows to the cells the regeneration of vital enzymes and proteins during normal aerobic life and to limitate the damage amount during situations of moderate oxidative stress. So the proteasome constitutes an important defense mechanism in aging process and in the minimization of damages related to the rising of pathologies induced by oxidation.

### ***1.6.2.1 The oxidative stress and the aging process***

During aging and the progression of some correlated pathologies, there is a generally diminution pf the proteolytic cell capacities. The importance of the proteolytic in order to maniatin the cell viability it was documented in several pathologies, including the Alzheimer disease, diabetes, arteriosclerosis, ischemia damages, where the lost of cell functionality seems to be associated to defects in the proteolytic cellular systems. Significateive changes in the activities of this systems in function of aginig, can contribute to the cellular fragility in older organism respect to younger organism, potentially through an altered ability to respond in a proper way to pato-physiological stimuli [153-156]. Lysosomes and proteasome, that constitute the two main intracellular systems involved in proteic degradation, suffer modification of some structural and functional propertiesin function of age.

An important role in such process is done by the presence of free radicals:

- aging and progression of several correlated pathologies are associated to a rising in free radicals production and of the relative levels of oxidatie modified proteins
- the proteins that suffer significative modifications derived from the presence of free radicals seems to resist to the proteolytic degradation and are able to act as inhibitors of the lysosomal idrolase and in proteasome;
- the proteasome itself is capable of oxidative modifications and inactivation.

### ***1.6.2.2 The processes of reparation of oxidative damaged proteins***

After the oxidation of proteins, cells tries to repair the damaged polypeptides and recuperate their function: cells contain a series of proteins capable of reconstitute the native structure of oxidised proteins [153]. Several shock proteins, or stress proteins, constitutive or inducible, are able to reconstitute the ternary proteic structure. On the other hand several enzymes are able to reduce the side chains of oxidised aminoacids:

- the system tioredoxin/tiredoxin reduces the disulphure bonds;

- the methionin sulphoxide reductase reduces the free sulphoxid methionins
- the methionin sulphossid reductase peptide, reduces the oxidised forms of methionin contained in peptides and proteins.

### ***1.6.2.3 The degradation of oxidised proteins***

After the exposition of proteins to oxidating conditions, is possible to verify the presence of an higher susceptibility to the proteolytic action in several protease, that results at the highest level at intermediate concentrations is principally due to the rising of hydrophobicity of the proteic substrate after the oxidation.

Infacts, the oxidation causes in proteins the exposition of hydrophobic portions, localized inside the native ternary structure, towards the exposed surface to the solvent. Since it's known that proteasome prefers to binds aromatic and hydrophobic aminoacids, the recognize of this hydrophobic and unfolded portions by the proteasome was widely reported in literature [153]. It was also demonstred that an excessive oxidation causes a diminution in the proteolytic susceptibility after the aggregation and the proteic cross-linking.

It's generally accepted that the removal of partially oxidised proteins constitutes an exential function for the maintaining of the cellular homeostasis and in the prevention of the accumulation of higly oxidised proteins and cross-linked that are no more degradable.

Several studies have demonstred a key role in the proteosomal system in the degradation of oxidised proteins: in also interesting to notice that such proteolysis, analyzed in cellular extracts, doesn't results ATP dependent, while the ATP presence inhibits the degradation of all the oxidised in the lysate analysed. On the other hand it has been reported several effects of the oxidative stress on the accumulation of ubiquinated proteins and on the ubiquitination system.

It is generally accepted that the cytosolic and nuclear proteins are generally degraded by the proteasome 20S by an ATP dependent mechanism, while the covalent attack of ubiquitin signs the protein for the ATP-dependent degradation from the proteasome 26S [153, 157, 158].

### ***1.6.2.4 Proteic oxidation and aging***

A significative rising in oxidised proteins it was reported in several human tissues: in cutaneous fibroblasts, in cheratinocytes, in erythrocytes and in brains. Such rising is related to age and is generated by direct oxidation of the aminoacid and by the formation of proteic

adduct with carbohydrates and products of lipidic peroxidation [156]. The degradation of important enzymes and the accumulation of damaged proteins in function of aging are able to modify the cellular integrity.

Infact the accumulation of oxidised proteins is associated to several pathologies like the formation of cataract, the Alzheimer and Parkinson disease, the lateral amyotrophic sclerosis and the rheumatoid arthritis [155]., In particular the progression of the Alzheimer disease is associated with a defective proteolytic processing of polypeptides like the  $\beta$ -amyloid protein precursor, with consequent formation of senile plates that bring to the neuronal degeneration. The Alzheimer disease is also characterized by the accumulation of proteic forms oxidative modified and ubiquitinated, suggesting a chain role in functionality of proteic lysosomal and proteosomal degradation systems [155]. The aging is correlated to a major predisposition to cardio hyschemic, characterized by a loss in the hemodynamic function, that provokes a rising in the level of oxidatively ubiquitinated and modified proteins. Such observation may suggest that some aging processes and the rising of some pathologies related to the accumulation of oxidative damaged proteins can be partially due to a non efficient functionality of the proteasomal system.

#### ***1.6.2.5 Degradation of the proteosomal structure and functionality during aging.***

Several studies have reported a diminution in the functionality of the proteasome in function of age, observable in several tissutal districts [156]. Literature reports the diminution of the ChT-L activity in hearth, in kidney, in liver and in lung of animal of different ages. It was evidenced a diminution of the activity of proteasome in function of age only in certain cerebral districts like the backbone, the hippocampus and the cerebral bark. A degradation of the proteosomal activity is recently demonstrated in the Parkinson and Alzheimer disease: such results are of particular interest since several studies have demonstrated have shown the inhibition of proteasome is sufficient to induce the neuronal death through events like the activation of the caspase, the liberation of cytochrome C, the high expression of p53, the fragmentation of chromatin and the opening of DNA. Moreover, in literature was reported the effect on proteasomal system of a dietetic ipocaloric regimen, the only known phenomenon capable of reduction of aging, is to maintain the PGPH activity in liver of older animals respect to those of young or adult rats. These evidences suggest a

direct implication of the modification correlated to aging with the proteosomal function in the turnover decline due to aging.

#### ***1.6.2.6 Diminution of the expression of the proteosomal subunits***

Recent studies on the variation of the genic expression in function of aging report that the transcription of some genes that decode the subunits of proteasome 20S and 26S, reduces with age. On the other hand the caloric restriction seems to maintain, or the enhance, the genetic expression of the proteosomal subunits and of the activator PA28 in cells of the skeletal muscle of rats. Besides, the accumulation of oxidized proteins in epithelial human cells is associated with the diminution of the activity and of the content of proteasome , suggesting that the expression of the proteasome diminishes with the age. The same is described for human embryonic fibroblasts aged or in fibroblasts derived by donors of different age [156, 159, 160].

#### ***1.6.2.7 Structural modifications of proteasome subunits.***

Particular attention has been applied to studies on the effects of the oxidation on the proteosomal system in order to appraising the effect of the oxidation on the functionality and on the structure of the enzyme[156]. Several results may differ in function in the considered oxidation system, by the assayed proteosomal activities and by the different cells and tissues analyzed. Studies conducted *in vitro* report the inactivation or the activation of the PGPH and T-L components of the proteasome 20S after the oxidation metal-catalyzed in function of the state, activated or latent, of the enzyme. Such results show a different susceptibility of the 20S and 26S form to the metal-catalyzed oxidising action [161]. Other describes the inactivation of the activities PGPH and T-L of the proteasome 20S in hepatic cells of rats after the treatment with iron-ascorbate [162]. The T-L activity is selective inactivated after treatment of the proteasome 20S with products of the HNE lipidic peroxidation, that damages the functionality of the enzyme by linking covalently to the proteasome [163, 164]. Further studies on proteasome 20S purified from different organs shows an inactivation correlated with age of several peptidasic activities and through bidimensional gel analyss, the presence of substitutions of the subunits and/or of post traductional modifications that may result responsible of the observer diminution of the peptidasic activity.



## **2 Materials and methods**

### **2.1 Materials**

#### **2.1.1 Thrombin-polyphenol, Plasmin-polyphenol, DHFR-polyphenol, Proteasome 20S-polyphenol interactions**

Human Thrombin (E.C.: 3.4.21.5, pdb-ID:1EB1), the synthetic substrate for spectrophotometric studies tosyl-gly-pro-arg-4-nitroanilide acetate (chromozym), plasmin and human plasminogen (E.C.: 3.4.21.7), PMSF, the flavonoids quercetin-3-rutinoside (rutyn), quercetin-3-D-galactoside (hyperosyde), luteolin, ellagic acid, epicatechin, catechin and Tween-20, NADPH, epigallocatechingallate, dihydrofolic acid, ascorbic acid were all of analytical grade and obtained from sigma-Aldrich. Carboxilate cuvettes and the immobilization kit containing N-idroxy-succinimide (NHS), 1-ethyl-3-(3-dimetilaminopropyl) carbodimide (EDC) and ethanolamine 1M, pH 8.5 were obtained from Affinity Sensors. NaOH, NaCl, Tris, KCl, CaCl<sub>2</sub>, NaH<sub>2</sub>PO<sub>4</sub>, KH<sub>2</sub>PO<sub>4</sub>, EDTA were of analytical grade and obtained from J.T.Baker. The experiments were conducted on a spectrophotometer Cary 1E from Varian Inc. Palo Alto, California, USA. The kinetic and thermodynamic studies were conducted on a Iasys Plus apparatus, from Affinity Sensors, Cambridge UK.

Fluorometric determinations were conducted on Shimazu RF-5301PC

The chromatographic column Mono-Q (HR 5/5) was obtained from Amersham Biosciences.

#### **2.1.2 Proteasome 20S-polyphenol interactions**

Bovine brain and thyme used for the purification of proteasome 20S, were obtained from local butcher. The antibody direct versus subunits X,Y,LMP7 and LMP2 were from Affiniti Research Products Ltd. (Mamhead, Exeter, UK). The membranes necessary for the electotransfer were of Immobilion P kind, buyed from Millipore and for immunorevelation were used kits ECL Western Blotting (Amersham Biosciences). The substrates used in order to test the activity ChT-L, PGPH and T-L were buyed from Sigma-Aldrich (suc-LLVY-MCA and Z-GGL-pNA, Z-LLE-MCA and Z-LLE-2NA, Z-GGR-MCA and Z-GGR-2NA). The

synthetic substrate used for testing the proteolytic activity BrAAP of proteasome was kindly obtained from Prof. M. Orłowski (Mount Sinai Medical School, New York). The aminopeptidase-N (Ap-N) necessary for testing this particular activity was purified following the Pfeleiderer protocol and the subsequent modifications from Almenoff [165]. Gallic acid and EGCG were directly dissolved in TRIS-HCl buffer 50 mM pH 8.0; resveratrol, (-)-epicatechin and rutin were dissolved in buffer-DMSO (1:1); hyperoside, ellagic acid and luteolin were dissolved in DMSO.

### **2.1.3 RP-HPLC, Folin-Ciocalteu, DPPH Assay, ORAC Assay**

Acetonitril, phosphoric acid, methanol, catechin, epicatechin, epigallocatechin gallate, gallic acid, fluorescein, AAPH, Trolox  $K_2HPO_4$  and  $NaH_2PO_4$  and water were all of HPLC grade and obtained from Sigma-Aldrich like for Folin Ciocalteu Reagent. DPPH was obtained from Calbiochem (Milan, Italy).

Chromatographic column Luna C18 4,6 x 250mm was obtained from Phenomenex.

### **2.1.4 Lipidic peroxides inhibition**

Chloroform, glacial acetic acid, potassium iodine, sodium thiosulphate potassium bichromate, BHT, BHA and starch paste were all obtained from Sigma

## **2.2 Methods**

### **2.2.1 Accelerated Solvent Extraction:**

Extraction of polyphenols were obtained through an ASE-100 (Dionex Corp.) equipped with a 10 ml cell filled with approximately 2g of grape seeds. Conditions were as following: pressure of 1500 psi, temperature of 150°C, 3 static cycles, flush volume 150%, purge time 100 sec. The solvent used for the extraction was water-ethanol (50:50). After extraction the obtained extract is vacuum-dried and weighted.

### 2.2.2 Folin-Ciocalteu assay:

Determination of polyphenols were obtained through Folin-Ciocalteu assay [166] and results indicated as gallic acid equivalents. Briefly standard of gallic acid from 50 to 500 mg/l are dissolved in water and 100  $\mu$ l are pipetted in a 10 ml volumetric flask with 7,9 ml of water and 0,5 ml of Folin-Ciocalteu; after 30 sec and before 8 min 1,5 ml of Na<sub>2</sub>CO<sub>3</sub> 20% m/v is added. The solution were maintained in dark and room temperature for 2 hours and readings were made on a double beam spectrophotometer at 760 nm using as blank a solution without gallic acid. Samples are prepared using a solution of 1mg/ml of dry extract dissolved in water and analyzed as indicated.

### 2.2.3 RP-HPLC assay:

Determination of gallic acid (GA), catechin (C), epicatechin (EC), epigallocatechin gallate (EGCG) were determined through RP-HPLC [167] using a LunaC-18 (Phenomenex) on a Varian Prostar HPLC system equipped with two 210 Prostar pumps and a 325 UV-VIS Prostar detector. A solvent gradient of 0,3% of phosphoric acid (A) and acetonitrile (B) was used as indicated in table 1. The solvent flux was 1 ml/min and readings were made at 278 nm with an injection volume of 20  $\mu$ l

Time (min)	% B (H <sub>3</sub> PO <sub>4</sub> 0.3%)
0	10
45	20
65	60

*Tab 1: RP-HPLC gradient pattern*

### 2.2.4 DPPH Assay

Antioxidant activity was measured through DPPH (1,1-diphenyl-2-picryl-hydrazyl) assay [168, 169].

In DPPH assay the odd electron of the free radical DPPH gives a strong absorption at 517 nm and it has a violet colour. When this radicalic species comes in contact with an antioxidant, the odd electron pairs off with an atom of hydrogen leading to the formation of the reduced species DPPH-H. This provokes a reduction of the absorbance recorded at 517 nm and when the reduction is complete, there is a contemporary change of color of the sample that from violet to yellow. The resultant decoloration is stoichiometric to the number of captured electrons. Briefly a 500 µl volume of each tested compound at various concentrations (10<sup>-5</sup>-2-1-0,5 mg/L in methanol) was mixed with 500 µl of a 8x10<sup>-5</sup> M of DPPH solution in methanol. After incubation of the mixture for 120 min, the absorbance of the remaining DPPH was determined colorimetrically at 517 nm. The scavenging activities were expressed as a percentage of the absorbance of the control DPPH solution. The results are expressed as mean of at least three independent experiments. Results were expressed as percentage activity. Mean inhibiting concentrations IC<sub>50</sub> were calculated by use of statistical software.

### **2.2.5 Lipidic peroxidation inhibition**

Chloroform and glacial acetic acid must be bubbled with nitrogen gas in order to make the solutions free from oxygen. A fresh made solution of 1% starch paste has to be made and must be free from iodine and iodide. The thiosulphate standardization is made with potassium dichromate. An appropriate amount of this standard has to be weighted in order to have a thiosulphate consumption (0.01 N or 0.02 N) of 45-50 ml; since dichromate has a low equivalent weight (MW/6) is preferable to prepare an aqueous solution of 250 ml containing 5 times the reactive necessary for the consumption of 40-45 ml of sodium thiosulphate and take each time 50 ml of this solution.

To this 50 ml 1,5-2 g of KI must be added with 2 ml of H<sub>2</sub>SO<sub>4</sub> 2N, than the solution is titrated with sodium thiosulphate (0.01 N or 0.02 N) until it reaches a pale-yellow coloration. At this point 2-3 ml of starch paste are added as indicator and titration is made until disappearing of the blue coloration of the complex starchpaste-I<sub>2</sub>.

The assay has to be made under diffused light or with artificial light. The sample has to be weighed in a range between 5 and 0,5 g based on expected peroxides number.

On appropriate flask add the sample. Add 10 ml of chloroform by dissolve the sample by manual shaking. Add 15 ml of acetic acid and then 1 ml of KI. Cap the solution rapidly, shake for 1 min and than make it stand for about 5 min, at a temperature between 15 and 25 °C.

Add 75 ml of distilled water. Titrate (preferably with a 10 ml burette) the free iodine with a solution of thiosulphate (0,002 N for values less than 12 and 0,01 N for values more than 12), and then shake the solution using the starch paste as indicator.

Results are expressed as numbers of peroxides (P.N.) expressed as milliequivalents of active oxygen/kg and is calculated by the formula:

$$P.N. = (V * T / m) * 1000$$

Where V is the number of ml of the standardized thiosulphate solution used in this assay, by taking in considerations also the blank sample; T is the exact normality of the thiosulphate solution used and M is the weight of the sample

### 2.2.6 ORAC

There is increasing interest in the use and measurement of antioxidant capacity in the food, pharmaceutical, and cosmetic industries. This interest is derived from the overwhelming evidence of importance of reactive oxygen/nitrogen species (ROS/RON) in aging and pathogenesis. Recently, Cao[170] . developed a method called oxygen radical absorbance capacity (ORAC), which measures antioxidant scavenging activity against peroxy radical induced by 2,2'-azobis(2- amidinopropane) dihydrochloride (AAPH) at 37 °C (5, 6). In this assay, B-phycoerythrin (B-PE), a protein isolated from *Porphyridium cruentum*, was the chosen fluorescent probe. The loss of fluorescence of B-PE is an indication of the extent of damage from its reaction with the peroxy radical. The protective effect of an antioxidant is measured by assessing the area under the fluorescence decay curve (AUC) of the sample as compared to that of the blank in which no antioxidant is present. The ORAC assay provides a very unique and complete assessment in which the inhibition time and inhibition degree are measured as the reaction goes to completion. However, the major limitation of the ORAC<sub>PE</sub> assay[171] is the use of  $\mu$ -PE as the probe. First,  $\mu$ -PE produces inconsistency from lot to lot, which results in variable reactivity to peroxy radical. Second, B-PE is not photostable, and after exposure to excitation light for certain time, it can be photobleached. This phenomenon was observed in a 96-well plate reader where the fluorescence signal was found to decline dramatically without the addition of AAPH (unpublished results). Third, it was observed that B-PE interacts with polyphenols due to the nonspecific protein binding. These disadvantages prompted us to utilize and validate a stable fluorescent probe to replace B-PE. For this reasons we have chosen to use fluorescein (FL) (3',6'-dihydroxyspiro[isobenzofuran-1[3H],9'[9H]-

xanthen]-3-one) as the fluorescent probe Unlike other popular antioxidant activity methods, the improved ORAC<sub>FL</sub> assay provides a direct measure of hydrophilic chain-breaking antioxidant capacity against peroxy radical.

Phosphate buffer and a fluorescein solution (FL) are preincubated at 37 °C in fluorimetric cuvettes before recording the initial fluorescence ( $f_0$ ). During each assay a blank and a standard must be analyzed. As blank it must be used 100 µl of buffer instead of 100 µl of sample. In standard case the sample must be substituted with 100 µl of a 20 µM Trolox solution.

Then in the cuvette are inserted 350 µl of phosphate buffer ( 75mM, pH 7,4), 900 µl of fluorescein solution (0,875 µM), 100 µl of sample ( i.e. for vegetal extracts 0,2 mg/l) and 450 µl of the AAPH solution (160mM). The reactions begins from the moment that AAPH is inserted. Immediately after the reaction starts the cuvette is vortexed and read immediately on a Shimadzu Spectrofluorimeter in order to obtain initial fluorescence value ( $f_0$ ) at 493 nm excitation wavelength and 515 nm emission wavelength. The fluorescence is read every 5 minutes until the fluorescence of the last reading is 5% of the initial reading. It's important that the solution is maintained constantly under dark conditions, thermostated and kept under agitation and capped in order to prevent solvent evaporation.

The final ORAC values were calculated by using a regression equation between the Trolox concentration and the net area under the FL decay curve and were expressed as Trolox equivalents as micromole per liter or per gram. The area under curve (AUC) was calculated as where  $f_0$  is the initial fluorescence reading at 0 min and  $f_i$  is the fluorescence reading at time i. The data were analyzed by in a Microsoft Excel spreadsheet to calculate the AUC

$$AUC = 1 + f_1/f_0 + f_2/f_0 + f_3/f_0 + f_4/f_0 + \dots + f_{55}/f_0 + f_{60}/f_0.$$

The net AUC was obtained by subtracting the AUC of the blank from that of the sample. The relative ORAC value (Trolox equivalents) was calculated as

$$\text{Orac Value } (\mu\text{M}) = 20 k (AUC_{\text{sample}} - AUC_{\text{blank}}) / (AUC_{\text{Trolox}} - AUC_{\text{blank}})$$

where k is the dilution factor .

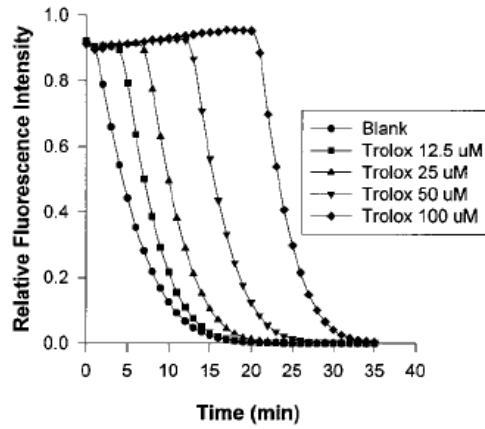


Fig. 17 : effects of Trolox concentration on FL decay curve

### 2.2.7 Spectrophotometric assay of enzymatic activity.

The equilibrium constant of dissociation  $K_i$  of the complex thrombin-flavonoid was measured by demonstrating the inhibitory effect over the amygdolitic activity towards a chromogenic substrate [172]. 0.25 nM of human thrombin was incubated with increasing concentrations of flavonoid in potassium phosphate buffer 50 mM, pH 7.5 at 25°C- After 10 minutes of preincubation (prolonged preincubation times didn't show an increase in inhibition rates), the residue activities were measured at 410 nm (maximum of absorbance of the product). The residue activity  $a_i$  was obtained by measuring the initial rates of formation of the product with ( $V_{0,i}$ ) and without ( $V_0$ ) a certain concentration of flavonoids  $[I]_i$ .

$$a_i = \frac{V_{0,i}}{V_0}$$

The data set was constituted by a series of residue activities  $a_i$  measured at increasing concentrations of flavonoids  $[I]_i$ . The constant of dissociation apparent or substrate-dependent ( $K_{iapp}$ ) was calculated for each concentration of substrate by using the standard Bieth equation [173]

$$a = 1 - \frac{[EI]}{[E^0]}$$

The apparent constant of dissociation ( $K_{iapp}$ ) is linked [173] with  $K_i$  by the equation:

$$K_{i_{app}} = K_i \cdot \left( 1 + \frac{[S^0]}{K_m} \right)$$

When  $K_m \approx K_i$  (like in our case), the effect of the concentration of substrate must be considered, by measuring the effect of increasing concentrations of substrate [173]. In our case, for each flavonoid studied, every set of experimental data was repeated for four increasing substrate concentration  $[S_0]$ , in the range between 1-12  $\mu\text{M}$ . The fitting of experimental data was realized by the software SigmaPlot 2002 ver. 8.01 produced by SPSS Inc.

## 2.2.8 Ligand immobilization.

The chemistry of immobilization most commonly used in protein application is coupling between carboxyl groups of carboxy-methyl-dextrane and the amminic primary groups of proteins ( N-terminal groups and lysine), through the EDC chemistry (1-ethyl-3-(3-dimethylaminopropyl)carbodiimide) and NHS (N-hydroxysuccinimide). This approach is also applicable to non-proteic biomolecules containing primary amminic groups.

The electrostatic absorbance of the biomolecule on the carboxylate matrix depends on its concentration in solution; the level of this dependence and the interval of pH where it happens depends on the isoelectric point of the molecule that has to be immobilized.

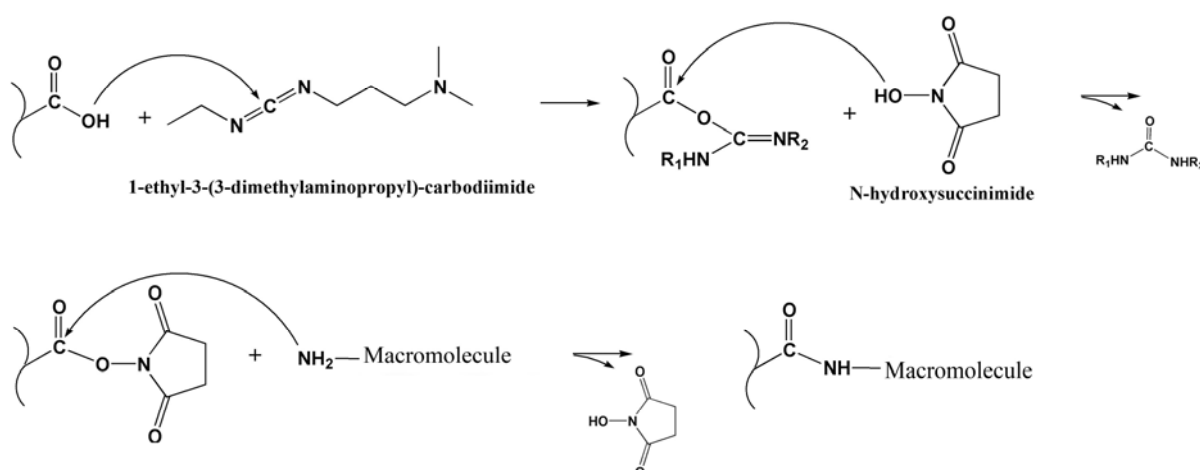


Fig. 18 Chemistry of immobilization of a macromolecule over carboxylate through EDC-NHS



### ***2.2.8.1 Immobilization of thrombin over a carboxylate layer.***

The cuvette of carboxylate is inserted in the IASYS biosensor and left for equilibration for 5 minutes at 25°C. Eventually impurities present inside of the cell of the cuvette are removed with washing of PBS-T (sodium phosphate 10mM, potassium chloride 2.7 mM, sodium chloride 138 mM and Tween-20 0.05% (w/w)). With the term washing we refer to a triple adding and removal made vary rapidly of the content of the cuvette with 75 µl of buffer. The binding was measured at 10 sec. The interval and the reading of the biosensor are expressed in arcseconds, and they correspond to the mass accumulation inside of the optical window on the binding layer. Every binding association was followed for 4 minutes.

Previously to the activation of the surface, the cell is washed with PBS ( potassium 10mM sodium phosphate, chloride 2.7mM, 138mM sodium chloride ): in fact, the exposure of the surface to buffer containing cleansing agent ( like for examples Tween of the buffer PBS-t ) immediately before the immobilization of the ligand it's not advisable, from the moment that the level of immobilization may result reduced , maybe due to a disguise of the reactive groups due to a deposit of the detergent on the surface.

The cell is again washed with PBS for 5 min, till the obtainment of a stable line of base ( fig.5, b ). Immediately before the use, equal volumes of the solutions of EDC and of NHS are mixed together : this solution constitutes the mixture of activation. The PBS buffer is then substituted with the mixture of activation of EDC/NHS ( 7 min ) in order to activate the carboxylic groups on the carboxylate surface ( fig.3.4, c ).

The mixture of activation is then removed by washing with the buffer PBS for 5 minutes ( fig. 5, d). The PBS is substituted with the buffer of immobilization ( acetate of 10mM sodium, pH 6 ) for 2 min (fig. 5, e). Finally the thrombin ( 100 G/ml, in sodium acetate) is added and incubated for 10 minutes ( fig. 5, f). The ligand not immobilized is removed by washing with PBS ( fig. 5, g). the remaining reactive groups, are deactivated with 1M ethanolamin, pH 8.5 ( 3 minutes.) ( fig. 5, h): this has the combined effect to block the remaining group of the ester of NHS and to remove the immobilized material electrostatically. This passage is followed by a washing with PBS, a washing with HCl 10mM ( buffer of regeneration ) and at last with PBS ( fig. 5, i). Then, the reaction environment is modified to the desired pH (potassium phosphate buffer, pH 7.5 ) and the flavonoids are added at various concentrations.

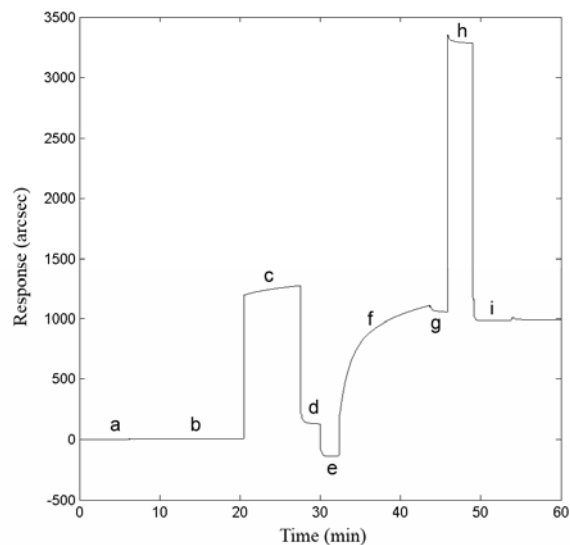


*Fig. 19 Immobilization of thrombin of the carboxylate surface through NHS-EDC*

### **2.2.9 Studies of coagulation.**

The human plasma has been obtained from blood centrifugation at 1200xg for 15 min, and subsequently incubated with quercetin at increasing concentrations ( 0-1mM ) for 10 min at 25°C. The time of thrombin (TT) of the plasma has been measured in accordance with a standard procedure [172, 174, 175] using a system STA-Rack ( Roche Diagnostics ).

### **2.2.10 Molecular docking of the interaction thrombin-flavonoid**

The purpose of the molecular docking is that to appraise the possible geometries of bond of a potential ligand with a target of which is known structures you/it three-dimensional. the fundamental stitches of a procedure of docking are: the characterization of the site of bond, the positioning of the ligand in the site of bond (orienting) and the evaluation of the force of for the specify interaction it complex receptor-ligand [176] (scoring).

The section for molecular docking of the MOE software ( Molecular Operating Environment, version 2001.01 [177] ) has been performed on a personal computer equipped with Intel Pentium4 processor: a docking box of 60×40×40 points with a grid of 0 , 375 Å has been put around the active site of the thrombin with the flavonoid at the entrance of this. The annealing based on the Monte Carlo [178] method ( 6 cycles for run, 8000 iterations for cycle,  $T_0=1000^{\circ}\text{K}$ ) has been simulated using the quercetin as model. Such procedure has used as energy function a Merck Molecular Force Field (MMFF94) [179]. The results of the

docking analysis have been expressed as an set of possible complex enzyme-ligand, ordered for decreasing stability.

### 2.2.11 QSAR Analysis

The analysis of three-dimensional QSAR has been used to draw a canonical model statistically meaningful and highly predictive [180]. Using the QSAR application of the MOE software, six descriptors have been selected: *Out of plane energy* [177], *Torsion energy* [177], *Molecular flexibility* (calculated as index of flexibility [181]), *Van der Waals acceptor surface area* e *Van der Waals donor surface area* (an approximation of the sum of the surface VdW areas of donor and acceptor of hydrogen bonds [182, 183]) and *Molecular globularity* (value assumed between 0 and 1, with the highest value for a perfect spherical molecule [184]). Then it has been performed the QSAR-Contingency<sup>TM</sup> e QSAR-Model<sup>TM</sup> using the pK<sub>d</sub> as range of activities and the molecular structures of the [177] ligands. A theoretical value of pK<sub>d</sub> for an inhibitor is calculated using the equation:

$$pK_d = Const + \sum_{i=1}^n C_i \cdot P_i$$

Where n is the number of descriptors and  $P_i$  is the value of the descriptor; *Const* and the weight of the  $i$  descriptor  $C_i$  are coefficients calculated from the module QSAR-Model<sup>TM</sup> [177].

### 2.2.12 Plasminogen purification

The human plasminogen was irreversibly inactivated by incubation with PMSF using a standard procedure [185]. The resulting solution was loaded on a Mono-Q column and eluted at a flux of 0.5 ml/min with the following gradient of buffer C (Tris-HCl 50 mM, pH 9) and D (Tris-HCl 50 mM, NaCl 1 M, pH 9) 0-25% D for 8 min., 10 min. at 25% D, 25-100% D for 20 min., 8 min. at 100% D and at the end 100-0% D for 4 min.

### **2.2.13 Spectrophotometric assay of enzymatic activity:**

The dissociation equilibrium constant  $K_d$  of the complex plasmin-flavonoid have been determined measuring the inhibitory effect on the amidolytic activity for a [186] chromogenic substrate. The human plasmin 60 nM has been incubated with increasing quantity of flavonoids in phosphate buffer 50 MM with NaCl 0.1M and PEG 6000 0.1 %, pH 7.5 at 25 °C. After 10 min. of preincubation (longer times has shown no further inhibition ), the residual activity has been measured at 410 nm using the chromozym-PL as substrate for the plasmin. The residual activities have been calculated in accordance with the procedure used for analogous study on thrombin.

### **2.2.14 Optical biosensor assay**

The cuvette of carboxylate has been washed with PBS-t (  $\text{NaH}_2\text{PO}_4$  10 mM, KCl 2.7 mM, NaCl 138 mM, Tween-20 0.05 % (v/v), pH 7.4 ) and equilibrated with PBS for 10 min. in order to obtain a stable line of base signal, at the temperature of 25 °C. The inactivated plasmin and plasminogen have been immobilized covalently on the matrix of carboxylate of the cuvette for medium using a standard procedure of immobilization [187]. The ligand not immobilized was removed by washing with PBS for 2 min. The reactive remaining groups were deactivated with ethanolamine 1M, which even assures that every kind of material electrostatically linked is removed. The immobilized quantity of plasmin and of plasminogen has been calculated, getting a value of 950 arcsec for both. At this conditions the partial mono-layer of an immobilized protein of 85 KDa results to be of 1.6 ng/mm<sup>2</sup>. Then, every flavonoid has been added at increasing concentrations. All the kinetics of association has been followed till the reaching of an equilibrium state. The dissociation and the following regeneration of the surface have been obtained by buffer addition.

The binding data have been analysed using the "Fast Fit" software in endowment to the apparatus; this software uses an iterative fit to the curves in order to determine the observed growth constant and the maximum response to the equilibrium for a certain concentration of ligand [L]. This software uses both monoexponential and biexponential models [1, 188]. A standard procedure F-test has been used then to determine which of the two patterns resulted better for the fitting [189]]. Moreover, data have been analysed globally [190, 191] using an monophasic curve:

$$R_t = R_{eq,[L]} \cdot \left(1 - e^{-(k_{ass}[L] + k_{diss})t}\right)$$

Where the response at the equilibrium state (extent) is:

$$R_{eq,[L]} = \frac{R_{max} k_{ass} [L]}{k_{ass} [L] + k_{diss}}$$

and  $R_{max}$  is the value of maximum concentration of the ligand. The responses measured at different concentrations of ligand can be simultaneously using the previous equations in order to determine  $k_{ass}$ ,  $k_{diss}$  and  $R_{max}$ .

### 2.2.15 Fluorometric determination

The human plasmin 23.5 NM has been incubated with increasing quantity of flavonoids ( 5-100  $\mu$ M) in phosphate buffer 50 mM with NaCl 0.1M, pH 7.5 at 25 °C. After 10 min. of preincubation, the intensity of fluorescence has been measured ( emission 348 nm and excitation 270 nm ). The quenching constant of Stern-Volmer  $K_{SV}$  has been then calculated using the following equation:

$$\frac{F}{F_0} = \frac{1}{\left(1 + K_{SV} [Q]^n\right)}$$

Where  $F_0$  and F are the fluorescence intensity in absence and in presence of flavonoid, and [Q] is the concentration of the flavonoid added. Moreover the value of  $n$  indicates the kind of binding stoichiometry between the two partners.

### 2.2.16 Molecular docking of the interaction plasmin-flavonoid.

The molecular docking was studied on a Pentium 4 platform using the Docking module and the Discover module of the InsightII software ( release 2005, Accelrys Ltd.) [176]. The crystallographic design of the light chain of the human plasmin 1DDJ [192] was obtained by the protein data bank [193]. The pattern of the complex plasmin-flavonoide has been optimized geometrically with the Discover module using a proper valence force field and an algorithm conjugated gradients to a derived RMS of 0.001. The intermolecular energy has been determined in the Evaluate section of the Docking module.

### **2.2.17 Spectrophotometric determinations of DHFR activity**

The activity of the DHFR has been determined at 25°C following the diminution of the absorbance of the NADPH and of the DHF at 340 nm by a spectrophotometric system Varian Cary 1E.

The experiments were conducted in buffer solution containing Na<sub>2</sub>(HPO<sub>4</sub>) 50 mM, EDTA 0.02 mM, pH 7 to 25°C. To prevent the oxidation of the catechins 1mM ascorbic acid has been added to the reaction mixture. The assay begins with the addition of enzyme (in absence of DHFR the diminution speed of of the absorbance is negligible).

### **2.2.18 Inhibition assay**

The inhibition from EGCG has been analysed by monitoring different the different rates of diminution of the absorbance of NADPH and DHF following the activation of the reaction by addition of DHFR, in presence of different concentrations of EGCG. The starting velocity of inhibition was determined at saturating and constants concentrations of NADPH ( 100 mM ) and varying the concentrations of DHF ( from 5 to 50 mM ) in the mixture of reaction and of inhibiting EGCG ( from 0 to 50 MM ) preincubated with the protein at 20°C for 15 minutes.

### **2.2.19 Purification of 20S proteasome from thymus and from bovine brain.**

The isolation and the purification of the complex 20S proteasome from thymus and from bovine brain has been performed in accordance with an experimental protocol developed by Eleuteri [194], based, essentially on a cut among the 40 and 60% of ammonium sulphate, a ion exchange chromatography and two molecular exclusion chromatography that favour the removal of contaminants with low molecular weight. A greater purification rate is obtained by adding a of hydrophobic interaction chromatography in order to separate the 20S proteasome from the co-eluting chaperonin Hsp90.

For the purification of the MPC from bovine modification have been used in order to eliminate the phospholipidic constituents in tissues.

### 2.2.20 Determination of the proteasomal activities.

The ChT activities-l, PGPH, t-l and BrAAP of the 20S proteasomal isolated have been determined spectrophotometrically as given previously 202, 203, using z-GGL-PNA, z-LLE-2NA, z-GGR-2NA and z-GPALG-PAB, respectively, as substrate, in accordance with the followings she/he/it/you conditions:

- 1) Cbz-Gly-Gly-Leu-PNA, concentration 0.4 MM in the assay, for the chimotripsin like activity;
- 2) Cbz-Leu-Leu-Glu-2NA, concentration 0.64 MM in the assay, for the peptidil glutamyl-idrolasic activity-;
- 3) Cbz-Leu-Leu-argon-2NA, concentration 0.4 MM in the assay, for the tripsin-like activity
- 4) Cbz-Gly-Pro-Ala-Leu-Gly-pAB, concentration 1 MM in the assay, for the BrAAP activity.

The mixture of reaction was constituted by 10 µg of enzymatic protein, the appropriate substrate for the activity that has to be measured ( dissolved in DMSO ) and TRIS-HCl buffer 0.05 M until a final volume of 250 ul.

The samples were incubated at 37 °C for 60 minutes and the reaction was stopped by addition of an equal volume of 10 % trichloroacetic acid . The released chromophore group was then , measured by diazotation. For such purpose 500 µl of a sodium nitrite 0.1 % solution were added in order to promote the formation of the diazonium salt. The sodium nitrite that didn't react were came destroyed by addition of an excess of ammonium sulphammate . The final reaction of copulation occurred between the salt of diazonium and N-1-naftiletilendiammine.

One unit of enzymatic activity was defined as the quantity of enzyme that catalyzed the release of 1 moles of chromophor group per hour. The specific activity is expressed in terms of unit for milligram of protein.

In the case of the BrAAP activity, in order to get the aromatic amine free in solution, it has to be added to the mixture of reaction an excess of Aminopeptidase N ( AP-n ). In fact, since the proteasome promotes the hydrolysis of the binding between the amino acid in P2 and the one in P3 of this substrate, the AP-N is necessary in order to release the p-A group-at the last aminoacid residue that is involved in the diazotation.

The chimotripsin-like activities ( ChT-L ), BrAAP and PGPH have been tested using the following synthetic fluorescent substrate: N-Succinil-Leu-Leu-Val-Tyr-7-amido-4-

metilcumarina( suc-LLVY-MCA ), Cbz-Gly-Pro-Ala-Leu-Gly-pAB ( Z-GPALG-PAB ) and Z-Leu-Leu-Glu-MCA ( Z-LLE-MCA )

The isolated proteasomes were incubated with the synthetic fluorescent substrate ( 5  $\mu$ M in this assay ) in the activity buffer ( TRIS-HCl 50 mM, pH 8.0 ): after 1h of incubation at 37°C, the measurement of the 7-amino-4-methyl-coumarine (AMC) and of the acid 4-aminobenzoic -(PABA)activity was measured through a Shimadzu fluorimeter RF-5301 ( AMC:  $\lambda_{ecc} = 380$  nm,  $\lambda_{em}=664$  nm; PABA:  $\lambda_{ecc} = 304$  nm,  $\lambda_{em}=664$  nm).

The specific activity using such substrates was calculated through a calibration curve obtained with solution of the two chromophore groups at increasing concentrations.

The activity of proteasomes 20S were tested in presence of increasing amounts of antioxidants: control assays were made on order to evaluate the interference of DMSO. Control experiments were also done in presence of specific inhibitors of proteasome: Z-GPFL-CHO e lactacistine (5  $\mu$ M).

### 2.2.21 Determination of IC<sub>50</sub>

The concentration of inhibitor that cause a 50% reduction of the enzymatic activity (IC<sub>50</sub>) was calculated from the equation:

$$IC_{50} = \frac{1}{1 + \frac{[I_0]}{a_r}}$$

where  $a_r$  represent the residual activity obtained at a certain concentration of antioxidant related to the control in absence of the polyphenolic compound;  $I_0$  is the concentration of the inhibitor. The IC<sub>50</sub> for the different polyphneolic compounds used in this present work, was calculated through statistical analysis software Matlab (ver. 6.5 release 13 by Mathworks Inc.) that allows to obtain the equation of function that best represents the ongoing of the residual activities obtained sperimentally, by means of increasing concentrations of antioxidants.

In the case of the presence of low concentrations of polyphenolic substances, able to induce a first phase of activation of the proteolytic component of the proteasome, followed by an inhibition step at increasing amounts of antioxidant, the value of IC<sub>50</sub> was obtained graphically taking in consideration only the inhibition phase.



### **2.2.22 Determination of the proteic concentration through Bradford method.**

The determination of the proteic concentration of the cellular lysates, was obtained through Bradford method [195]. This assay allows to determine through a spectrophotometer set at 595 nm the absorbance of the complex that proteins made with Biorad reagent (constituted by 100 mg/ml of Comassie Brilliant Blue G-250, ethanol and phosphoric acid). Since such absorbance is proportional to proteic concentration, in order to know the concentration of the samples, is necessary to make a calibration curve with known amounts of bovine serum albumine (BSA).

## 3 Experimental

The main object of our research was to find a valid source of polyphenols in order to be used for possible nutraceutical applications. Our main attention was put towards grape seeds. The Marche is an Italian region with an high tradition about wine and there are several sources of this important raw material.

We have identified during this research, a method in order to obtain the highest quantity of polyphenol with the most appropriate chemical pattern. This technology is subject of a patent realized by researchers of University of Camerino and gave rise to a spin-off called Biophenolix.

The grape seed extracts developed by this research has several important characteristics:

- the low catechin content
- high concentration of proanthocyanidines
- no degradation of active molecules during all the industrial process
- organic origin of the raw material and possibility of obtaining the organic certification for all the industrial process

This research was also financed by Italian Ministry of University and Research

### ***3.1 Characterization of Biophenolix grape seeds extract***

Biophenolix grape seed extract is a primary extract obtained by extraction with water:ethanol mixture (30:70). It can be used for several applications ranging from nutraceutical use to cosmetic and pet-food.

The extract is characterized by a at least 28% polyphenolic content with a catechin content of not more than 5%.

In table 2 is reported the comparative analysis for Biophenolix with other commercial available grape seed extract

	Biophenolix	Leucoselect	China
Gallic Acid	0,83	1,01	1,1
Epigallocatechin gallate	2,50	16,03	16,3
Catechin	1,37	12,01	12,1
Epicatechin	0,90	8,02	8,2
Total monomeric species	5,60	37,07	37,7
Purity	30,02	86,44	70,72
ORAC $\mu\text{eq Trolox/gr}$	2000,00	6700	4600
DPPH EC50 (mg/l)	84,04	24,01	24,28

Tab 2: Chemical caharacteritics of grape seed extracts

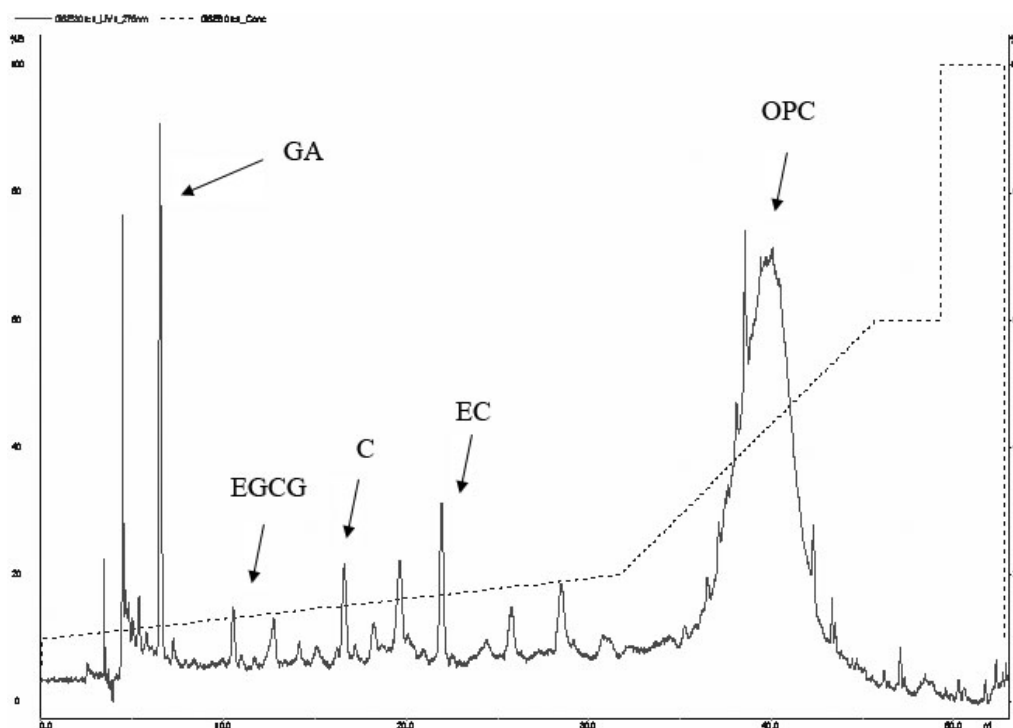


Fig. 20: RP-HPLC chromatogram of Biophenolix grape seed extract (GA: gallic acid; EGCG: epigallocatechin gallate; C: catechin; EC:epicatechin).

### 3.2 Purification of grape seed extract on polystyrenic resins

Since Biophenolix extract has a low purity, we have developed a process capable of being organic certified, in order to improve the extract purity. Due to organic regulations we can use only water and ethanol as solvents and we have limited possibilities for the utilization of production coadiuvants. Polystyrenic resins respond to organic regulations and are low-cost

and intensive use. We have tested different commercially available resins and developed a method on lab scale ready to be used on a pilot-scale production.

### **Extraction**

The chosen extraction solvent was ethanol at 50%. It was warmed at 55 °C; then the grape seeds were added. The ratio grape seeds/extraction solvent was 1/10. The experiment was conducted from 180 gr of grape seeds and 1800 ml of EtOH at 50%. The grape seeds were maintained in contact with the solvent for a period of 4 hours under magnetic stirring. Then the extraction was stopped and the seeds were removed by filtration. The seeds were washed with 100 ml of distilled water.

### **Concentration**

The extract obtained was concentrated by rotavapor under vacuum at 43 °C to remove ethanol. The final volume was 500 ml. Then ethanol (43,5 ml) was added to the water solution to reach a final concentration of 8%. Therefore we had 543,5 ml of a grape seed extract in ethanol at 8%. At this step we obtained, in respect with the seeds weight, yield of 8,02% for dry material, yield of 2,64% for polyphenols and a purity grade of 32,87%.

### **Centrifugation**

The ethanolic extract was centrifugated at 3000 rpm for a period of 15 minutes. The supernatant had a yield of 7,03% for dry material, yield of 2,55% for polyphenols, and a purity grade of 36,21%. The pellet contained the 9,5% of the dry material extracted and 2,54% of the total polyphenols extracted. The dry material and polyphenols loss was minimum at this step: the 87,68% of dry material and 96,63% of polyphenols remained in solution.

The three steps were summarized in the table 3; the percentages are referred to the dry material and polyphenols obtained from the extraction step:

		<b>Dry mat. (g)</b>	<b>Dry mat. (%)</b>	<b>Polyph. (g)</b>	<b>Polyph. (%)</b>
<b>Extraction</b>		14,4343		4,744	
<b>Centrifugation</b>	<b>Supernatant</b>	12,6567	87,68	4,5841	96,63
	<b>Pellet</b>	1,3751	9,53	0,1204	2,54

*Tab 3: pre-centrifugation step for chromatographic purification*

The yields of the primary extract in respect of the seeds weight were 8.02% for dry material and 2.64% for polyphenols. Otherwise the supernatant obtained from the centrifugation process had yield of 7,03% for dry material and of 2.55% for polyphenols.

## **Purification**

### **Loading on XAD 7-HP**

The XAD 7-HP (120 ml) was previously equilibrated with ethanol at 8%. The supernatant obtained from the centrifugation step was loaded on the resin. Then we wash the polymer with 13 column volume (CV) of ethanol at 8%. The total loading volume (LOAD 1) was 1880 ml (15,7 CV). At this step 59,12% of dry material and 9,67% of the total polyphenols loaded were eluted.

Then we made another loading step (LOAD 2) with 900 ml of ethanol at 8% (7,5 CV). The dry material eluted was 0,76% in absence of polyphenols.

### **Elution with ethanol at 45%**

The elution step was carried out directly with ethanol at 45%. We obtained 1800 ml (15 CV). During this phase 33,89% of dry material and 78,62% of polyphenols were recovered. The purity grade was 84.01%.

### **Elution with ethanol at 70%**

This was considered the resin regeneration step. During this step we obtained 790 ml (6,6 CV). In the course of this phase we eluted the remaining material: 6,23% of dry material and 11,71% of the polyphenols loaded. The purity grade was 68.07%.

The purification steps were summarize below, the percentage are refered to the dry material and polyphenols loaded on chromatographic column:

	<b>Elution volume (CV)</b>	<b>Dry mat. (g)</b>	<b>Dry mat. (%)</b>	<b>Polyph. (g)</b>	<b>Polyph. (%)</b>	<b>Purezza (%)</b>
<b>Load 1</b>	15,7	7,4826	59,12	0,4433	9,67	5,92
<b>Load 2</b>	7,5	0,0956	0,76	0	0,00	0,00
<b>EtOH 45%</b>	15	4,2895	33,89	3,6038	78,62	84,01
<b>EtOH 70%</b>	6,6	0,7889	6,23	0,537	11,71	68,07

*Tab 4: Purification steps on XAD-7HP*

The yields of the purified fraction in respect of the seeds weight were 2,38% for dry material and 2% for polyphenols.

The product obtained after purification on XAD-7HP resins with the suggested method has the following characteristics:

	<b>Biophenolix Purified</b>
Gallic Acid	0,15
Epigallocatechin gallate	3,25
Catechin	2,91
Epicatechin	2,50
Total monomeric species	8,80
Purity	82,60
ORAC $\mu$ eq Trolox/gr	6313
DPPH EC50 (mg/l)	23,54

Tab 5: chemical characterization of purified GSE by XAD-7HP

### ***3.3 Characterization of catechins in grape seeds during ripening***

Catechins are unwanted molecules in grape seed extracts; this is due for their low antioxidant activity, for their possible toxic effects and for being a marker of degradation of raw material. Catechins are the base unit of proanthocyanidines and are found both in skin and seeds. Our aim was to find if there is a correlation between ripening and catechin content, in order to find the best ratio between catechin content and total polyphenolic content.

We have studied the ripening of three vintages, from 2003 to 2005, by collecting grape from the same plant of *Vitis Vinifera* variety Sangiovese from a organic producer in the surroundings of Offida (Italy). Seeds were manually separated and dried at 45°C for 72 hours. The seeds were then extracted with a water:ethanol (30:70) mixture.

For seasons 2003 and 2004 a Soxhlet extraction was used while for 2005 accelerated solvent extraction was used. For 2005 vintage we have also verified the antioxidant activity using DPPH assay. Total polyphenolic content was determined with Folin-Ciocalteu assay and single catechins content through RP-HPLC assay.

In literature (...) is reported that during ripening there is a rising in polyphenolic content, until grape reaches maturation. After maturation is reached, there polyphenols decrease while sugars rise their concentration. Grapes are collected depending on their application: for grape juice is preferred to collect grapes just maturation is reached while for wine production it is preferable to wait 10-15 days. Catechins are also responsible of sensorial properties and the determination of these molecules are important in wine production.

Date	TPC (%)	GA (%)	C (%)	EC (%)	TM (%)
21/08/03	26,67	1,99E-01	1,26E+00	4,70	6,16
29/08/03	11,79	9,70E-02	3,84E-01	2,11	2,59
03/09/03	19,36	1,43E-01	7,46E-01	3,36	4,25
10/09/03	10,33	8,52E-02	3,19E-01	1,56	1,97
18/09/03	12,16	7,74E-02	2,69E-01	1,60	1,95
25/09/03	8,93	9,94E-02	3,49E-01	1,50	1,95

Tab 6: Evolution of catechins during 2003 vintage. TPC: total polyphenolic content; GA: gallic acid; C: catechin; EC: epicatechin; TM:total monomeric content.

Date	TPC (%)	GA (%)	C (%)	EC (%)	TM (%)
24-08-2004	5,89	5,92E-02	6,90E-01	1,930308	2,679183
09-09-2004	3,19	5,08E-02	3,47E-01	1,271279	1,668657
23-09-2004	2,65	2,31E-02	2,23E-01	0,604663	0,850888
30-09-2004	1,76	1,57E-02	8,50E-02	0,334728	0,435356
07-10-2004	2,62	2,26E-03	7,29E-02	0,185819	0,261004
14-10-2004	1,68	8,41E-03	5,83E-02	0,157347	0,224032

Tab 7: Evolution of catechins during 2004 vintage. TPC: total polyphenolic content; GA: gallic acid; C: catechin; EC: epicatechin; TM:total monomeric content.

ate	TPC (%)	GA (%)	C (%)	EC (%)	EGCG (%)	TM (%)
19/08/06	9,17	0,31	1,72	1,86	0,12	4,02
25/08/06	10,19	0,35	1,54	2,43	0,07	4,39
02/09/06	8,71	0,38	1,65	2,12	0,23	4,39
13/09/06	7,73	0,28	1,16	1,33	0,52	3,30
19/09/06	7,78	0,39	0,86	0,92	0,57	2,73
24/09/06	7,22	0,29	0,65	0,67	0,46	2,07
03/10/06	7,02	0,46	0,79	0,71	0,50	2,46

Tab 8: Evolution of catechins during 2005 vintage. TPC: total polyphenolic content; GA: gallic acid; C: catechin; EC: epicatechin; EGCG:epigallocatechin gallate; TM:total monomeric content

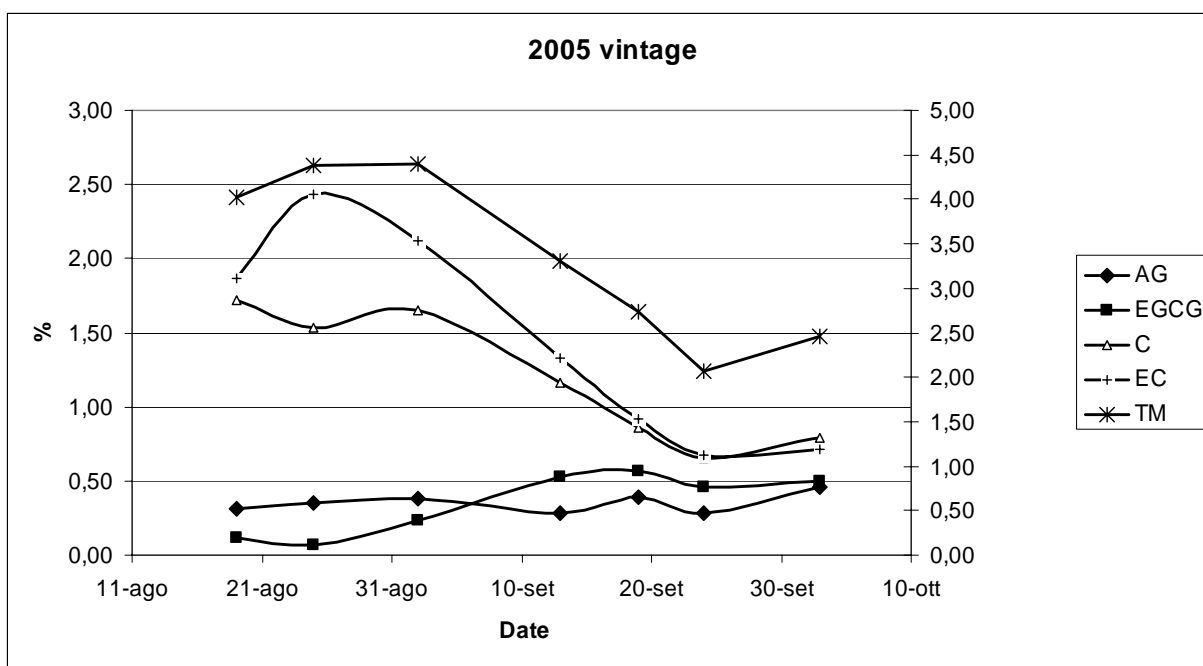


Fig. 21: Evolution of flavonoids during ripening ( AG: gallic acid, EGCG: epigallocatechingallate, C:catechin, EC:epicatechin, TM: total monomeric flavonoids)

As is possible to observe from tables 6, 7 and 8, absolute values are highly influenced by seasonability. Anyway catechin ( C, EC) pattern follows always after reaching a maturation as second order kinetic. The ratio between total polyphenols and total monomers remains almost the same, indicating that there isn't a correlation between low monomeric content and period of collection of grapes. This parameter is mainly influenced by other factors, like for example grape variety, soil and climate conditions. The main parameter influenced during ripening is total polyphenolic content; for this reason in order to achieve the best yield and ratio of polyphenols is better to collect grape for grape seeds extract production at the very early stage of maturation. For this reason it is also preferable to use seeds used for grape juice production and not those used for wine production.

For 2005 vintage we have also evaluated the antioxidant activity and the results are presented in table 9 and figure 8:



Date	EC <sub>50</sub>	Eq. Trolox Norm	AE (1/EC <sub>50</sub> )
19-ago	0,433821	0,02044	2,305098
25-ago	0,391501	0,02229	2,554269
02-set	0,388062	0,02097	2,576908
13-set	0,513964	0,02028	1,945662
19-set	0,488035	0,02028	2,049034
24-set	0,608904	0,01944	1,642296
03-ott	0,429916	0,02433	2,326033

Tab 9: Evolution of antioxidant activity during ripening

The antioxidant activity is normalized with the percentage of polyphenols of each extract in order to normalize the values obtained, since the activity depends from the polyphenolic content; with this normalized value it's possible to evaluate the strength of antioxidant activity independently from its polyphenolic content. It's evident that antioxidant activity is strictly correlated with the total polyphenolic content. Since there is no variation in the ratio between catechins and proanthocyanidines during ripening the antioxidant activity follows the same pattern of the polyphenolic content.

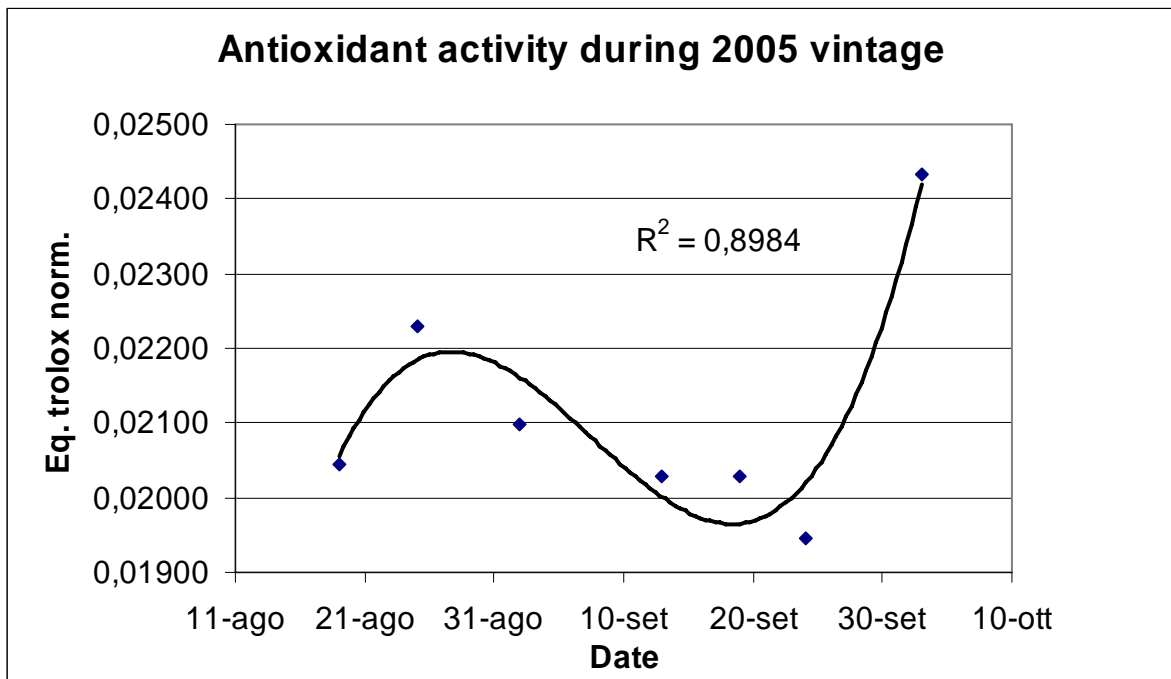


Fig. 22: Evolution of antioxidant activity during ripening

### 3.4 Determination of peroxidation inhibition activity in lipidic matrix.

The ability of the GSE to inhibit the lipidic peroxidation was determined in olive oil.

Quantities of 100 and 500 ppm of GSE were added to 100 ml of olive oil and comparisons were made with a mixture of 50 ppm of BHT and 50 ppm BHA. Olive oil was maintained in dark at 45°C and peroxides were determined by titration.

The results are indicated in table 10 and fig 9.

Days	0	3	6	10	14	17	20	27	35	44	49
Olive Oil	1,81	5,75	5,41	2,76	4,77	3,34	6,75	27,33	69,11	134,86	176,57
GSE 100	1,81	1,68	3,27	2,71	3,48	3,22	5,88	17,60	51,66	110,03	146,77
GSE 500	1,81	1,59	4,79	2,85	3,55	3,87	4,73	24,39	64,16	128,46	168,44
BHT+BHA	1,81	2,81	3,20	2,64	4,16	4,05	5,75	11,81	21,12	39,05	51,90

Tab 10 : number of peroxides determined in olive oil with and without addition of antioxidants

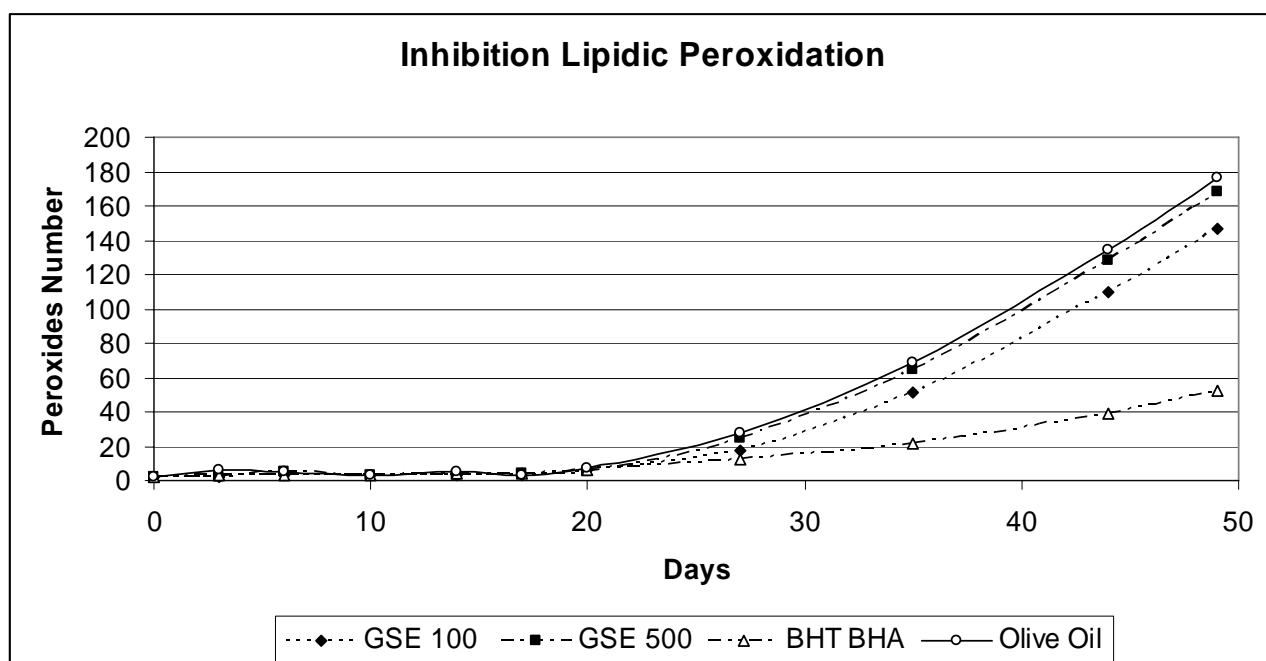


Fig. 23: Number of of peroxides determined in olive oil with and without addition of antioxidants

### 3.5 Characterization of possible alternative sources of polyphenols

Grape seed is not the only source of natural polyphenols. Since they are found in almost all vegetables we have tried to identify, based also on natural availability of possible alternative sources.

#### 3.5.1 Pomegranate

Pomegranate is a fruit widely present in Europe and in Asia, especially in areas with Ripened pomegranate (*Punica Granatum L. Var. Sativa K. Maly*) of variety Ferdoes (A) and Feyzabadwere (B) were obtained from an Iranian producer. All fruit components have been manually separated obtaining. Seed pomace has been manually pressed to separate the liquid part, called juice. The drying process has been obtained by drying at 40°C for 48 hours. All the components (5 g for each fruit component and variety) were then extracted in a Soxhlet system with 100 ml of EtOH 70% for 4 hours. The extracts were then concentrated under vacuum (Buchi, Switzerland) to evaporate the EtOH and finally lyophilized to remove water. The obtained product was used for RP-HPLC and total polyphenolic content determination and enzyme inhibition studies.

The polyphenolic content is contained in the table 11:

	Total Polyphenolic content (%)	Ellagic Acid(%)	Catechin (%)	Epicatechin (%)
<b>Peel A</b>	12,96	0,10	15,36	1,28
<b>Skin A</b>	9,22	0,05	6,28	0,81
<b>Peel B</b>	17,34	0,02	8,54	0,21
<b>Skin B</b>	19,71	0,05	2,80	0,51
<b>Seeds A</b>	1,64	0,00	N.D.	N.D.
<b>Seeds B</b>	0,55	0,00	N.D.	N.D.
<b>Seeds A*</b>	1,19	0,00	N.D.	N.D.
<b>Seeds B*</b>	0,55	0,00	N.D.	N.D.
<b>Juice A</b>	N.D.	0,00	N.D.	N.D.
<b>Juice B</b>	N.D.	0,00	0,06	N.D.

Tab 11 : Determination of monomeric polyphenols in pomegranate Ferdoes (A) and Feyzabadwere (B)

variety components

The typical chromatogram for each fruit component is shown in following chromatogram. Analysis of the chromatograms shows that the main constituents of the extracts are

monomeric flavonoids like catechin, epicatechin and ellagic acid. Ellagic acid is the most present in all the constituents even if at not very high concentrations.

The main flavonoid present in pomegranate is catechin which is present in peel and skin at high concentrations.

Ellagic acid is present in all the components but at concentration under 0.1%.

The species B is the richest of flavonoids at a concentration more than 4% in both skin and peel.

All the extracts have a very low concentration of polymeric flavonoids, while they are rich in monomeric ones.

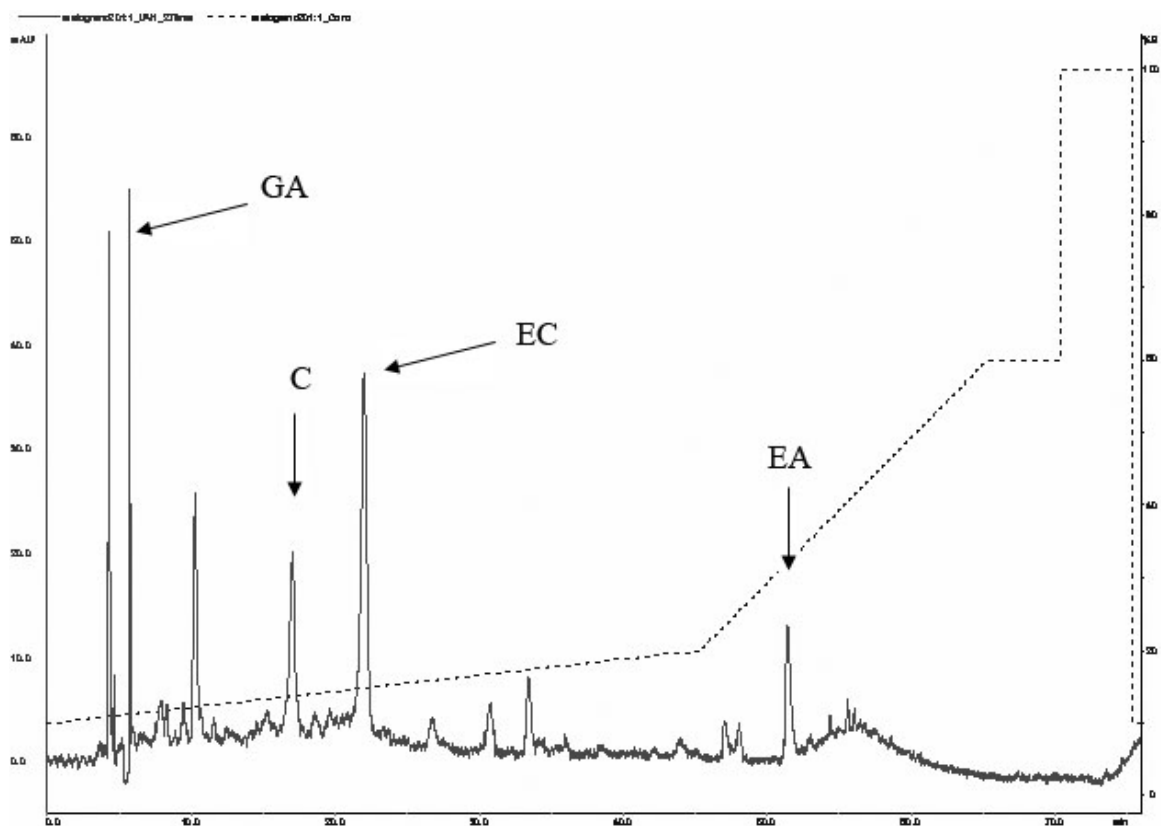


Fig. 24: RP-HPLC chromatogram of typical pomegranate extract (GA: gallic acid; EA: ellagic acid; C: catechin; EC:epicatechin).

### 3.5.2 Prunus Spinosa

*Prunus Spinosa* is a spontaneous plant that grows in Mediterranean zone. It's characterized by elevated astringency and bitter taste, that indicates the presence of polyphenols.

Samples of prunus spinosa were collected in the Sibillini Mountains Natural Park and the fruit components were manually separated. Then samples were dried at 45°C for 72 hours and

the extraction of polyphenols was carried by Soxhlet extraction with mixture of water:ethanol (30:70) for 4 hours. The extracts were then concentrated under vacuum (Buchi,Switzerland) to evaporate the EtOH and finally lyophilized to remove water. The obtained product was used for RP-HPLC and total polyphenolic content determination

The polyphenolic and catechin content of the fruit components were investigated and the results are presented in the table 12 and figure 11.

	Total Polyphenolic Content (%)	Gallic Acid (%)	Catechin (%)	Epicatechin (%)
<b>Fruit</b>	0,796	0,037	5,664	0,472
<b>Pulp</b>	0,504	0,014	1,820	0,235
<b>Skin</b>	1,670	0,008	3,347	0,083
<b>Seed</b>	0,564	0,013	0,778	0,143

Tab 12 : determination of monomeric polyphenols in *Prunus Spinosa* components

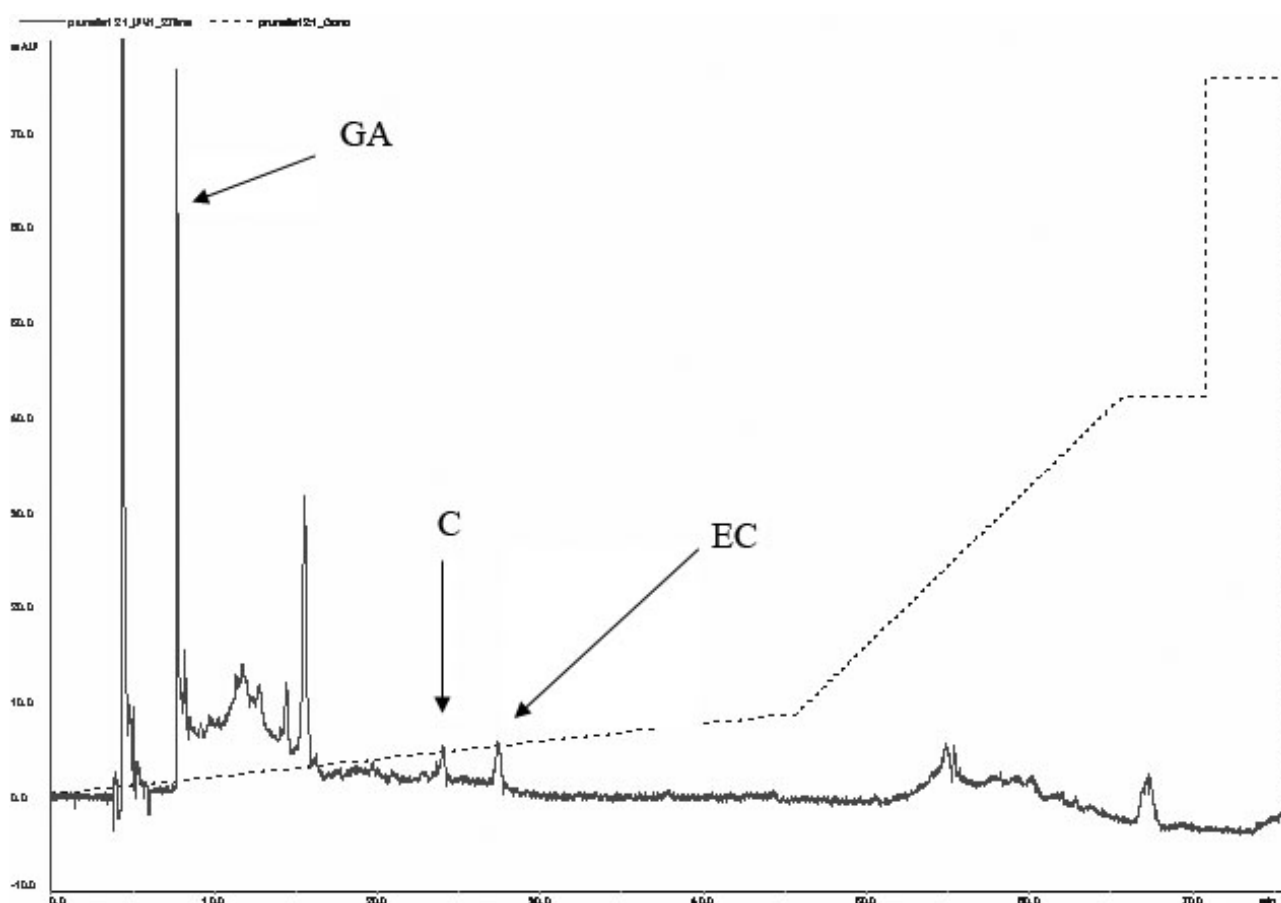


Fig. 25: RP-HPLC chromatogram of typical *prunus spinosa* extract (GA: gallic acid;; C: catechin; EC:epicatechin).

### 3.5.3 Rosemary

Rosemary (*Rosmarinus officinalis*) is a widely distributed plant of the Mediterranean region. It's used as spice in Mediterranean diet and it's known for its utilization as natural antioxidant. In the immediate future, rosemary will be recognized as natural antioxidant by EU food authority and it will be used in meat applications in order to prevent oxidation phenomenon. In this study we will consider the differences between spontaneous and cultivated rosemary, in order to evaluate possible differences and future applications.

Rosemary samples were hand collected by a local Sardinian producer and dried at 45°C for 72 hours.

A sample of cultivated rosemary was also used to find the best extraction conditions with ASE in order to propose also a possible scale-up for industrial applications.

5 g of rosemary were extracted with different mixtures of water:ethanol at different cycles and temperature in order to find the best extraction capabilities. The extracts were then concentrated under vacuum (Buchi, Switzerland) to evaporate the EtOH and finally lyophilized to remove water. The obtained product was used for RP-HPLC in order to determine and total polyphenolic content determination

The results are presented in the following tables and graphs:

After having defined the optimal extraction parameters, we have extracted the samples with ASE. The results are presented in the following tables:

% EtOH	Dry Yield(%)	Polyphenols Yield (%)	Purity (%)
80	37,7	6,13	16,260
50	52,36	9,1	17,380
40	48,86	8,7	17,806
20	39,9	8,03	20,125
0	36,7	6,4	17,439

Tab 13 : influence of EtOH concentration on ASE extraction

°C	Dry Yield(%)	Polyphenols Yield (%)	Purity (%)
100	33,75	6,08	18,01
150	45,36	8,14	17,95
200	64,1	13,3	20,75

Tab 14 : influence of temperature on ASE extraction with EtOH 50%

Cycles n°	Dry Yield(%)	Polyphenols Yield (%)	Purity (%)
1	61,7	14,56	23,60
2	64,3	13,26	20,62
3	64,1	13,3	20,75

Tab 15 : influence of number of cycles on ASE extraction with EtOH 50% and 200 °C

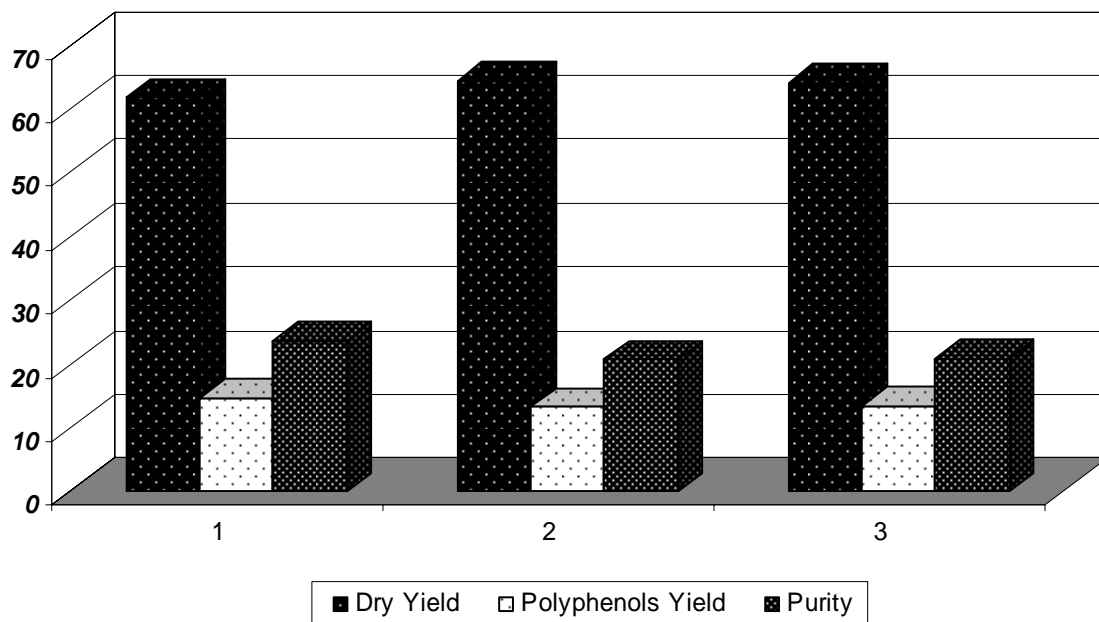


Fig. 26: influence of number of cycles on ASE extraction

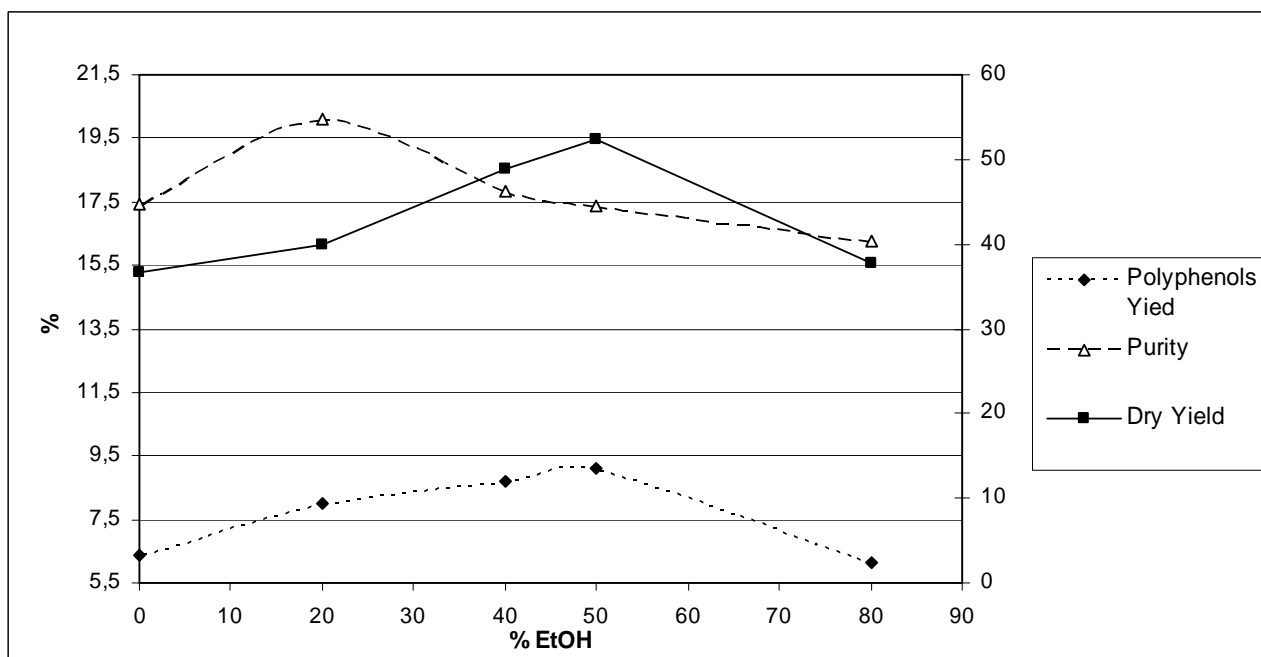


Fig. 27: influence of ethanol concentration on ASE extraction

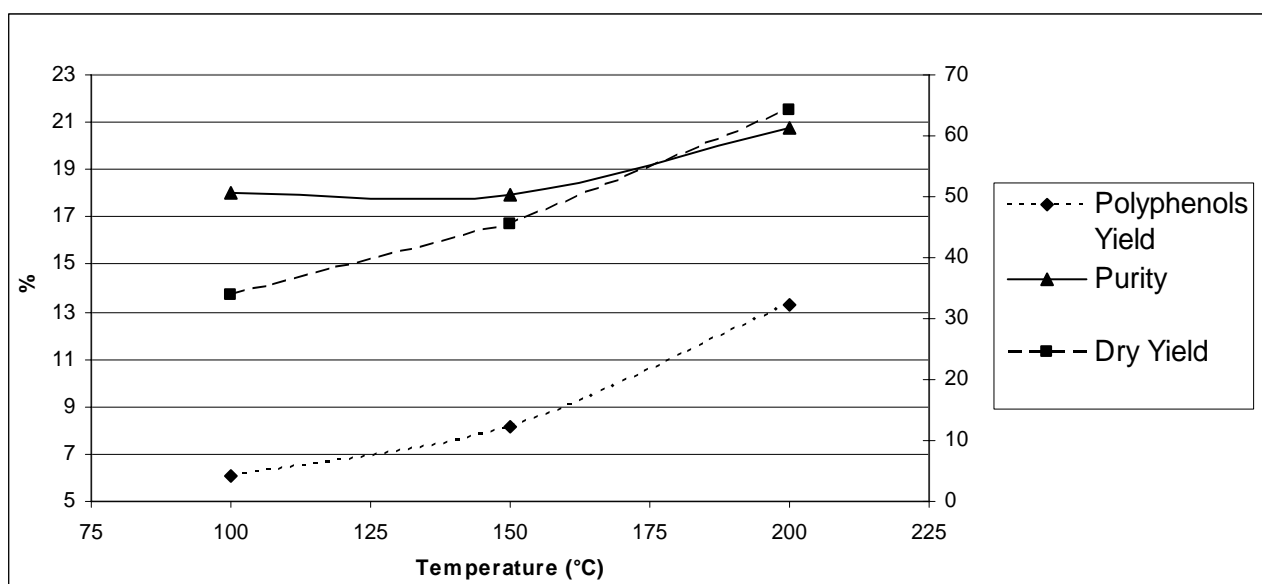


Fig. 28: influence of temperature on ASE extraction

As is possible to observe the best water:ethanol mixture is a 50:50 ratio; even if the purity is not the highest available, it will be able to extract the maximum amount of polyphenols present in the rosemary. It would be best also to use the highest possible temperature in order to maximise polyphenols extraction. This is not a limitation since ASE operates in sub-critical conditions for the solvent using 1500 psi pressure, while in industrial applications the possibility of pressurize the extraction ambient is limited, and very economically non convenient. The number of cycles is not influencing the extraction conditions, since one cycle at 200 °C with water:ethanol 50:50 is capable of extracting most of the polyphenols contained in rosemary. The extracts were then concentrated under vacuum (Buchi,Switzerland) to evaporate the EtOH and finally lyophilized to remove water. The obtained product was used for RP-HPLC in order to determine and total polyphenolic content determination

After having defined the optimal extraction parameters, we have extracted the samples with ASE. The results are presented in the following table where the rosmarinic and carnosic acid are expressed as percentage of the extract obtained:

	Dry Yield (%)	Polyphenols Yield (%)	Purity (%)	Rosmarinic acid (%)	Carnosic acid (%)
<b>Leaves cultivated</b>	64,75	10,99	16,97	2,34	10,30
<b>Leaves Spontaneous</b>	61,06	11,07	18,12	2,45	9,23
<b>Stems cultivated</b>	30,23	5,20	17,19	1,96	1,66
<b>Stems Spontaneous</b>	32,60	4,48	13,75	2,29	0,89

Tab 16 : determination of polyphenols on rosemary extracts



Antioxidant activity by DPPH assay was also determined and result are presented in table 17:

	<b>EC<sub>50</sub></b>	<b>Equ. Trolox norm</b>	<b>AE (1/EC<sub>50</sub>)</b>
<b>Leaves cultivated</b>	0,635426499	0,00825	1,573746
<b>Leaves Spontaneuous</b>	0,992364988	0,00816	1,007694
<b>Stems cultivated</b>	1,166401187	0,01287	0,857338
<b>Stems Spontaneous</b>	1,148355121	0,01291	0,870811

*Tab 17 : determination of antioxidant values (DPPH assay) on rosemary extracts*

In order to verify the results obtained with ASE and to propose an industrial method for extraction of the raw material, the data obtained was used to design a 50 g scale extract production.

Cultivated rosemary (leaves and stems) was dried at 45°C for 48 hours, then the dried material was milled.. The chosen extraction solvent was ethanol at 50%. The solvent was warmed at 55 °C; then dried rosemary was added. The ratio rosemary/extraction solvent was 1/10. The experiment was conducted from 50 gr of dried rosemary and 500 ml of EtOH at 50%. The rosemary was maintained in contact with the solvent for a period of 4 hours and 30 minutes under magnetic stirring. Then the extraction was stopped and solid residues were removed by filtration. The solids were washed with 100 ml of distilled water. The extract obtained was concentrated at rotavapor and analyzed by Folin-Ciocalteu assay.

The yields obtained in respect with the dried rosemary weight were:

Purity (%)	25
Dry Yield (%)	17,8
Polyphenols Yield (%)	4,5

*Tab 18 : yield of cultivated rosemary extract*

The data obtained shows that is not possible to reach values obtained by ASE; anyway the results obtained on the proposed process are comparable with other vegetal extracts already present in the market

## 3.6 Interaction Polyphenols-Thrombin

### 3.6.1 Spectrophotometric tests.

The increasing flavonoid addition to a fixed amount of thrombin has produced a range of isothermal inhibition hyperbolic curves, showing an increasing slope proportional to the decrease of the substrate concentration (Fig. 17). These inhibition data have been analysed by a mathematical model 1:1 for a reversible competitive inhibition binding with the enzyme [173].

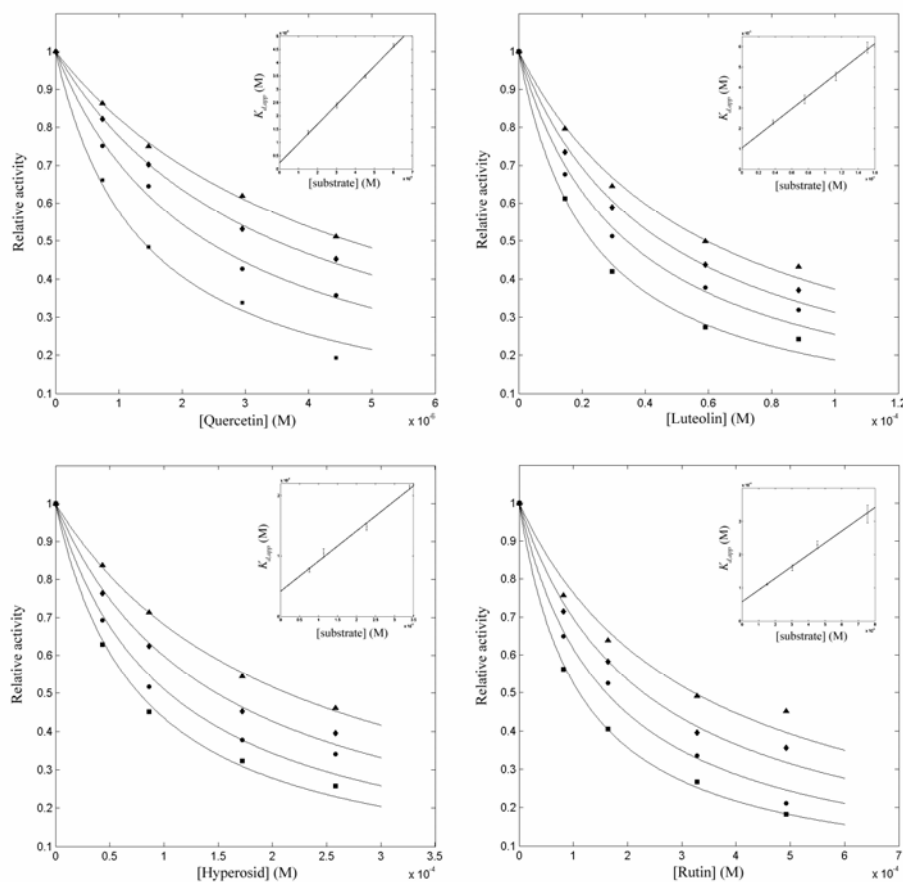


Fig. 29: Inhibitory effect of some flavonoid on the amilolytic activity of thrombin: the relative activity has been measured at four different substrate concentrations.

The substrate dependent thrombin-ligand dissociation constant,  $K_{iapp}$ , has been obtained for each single studied flavonoid.  $K_{iapp}$  is directly related to the substrate concentration, as shown in the figure 17 (box) [173]. From the analysis of these values with the  $K_{iapp} = K_i \cdot \left( 1 + \frac{[S^0]}{K_m} \right)$

it is possible to calculate the  $K_i^*$  (tab. 20) and the  $K_m$ . The experimental  $K_m$  value, measured with this procedure, is  $7,2 \pm 0,6 \mu\text{M}$ , in agreement with previously published data [196].

### 3.6.2 SPR analysis

The thrombin immobilization on the carboxylate layer has required 900 arc seconds (surface density  $1.7 \text{ ng/mm}^2$ , equivalent to  $7 \text{ mg/ml}$  concentration). This result can be also qualitatively obtained from the information derived from the molecular weight of the ligand able to saturate the surface in a monomolecular Langmuir surface.

The flavonoid-thrombin binding has been studied adding specific increasing concentrations of flavonoid in phosphate buffer and testing the association kinetics within one minute intervals. The dissociation has been obtained by removal of the flavonoid with buffer addition until the baseline attainment. As shown in the figures 19-22, monophasic association and dissociation kinetics have been obtained. According to the procedures described in Materials and Methods, it has been possible to calculate the  $k_{ass}$ ,  $k_{diss}$  e  $K_i$  constants for each tested flavonoid (tab. 20), with Luteolin exception, because of the lack of detectable specific interaction.

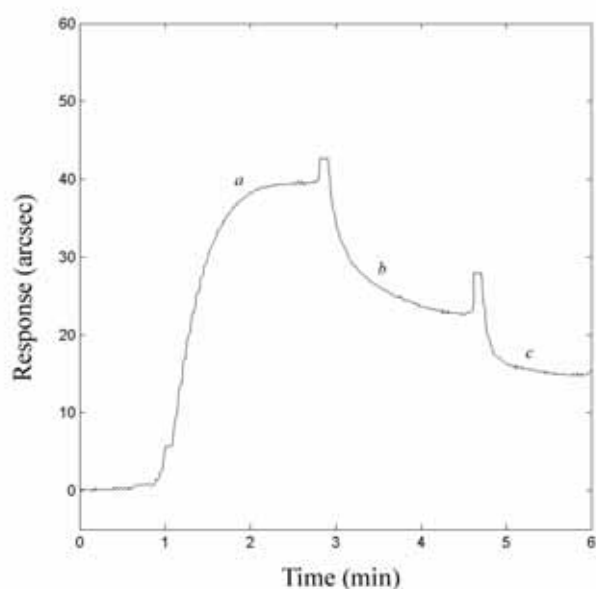


Fig. 30: Binding plot: association (a), dissociation (b) and partial regeneration (c)

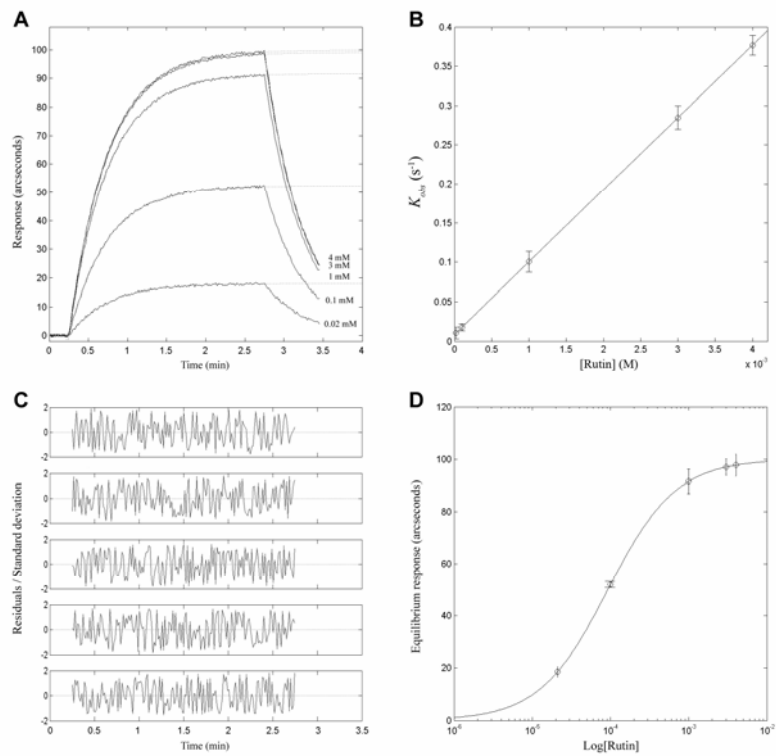


Fig. 31: Association plots at different rutin concentrations

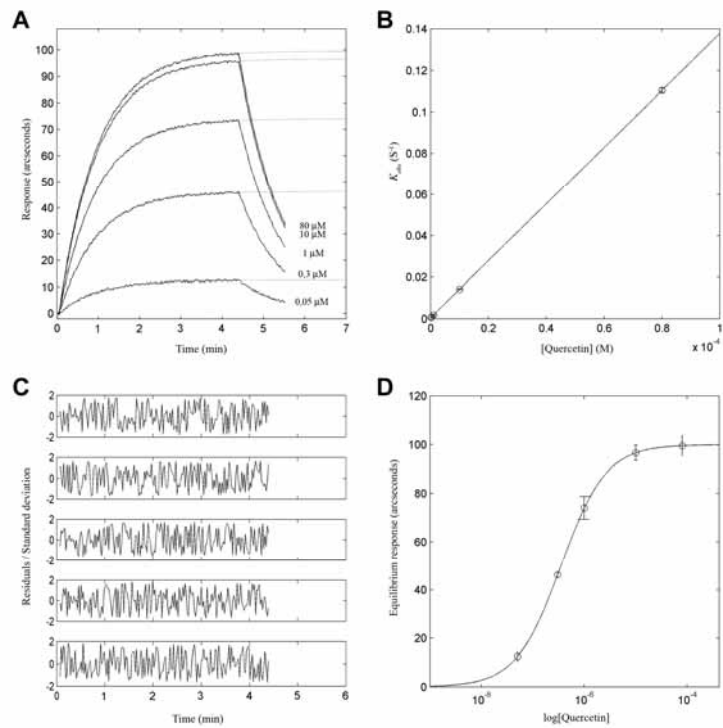


Fig. 32: Association plots at different quercetin concentrations.

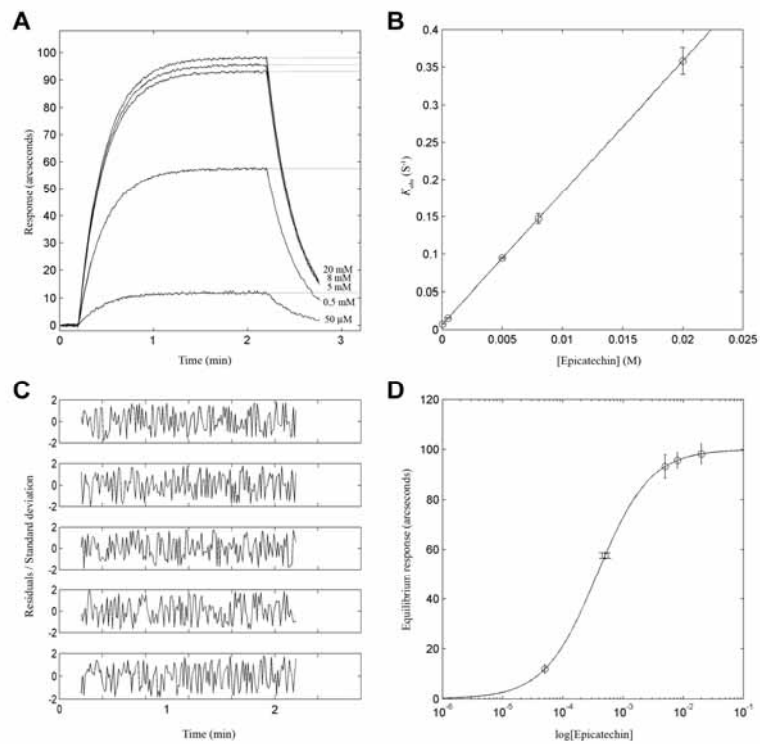


Fig. 33: Association plots at different epicatechin concentrations.

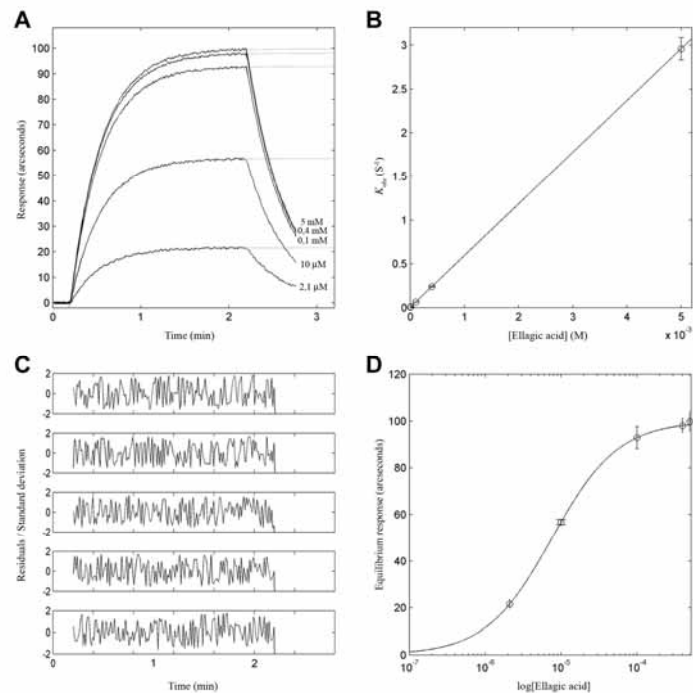


Fig. 34: Association plots at different ellagic acid concentrations.

The inhibition constants calculated with the spectrophotometric test in solution ( $K_i^*$ ) were in agreement with those calculated by the interactions on the probe surface. Such data have suggested an intermediate affinity binding of the flavonoids with the trombin. Among the

others quercetin shows the lowest inhibition constant ( $K_i=0.35 \pm 0.04 \mu\text{M}$ ,  $K_{i^*}=0.23 \pm 0.07 \mu\text{M}$ ). This value is similar to that one of argatroban, the powerful synthetic inhibitor ( $K_i=0,019 \mu\text{M}$ ) [197]. The polyphenols having a planar structure, similar to quercetin (rutin, hyperoside and luteolin), show a different affinity for the human thrombin.

This difference could be partially induced by the steric hindrance of the bulky groups of rutin and iperoside, partially for the impossibility for the luteolin to produce a hydrogen bond between the O-3, absent in this flavonoid, and the His57 of the thrombin catalytic site. This point can partially explain the lack of any detectable specific interaction with the trombin immobilised on the probe surface. The tested antocyaninidins, in particular the epicatechin ( $K_i=396 \pm 128 \mu\text{M}$ ,  $K_{i^*}=320 \pm 14 \mu\text{M}$ ), form less stable complexes with the human thrombin, while the ellagic acid shows a quite strong inhibitory activity ( $K_i=7.6 \pm 0.5 \mu\text{M}$ ,  $K_{i^*}=1.4 \pm 0.5 \mu\text{M}$ ).

The determination of the association ( $k_{ass}$ ) and dissociation ( $k_{diss}$ ) constants of the thrombin-flavonoid binding further defines the mechanistic properties of the process. Among the tested flavonoids, the trombin-quercetin bond is the kinetically favoured one ( $k_{ass}=1374 \pm 32 \text{ M}^{-1}\text{s}^{-1}$ ), while epicatechin shows the less fast kinetic ( $k_{ass}=17.6 \pm 5.7 \text{ M}^{-1}\text{s}^{-1}$ ). With regard to the dissociation kinetic, all the tested flavonoids, with the exception of quercetin, present  $k_{diss}$  values in a narrow range ( $3.4 \pm 0.3 < k_{diss} < 8.5 \pm 0.5 \text{ ms}^{-1}$ ). We can deduce that the heterogeneity of the inhibition constants is almost due to the association constant contribution.

### 3.6.3 Coagulation studies

The quercetin effect on the coagulation time has been evaluated with TT tests on human plasma. Quercetin ha produced a TT increase showing an anti-clotting effect at submillimolar concentrations (Fig.23). The minimal concentration necessary for the detection of a quercetin anti-clotting effect has been higher than expected, if related to the dissociation constant of the quercetin-thrombin complex ( $K_d= 0.35 \mu\text{M}$ ), also because of its binding with other plasma proteins [172, 174, 175]. In any case the quercetin concentration range used in our work has been always lower than the toxicity levels of this class of compounds [198-200].

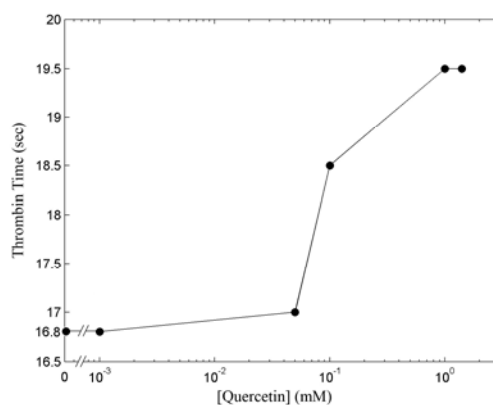


Fig. 35: Quercetin anti-clotting activity: effect of increasing quercetin concentrations on plasmatic TT

### 3.6.4 Extracts effect on thrombin

As a consequence of the observed thrombin inhibition shown by different polyphenolic molecules, we have tested the action of the Biophenolix grape seed extract and of other extracts. In figure 24 it is shown the plot of the residual thrombin activity vs. the grape seed extract concentration, expressed as  $\mu\text{g}$  of gallic acid equivalents per ml of the reaction mixture.

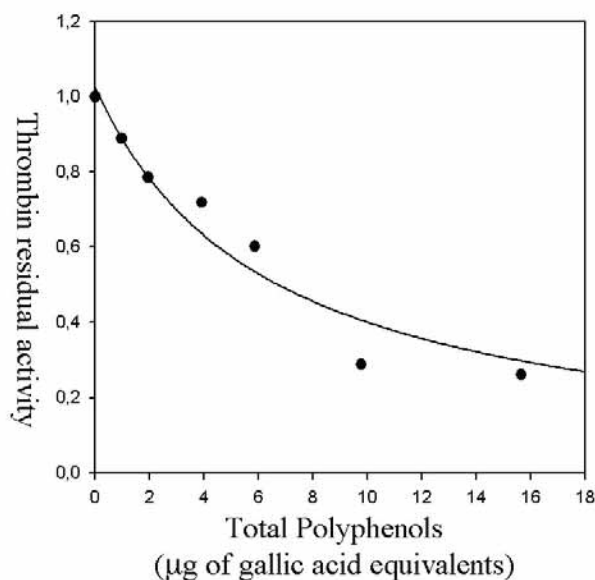


Fig. 36: Residual thrombin activity vs. increasing concentrations of grape seed extract

Such behaviour can be directly related to the monomers detected on the extract, as deduced from the respective inhibition constants, although the extract is particularly rich in polymeric species.

The activity of other vegetal extracts have been tested and the result are shown in table 19.

	Extract	Flavonoid Conc.	Ki app (ug/ml)
	Grape Seed	30%	6,89 ± 1,27
	Green Tea	80%	11,94 ± 1,68
Prunus Spinosa	Seed	0,80%	340,50 ± 52,96
	Skin	1,67%	450,30 ± 70,46
Pomegranate	Peel A	12,95%	2,09 ± 0,24
	Skin A	9,22%	1,93 ± 0,24
	Peel B	17,33%	2,65 ± 0,33
	Skin B	19,71%	2,670 ± 0,3579

Tab 19: Inhibition data of different extracts on thrombin

### 3.6.5 Molecular docking

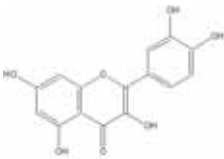
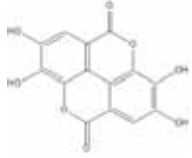
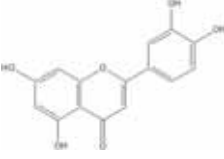
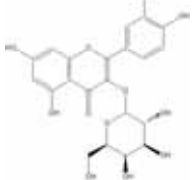
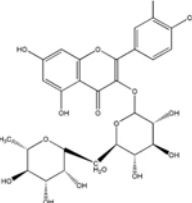
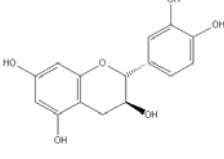
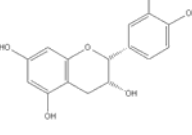
Like the results of the inhibition constants, also the docking test has confirmed the trombin-quercetin complex is the most stable complex. The model parameters of the complex are the followings:

- ✓ Total free energy = -9.06 kcal/mole;
- ✓ Trombin free energy = -20.33 kcal/mole;
- ✓ Van der Waals free energy= -14.38 kcal/mole;

As previously assumed, the model shows the presence of a 2,6 Å critical hydrogen bonding between the His57 of the thrombin catalytic site the O-3 of the flavonoids (Fig. 25) in addition to the insertion of these molecules in the narrow catalytic hydrophilic sac of this catalytic site (His57, Lys60f, Glu192 e Ser195). The Trp60d, the only non polar residue exposed in the catalytic sac, could also play a stabilising role through a hydrophobic effect.

The crystallographic data of the argatromban-thrombin complex shows a ligand orientation different from the quercetin-thrombin model (Fig. 26). In effect, the argatromban molecule interact with the thrombin catalytic sac trough an hydrophobic packing between the quinolic group and the thrombin P-pocket (Tyr60a, Trp60d e His57) [201].



Name	Molecular structure	$Ki^*$ ( $\mu\text{M}$ )	$Ki$ ( $\mu\text{M}$ )	$k_{ass}$ ( $\text{M}^{-1}\text{s}^{-1}$ ) e $k_{diss}$ ( $\text{ms}^{-1}$ )
Quercetin		$0,23 \pm 0,07$	$0,35 \pm 0,04$	$1374 \pm 32$ $0,48 \pm 0,05$
Ellagic Acid		$1,4 \pm 0,5$	$7,6 \pm 0,5$	$591 \pm 4$ $4,5 \pm 0,3$
Luteolin		$10,5 \pm 0,1$	/	/
Hyperoside		$41,9 \pm 0,7$	$38,3 \pm 3,8$	$87,9 \pm 3,7$ $3,4 \pm 0,3$
Rutin		$58,4 \pm 0,9$	$92,3 \pm 6,8$	$92,1 \pm 3,2$ $8,5 \pm 0,5$
Catechin		$260 \pm 12$	$209 \pm 31$	$34,5 \pm 3$ $7,2 \pm 0,9$
Epicatechin		$320 \pm 14$	$369 \pm 128$	$17,6 \pm 5,7$ $6,5 \pm 0,8$

Tab 20: -  $Ki$ ,  $k_{ass}$  e  $k_{diss}$  values obtained from the optical bioprobe; the  $Ki^*$  values have been obtained from the spectrophotometric test..

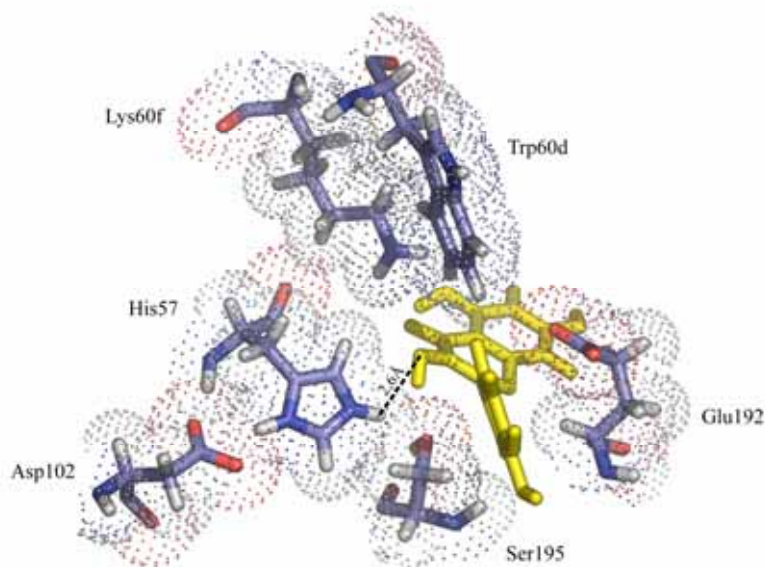


Fig. 37 :Three-dimensional docking of the thrombin-quercetin complex: the His57-quercetin hydrogen bonding, the catalytic triad and the residues in close contact with the flavonoids are shown

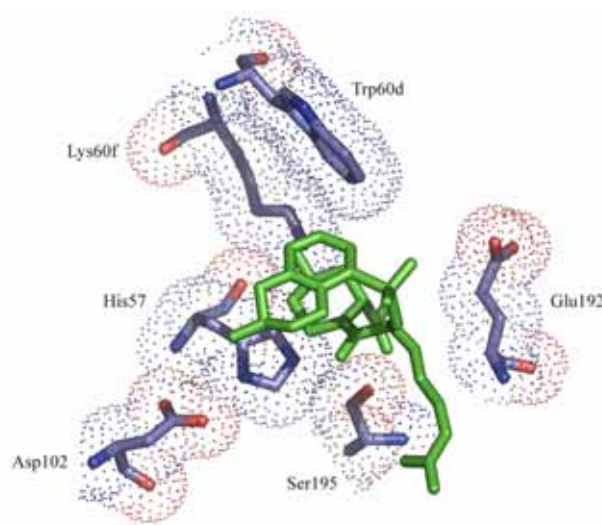


Fig. 38: The crystallographic structure shows the argotraban-thrombin binding (pdb-ID: 1DWC) [202].

### 3.6.6 QSAR analysis

We do not have examined a high number of flavonoids; nevertheless the results of this analysis have been statistically significant because their inhibitory activity range cover a three

order size. The application of the QSAR-Contingency<sup>TM</sup> analysis shows that only the *Torsion energy*, *Molecular flexibility*, *Van der Waals acceptor surface area* e *Molecular globularity* descriptors have been accepted for the QSAR analysis, among the six previously selected, because their *contingency C coefficients* were > 0.6 and their *Cramer V coefficients* were >0.2 [177]. Furthermore these descriptors resulted linearly independent for the set of the examined flavonoids. The results of the QSAR-Model<sup>TM</sup> are shown in the Tab. 3.2, the value of the constant *Const* = 6.49.

Descriptors	Estimated linear model ( $C_j$ )	Relative importance
Molecular Flexibility	-1,31	1,00
Torsion Energy	+0,31	0,85
VdW Acceptor Surface Area	+0,05	0,21
Molecular Globularity	-0,69	0,03

Tab 21: Results of the QSAR-Model<sup>TM</sup>.

The QSAR analysis suggests that thrombin makes stable complexes molecules having an high torsion energy, low flexibility, large WdW surface accepting hydrogen bonds, low globularity value. But, as shown in the table 21, not all these descriptors have the same importance. The torsion energy and the molecular flexibility are the most important descriptors and can determine the choice of the best thrombin inhibitor. The inhibitor must have an enough rigid and planar structure, a suitable WdW surface, possibly the oxygen in C-3 accepting the hydrogen bond (as suggested from the docking analysis).

These results are in agreement with the previously described hypothesis: the kinetically limiting event is the entrance and positioning of the ligand within the thrombin catalytic sac. Because of its partial occlusion, the catalytic sac discriminate planar and rigid ligands. Quercetin and partially the ellagic acid show a more rigid and planar structure than the two antocyanidins, these characteristics facilitate the access within the catalytic sac, as confirmed from their high association constants, while luteolin is jeopardised only from the lack of the O-3.

## 3.7 Polyphenols-Plasmin interactions

### 3.7.1 Spectrophotometric test of the enzymatic activity.

We have measured the variation of the plasmin amilolytic activity on a chromogenic substrate in the presence of increasing amounts of the flavonoid and we have obtained an inhibition hyperbolic isotherm, whose slope decreases with the substrate concentration increase (Fig.3 A e C).

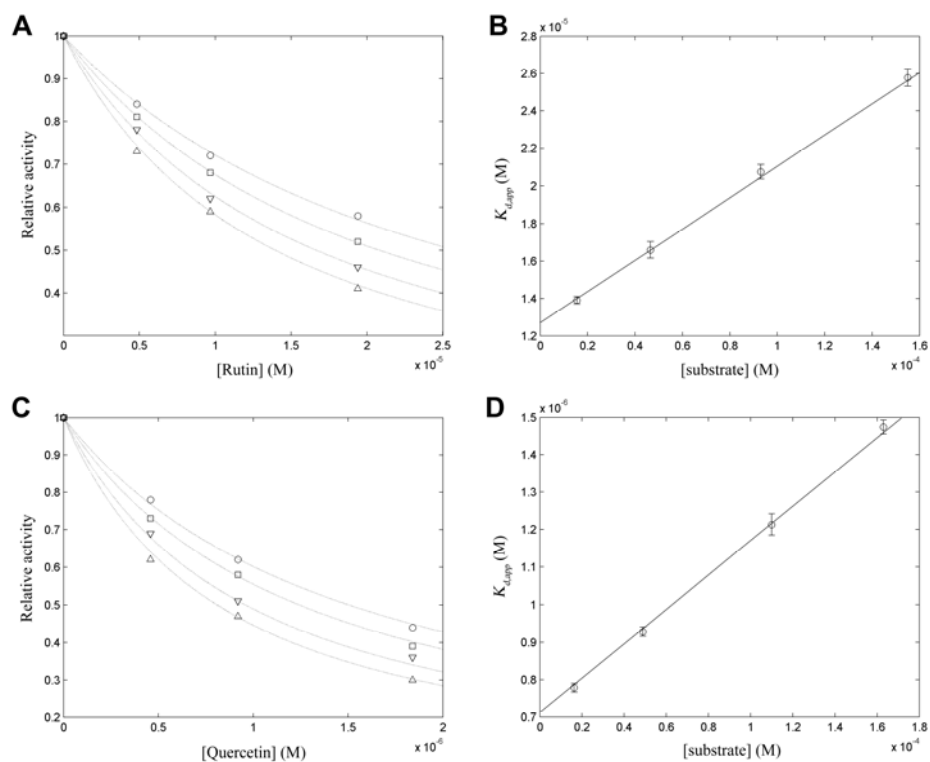


Fig. 39: (A, C) the relative plasmin activity vs. the flavonoid concentration measured at four different substrate concentrations; (B, D) the  $K_{d,app}$  measured for the plasmin-flavonoid interaction vs. the substrate concentration  $[S_0]$  from which the  $K_d$  has been determined.

These inhibition data can be fitted using a stoichiometric model 1:1 ( $K_{i,app} = K_i \cdot \left(1 + \frac{[S_0]}{K_m}\right)$ ) for the bonding of an enzyme with a reversible competitive enzyme [203]: this hypothesis has been confirmed by a Dixon plot analysis [204]. Furthermore the  $K_{d,app}$ , the equilibrium constant of the substrate dependent dissociation of the plasmin-flavonoid complex, obtained for both the studied flavonoids, is linearly dependent from the substrate concentration (Fig.30 B e D)

[203]. This result confirms the competitive type inhibition. The experimentally measured  $K_m$  was  $= 138.06 \pm 7.87 \mu\text{M}$ , in accord with the literature data [205].

### 3.7.2 SPR studies: equilibrium analysis.

The results of the spectrophotometric test have been confirmed with bioprobe studies. The Fast Fit and Global Fit analysis has shown monophasic association and dissociation kinetics (Fig.31 A).

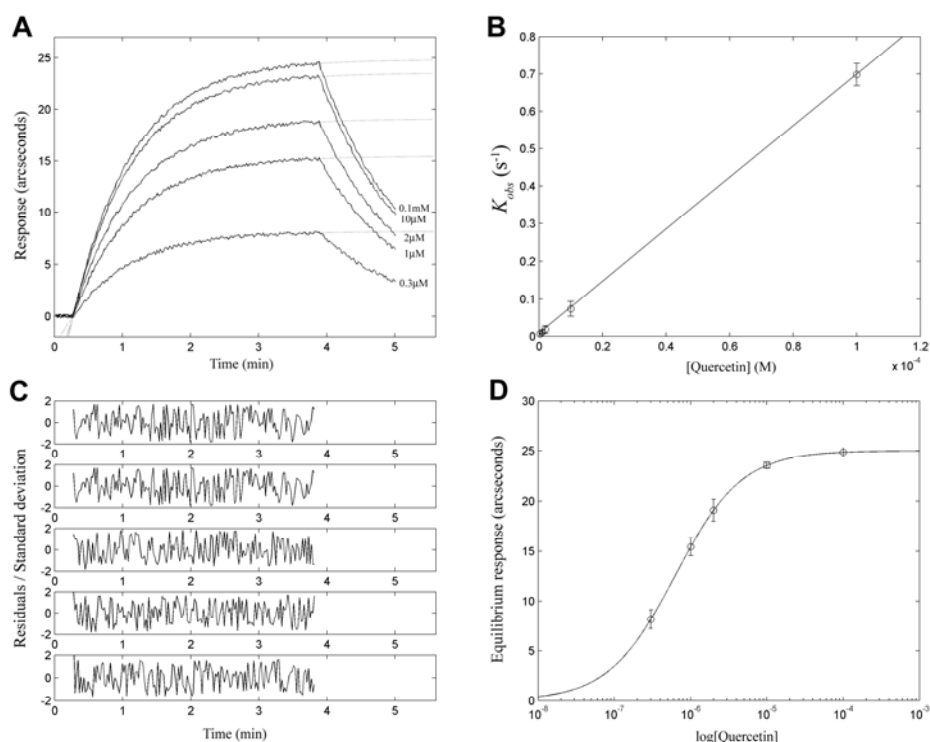


Fig. 40: (A) Overlapped association and dissociation curves measured at increasing quercetin concentrations; (B) linear relation between the quercetin concentration and the  $K_{obs}$ ; (C) residues normalised for standard deviation computed for a monophasic fitting of the association data; (D) bond extent.

Furthermore, the monoexponential analysis of the association curves was error-free (Fig. 31 C) and the biexponential model does not increased the reliability of the fit on the basis of the F-test (95% confidence)

Complesso	$K_d^*$ (M)	$K_d$ (M)	$k_{ass}$ ( $M^{-1}s^{-1}$ ) e $k_{diss}$ ( $ms^{-1}$ )	$K_{SV}^{-1}$ (M)
Plasminogen-Quercetin	/	$7.6e^{-7} \pm 0.8e^{-7}$	$7303.33 \pm 298.68$ $5.6 \pm 0.5$	/
Plasmin-Quercetin	$7.15e^{-7} \pm 0.96e^{-7}$	$6.2e^{-7} \pm 2.9e^{-7}$	$6944.87 \pm 1261.83$ $4.3 \pm 1.9$	$10.35e^{-6} \pm 1.27e^{-6}$
Plasminogen-Rutin	/	$9.5e^{-6} \pm 6.2e^{-6}$	$112.76 \pm 13.48$ $1.1 \pm 0.7$	/
Plasmin-Rutin	$12.98e^{-6} \pm 0.76e^{-6}$	$10.7e^{-6} \pm 0.9e^{-6}$	$220.63 \pm 3.73$ $2.4 \pm 0.2$	$16.82e^{-6} \pm 1.47 e^{-6}$

Tab 22: The  $K_d^*$  have been calculated with spectrophotometric tests;  $K_d$ ,  $k_{ass}$  and  $k_{diss}$  have been obtained with the optic bioprobe; the reciprocal value of the Stern-Volmer  $K_{SV}^{-1}$  quencin constant has been calculated from the fluorimetric data

The dissociation constants at equilibrium (Tab. 22) obtained either with spectrophotometric tests ( $K_d^*$ ) than with bioprobe studies ( $K_d$ ) result comparable with each other, suggesting the plasmin-flavonoid complexes show a similar functional behaviour both in solution and immobilised on the bioprobe surface. Furthermore, the comparison of the  $K_d$  values measured for the complexes between the plasmin (plasminogen) and the flavonoid suggest the bonding site is not affected from modifications after the zymogen activation. The  $K_d$  calculated values (included in the range  $10^{-6} - 10^{-7}$  M) and the saturation reached at the asymptote at high flavonoid concentrations suggest the presence of a specific flavonoid binding site within the enzyme.

### 3.7.3 SPR studies: kinetic analysis

The measured association ( $k_{ass}$ ) and dissociation ( $k_{diss}$ ) constants furnish further information concerning the mechanistic properties of the macromolecular identification process. Between the two tested flavonoids, the quercetin association to plasmin and plasminogen is kinetically preferred to rutin (Tab. 22). The analysis of the dissociation kinetics shows similar  $k_{diss}$  for the two flavonoids. Such behaviour can explain the differences between the equilibrium constants simply in terms of variability in the association constants.

### 3.7.4 Fluorimetric tests

The measured Stern-Volmer quenching constants show the quercetin interact more positively with plasmin (tab. 22), as demonstrated from the faster decrease of the relative fluorescence intensity following the plasmin-quercetin interaction (Fig. 32). Furthermore, the  $n$  variable values obtained from the fitting of the experimental data with the  $\frac{F}{F_0} = \frac{1}{(1 + K_{SV}[Q]^n)}$  equation ( $1.25 \pm 0.10$  for quercetin and  $1.08 \pm 0.09$  for rutin), show a 1:1 stoichiometry in the quenching process. We can suppose the plasmin-flavonoid interaction takes place in the catalytic site near the Trp761.

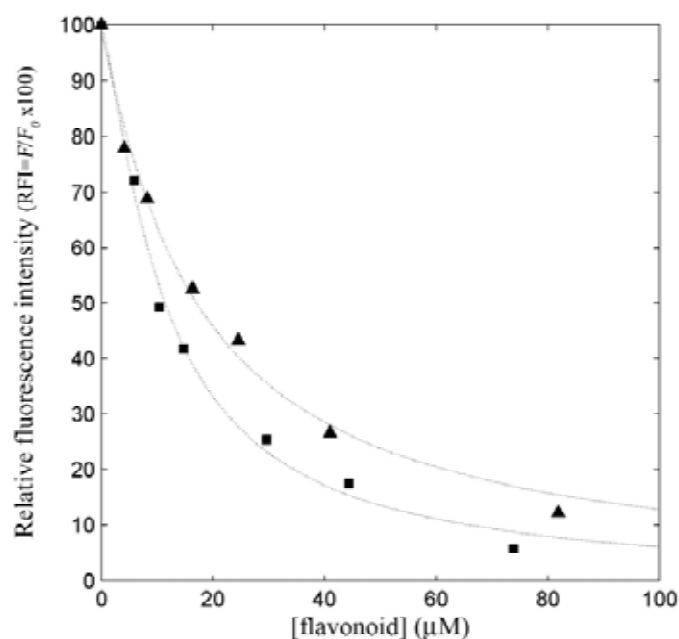


Fig. 41: The Trp761 fluorescence quenching represented as relative fluorescence intensity RFI vs. the quercetin ■ and rutin ▲ ( $\lambda_{ex} = 270 \text{ nm}$  e  $\lambda_{em} = 348 \text{ nm}$ ).

### 3.7.5 Grape seed extract effect on plasmin

Because of the inhibiting effect of the single polyphenolic compounds on plasmin, than we have also tested the Biophenolix grape seed extract activity. The following plot shows the plasmin residual activity vs. the concentration of the extract, expressed as  $\mu\text{g}$  of gallic acid equivalents per ml of the reaction mixture.

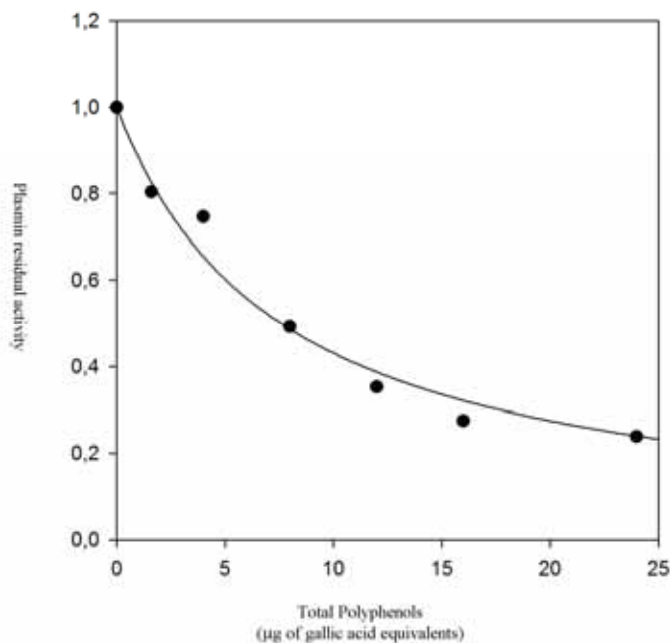


Fig. 3.9 – Plasmin residual activity vs. grape seed extract concentration

This trend ( $K_i=7.572\pm 0.660 \mu\text{g/ml}$ ) can be directly related to the monomeric species of the extract, even though it is extremely rich of only partly characterised polymeric species.

### 3.7.6 Molecular docking of the plasmin-flavonoid interaction.

The docking has demonstrated an essentially electrostatic difference between the two complexes plasmin-quercetin and plasmin-rutin; a positive difference for the first complex. In effect, the energetic values of the complexes (-58.4609 kcal/mol for quercetin and -52.9895 kcal/mol for rutin) are different only because of the electrostatic contribution (-17.6323 kcal/mol for quercetin and -13.4532 kcal/mol for rutin). The difference is explained from the presence of 6 hydrogen bonds in the plasmin-quercetin complex (Trp761 and OH in position 3 of the 2-diidroxyphenil; Arg644 and OH in position 7; Arg644 and carbonyl OH in position 4; Asp646 e Arg644 and carbonyl OH in position 4; Glu606 Arg644 and carbonyl OH in position 4; Glu606 and OH in position 3) while the plasmin-rutin complex posse 3 hydrogen bonds (Asp646 and OH in position 7; Arg644 and OH in position 7; His603 and OH in position 3 of the 2-diidroxyphenil).



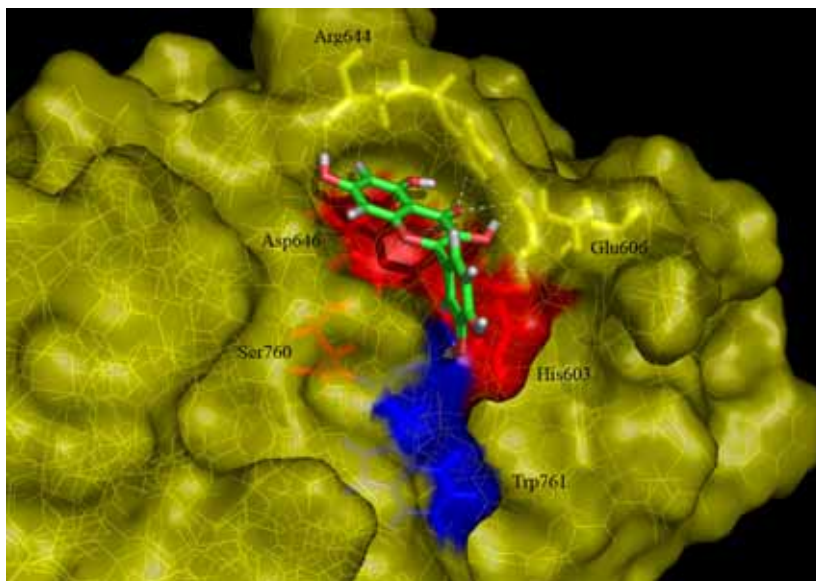


*Fig. 42: The plasmin-quercetin complex showing the catalytic triad (red) and the Trp761 responsible of the fluorescence emission effect. Also shows (white) the 6 hydrogen bonds*

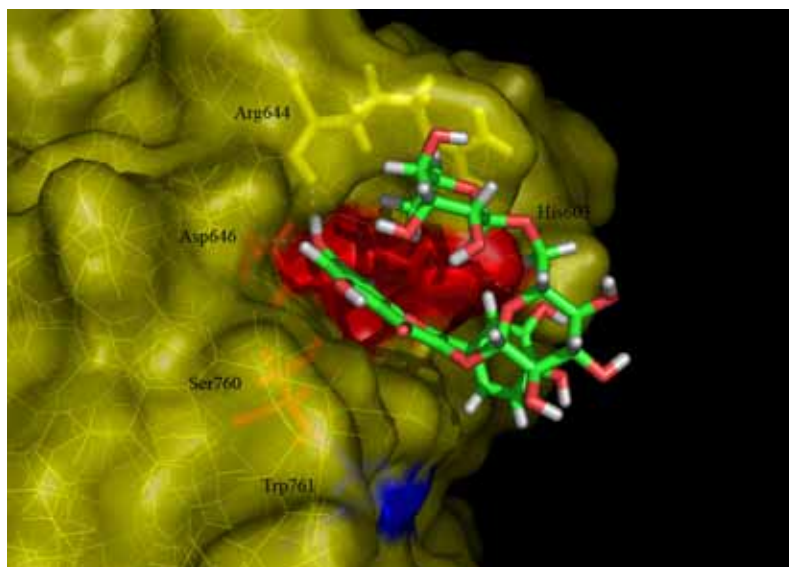


*Fig. 43: The plasmin-rutin complex showing the catalytic triad (red) and the Trp761 responsible of the fluorescence emission effect. Also shows (white) the 3 hydrogen bonds*

### 3.8 Polyphenols-DHFR interactions

#### 3.8.1 Wt-DHFR inhibition by monomeric catechins

The inhibition data are obtained by the contemporary pre-incubation of the catechin with the enzyme or by the enzyme addition to incubation mixture, containing the flavonoid and the substrate (DHF). The addition of increasing amounts of EGCG to a fixed wt-DHFR concentration produced an inhibition hyperbolic isotherm. All the experiments have been performed by catechin pre-incubation with the protein at different intervals. The results have shown a “*slow-binding inhibitor*” [206] trend for the EGCG and also an incubation time dependent inhibition.

Incubation (min)	% Inhibition
0	12,15%
5	32,56%
10	93.57%
15	93.5%

Tab 23: percentage of inhibition at different incubation time of the protein with EGCG.

[EGCG] = 100  $\mu$ M, [wt-DHFR] = 40 nM, [DHF] = 30  $\mu$ M.

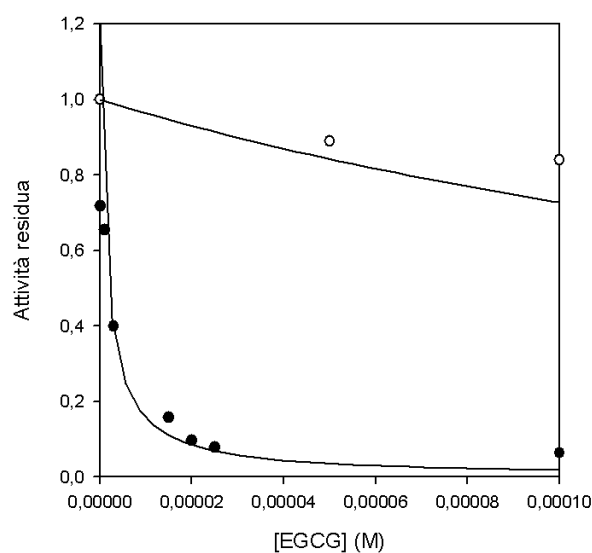


Fig. 44: EGCG inhibitory effect on the wt-DHFR enzymatic activity after 15 min pre-incubation (●) and without pre-incubation (○).

All the experiments have been performed after 15 min pre-incubation of the EGCG with the protein; longer incubation intervals did not produced any significant variations of the residual activities.

### 3.8.2 $K_m$ determination at different EGCG concentrations.

The Michaelis constant ( $K_m^{DHF}$ ) for the substrate has been experimentally determined plotting the initial speed  $V_i$  (measured when a small substrate amount has reacted) vs. increasing DHF concentrations. Fig. 40 shows the Michaelis curves obtained at different EGCG concentrations.

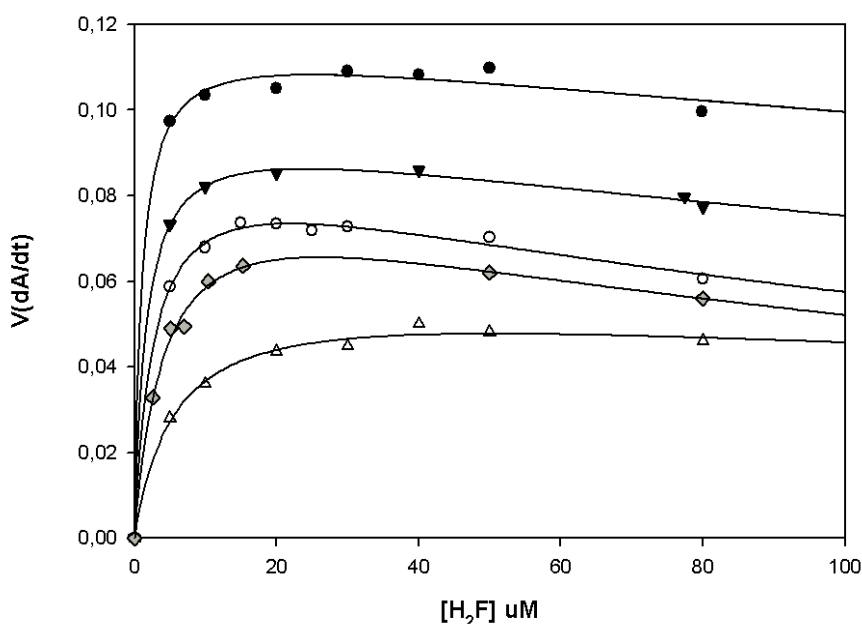


Fig. 45: Substrate concentration effect on the speed of the enzymatic activity, at different EGCG concentrations.

●: [EGCG] = 0 μM; ▼: [EGCG] = 5 μM; ○: [EGCG] = 12,5 μM; ◇: [EGCG] = 20 μM; △: [EGCG] = 28,5 μM.

The fit of each curve has been evaluated taking in account the recently published substrate inhibition data [207].

The Michaelis curves analysis has shown the substrate inhibition, as recently published [207], and the corresponding data fit has been done with the use of the Nakano equation, modified for substrate inhibition.

$$V = \frac{V_{\max}}{1 + \frac{K_m^{DHF}}{[S]} + \frac{[S]}{k_i}}$$

where  $[S]$  stands for the substrate concentration,  $K_m^{DHF}$  indicates the Michaelis constant for the DHF substrate and  $V_{\max}$  the top speed.

$K_m^{DHF}$ ,  $V_{\max}$  and the catalytic constant  $k_{cat}$  for each EGCG concentration have been derived from the data analysis (Fig. 5.7)

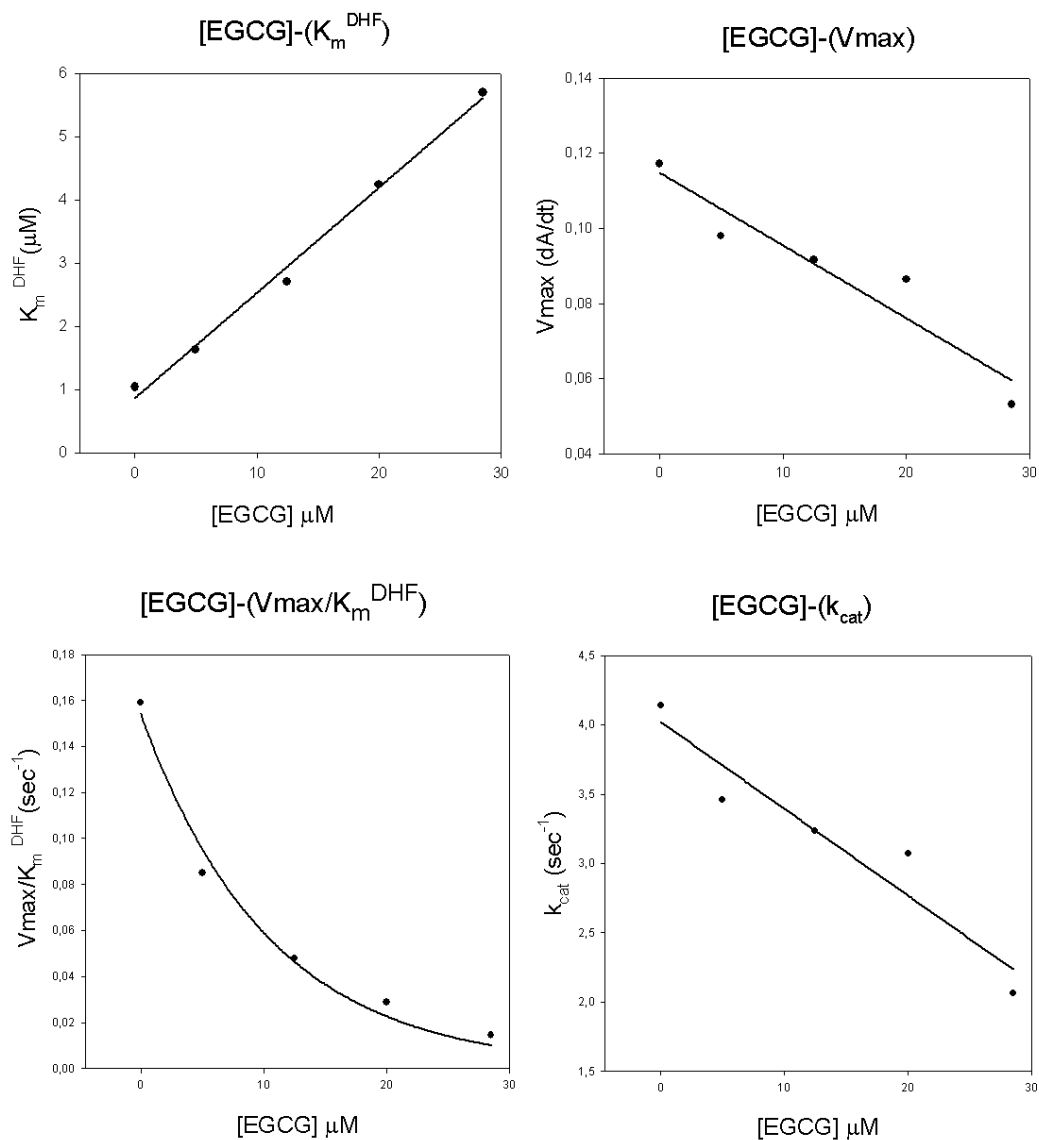


Fig. 46 : the different plots show  $K_m^{DHF}$ ,  $V_{\max}$ ,  $V_{\max}/K_m^{DHF}$ ,  $k_{cat}$  vs. the EGCG concentration.

The results clearly indicate a mixed inhibition of the EGCG on the wt-DHFR. The EGCG behaves both like a competitive inhibitor (the  $K_m^{DHF}$  increase with the inhibitor concentration

indicates a reversible competitive inhibition) and like a non competitive inhibitor (the  $V_{\max}$  decrease with the inhibitor concentration decrease indicates a non competitive inhibition).

### 3.8.3 Inhibition constants determination

In case of mixed inhibitions, the competitive ( $K_{ic}$ ) and non competitive ( $K_{iu}$ ) inhibition constants can be with good approximation determined using classic analysis methods [208]. Plotting the reciprocal speed vs. the inhibitor concentration [I] at different substrate concentration, a straight lines set is obtained, intersecting each others at a coordinate point  $[I] = -K_{ic}$ , as referred in [208]. Both plots allow us directly to determine the  $i_{50}$ , i.e. the inhibitor concentration producing 50% enzyme inhibition at a defined substrate concentration. If the  $S/v$  or  $1/v$  vs.  $I$  plots produce a linear relationship,  $i_{50}$  is the value furnished from the straight line intercept with the abscissa [I]. The various straight lines intercepts obtained at different substrate concentrations vs. [I] in the  $S/v$  or  $1/v$  plots indicates the possible inhibition classes: competitive, mixed competitive, non competitive, mixed non competitive, uncompetitive [208].

The ordinate is equal to:

$$\frac{[S]}{V} = K_m^{DHF} \cdot \frac{1 - \frac{K_{iu}}{K_{ic}}}{V_{\max}}$$

Where  $K_m^{DHF}$  e  $V_{\max}$  are respectively the substrate Michaelis constant and the top reaction speed in absence of the inhibitor.

It has been demonstrated the EGCG-DHFR is mixed type with relevant competitive character (the intercept is positioned under the abscissa in an  $S/v$  vs. [I] plot, while it is positive in a  $1/v$  vs. [I] plot,  $K_{ic} = 4.9 \pm 1.9 \mu\text{M}$ ,  $K_{iu} = 25.0 \pm 1.9 \mu\text{M}$ ). In such inhibition type, using the  $S/v$  ratios, the  $i_{50}$  increases proportionally to [S].

### 3.8.4 Grape seed extract effect on DHFR

After the verification of the gallate polyphenols inhibition on the DHFR, we have tried to test the effect of the Biophenolix grape seed extract. Unfortunately the high level of polymeric polyphenols has produced the DHFR aggregation and the following precipitation, preventing the interaction characterization.

## ***3.9 Polyphenols-Proteasome 20S interactions***

### **3.9.1 Isolation and purification of the bovine brain multicatalytic protease.**

In order to isolate and purify the bovine brain multicatalytic protease complex, the organ was previously washed in physiological solution and the external membrane was taken away, than the grey substance was separated from the white, contemporarily the fat and fibrous parts were removed. The isolated grey substance, 235 gr., was firstly homogenised with Waring-Blendor in Tris-HCl 50 mM, KCl 150 mM, EDTA 2 mM, pH 7.5 buffer (ratio 1:2.5 tissue/buffer). The collected suspension was again homogenised with Potter-Elvehjem. All the described operations were carried out at 4°C. In order to help the extraction, the homogenate was kept overnight in ice under mild stirring.

After a 13500 x g centrifugation x 1h, the surnatant was added with solid ammonium sulphate to a 40% - 60% salt saturation. The precipitate was suspended in Tris-EDTA 50 mM + KCl 150 mM, pH 8.3 buffer, and dialysed with the same buffer overnight. Than it was carried out a first separation by gel-filtration on a Sephacryl S200 column, equilibrated with Tris-EDTA 50 mM, KCl 150 mM a pH 8.3 buffer. This step removes the higher part of phospholipids. The proteasome fractions were identified on the basis of their chemotropism-like activity, than collected and concentrated by ultra filtration (YM10 membrane) under nitrogen atmosphere.

The concentrated sample was loaded on a DEAE-Sephacel column, equilibrated with Tris-EDTA 50 mM, pH 7.5 buffer and eluted in KCl (0-0.8 M) linear gradient. The active fractions were collected and dialysed in Tris-EDTA 50 mM, KCl 150 mM, pH 7.5 buffer, concentrated and loaded on a Superose 6 FPCL column. The gel-filtration eluted peak was again loaded on a Phenyl Sepharose CL/4B FPLC column, equilibrated in Tris-EDTA 20 mM,  $(\text{NH}_4)_2\text{SO}_4$  at 30%, pH 7.5 buffer and eluted in an ammonium sulphate (30%-0%) linear gradient.

In the figure 46 are shown the results of polyacrilammide (12%) gel electrophoresis carried out in denaturing conditions. The MPC characteristic electrophoretic profile is formed from 10 protein bands showing, on the basis of a comparison with known protein markers (not shown), molecular weight range between 21 and 32 kDa.

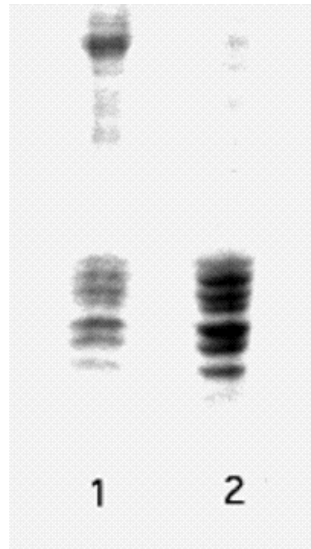


Fig. 47 Poliacrilamide (12%) gel electrophoresis carried out in denaturing conditions, after Superose 6 elution (lane 1) and after Phenyl Sepharose CL/4B elution (lane 2)

In table 25 are collected all the quantitative data related to the bovine brain 20s proteasome purification steps.

All the purification steps have been carried out at a  $<4^{\circ}$  process temperature. The protein concentration has been measured with the Lowry method [209] for the first four steps, and with the Bradford method for the following steps. The chemotropism-like activity has been measured according to Materials and Methods.

<b>Purification step</b>	<b>volume (ml)</b>	<b>Protein (mg/ml)</b>	<b>Total activity</b>	<b>Spec. act. (U/mg)</b>	<b>recovery %</b>	<b>Purific. index</b>
homogenate	780	80.7	969.6	0.015	100	1
surnatant	612	4.8	146.9	0.05	15.15	3.33
(NH <sub>4</sub> ) <sub>2</sub> SO <sub>4</sub> precipitation	28	14.4	30.94	0.077	3.19	5.13
Sephacryl S200	38	1.4	13.9	0.26	1.4	17.3
DEAE-Sephacel	126	0.39	10.71	0.21	1.1	14
Superose 6	5,5	0.91	1.22	0.24	0.126	16
Phenyl Sepharose	7	0.17	1.64	1.35	0.17	90

Tab 24: Bovine brain 20s proteasome purification scheme

Tab. 25 shows the specific activity of the proteolytic components of the bovine brain purified MPC.

Component	Substrate Conc. (mM)	Specific activity ( $\mu\text{mol}/\text{mg}/\text{h}$ )
BrAAP	Z-GPALG-pAB (1.0)	1.24
PGPH	Z-LLE-2Na (0.64)	1.53
ChT-L	Z-GGL-pNA (0.4)	3.60
T-L	Z-LLR-2Na (0.4)	0.42
SNAAP	Z-GPAGG-pAB (1.0)	0.55

Tab 25: Bovine brain MPC proteolytic activity

The proteolytic activities have been determined according to Materials and Methods.

Figure 47 shows the immunoblotting autoradiographic film, discriminating the constitutive from immunogenic type of the brain enzymatic system.

The incubation with specific antibodies for the  $\beta$ , X, Y e Z subunits has shown the presence of a constitutive proteasome characteristic subunits (XYZ-MPC).

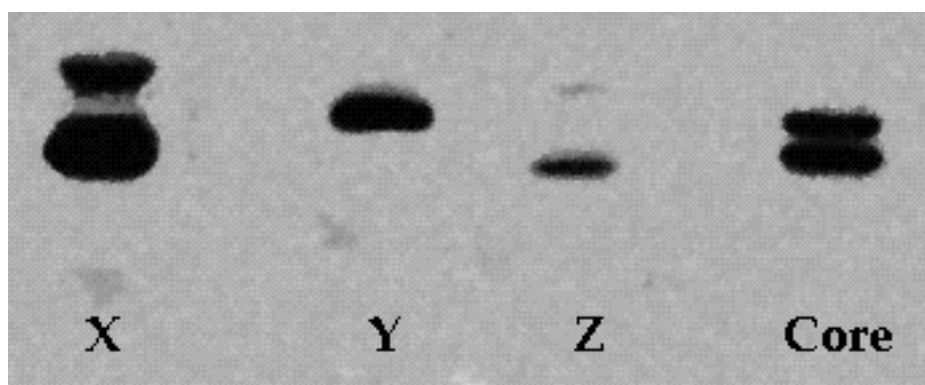


Fig. 48: Immunorevelation of the  $\beta$  X, Y e Z subunits and of the 20S Core carried out on the bovine brain purified MPC. The test has been performed according to Materials and Methods, the four membrane segments have been incubated with primary antibodies specific for the single subunits.

### 3.9.2 Isolation and purification of the bovine thymus multicatalytic protease.

The bovine thymus protease purification procedure has been similar to that one previously described bovine brain isolation. In details, 270 gr. of tissue, after the accurate fat removal, were firstly homogenised with a Waring-Blendor in Tris-HCl 10 mM, pH 7,5 buffer, than centrifuged at 13500 x g per one hour. The collected surnatant was added with 1% final



streptomycin solution, in order to precipitate nucleic acids and nucleo-proteins. Then it was carried out the fractionated precipitation with solid ammonium sulphate. The precipitate was obtained in the 40-60% saturation interval, it was suspended in Tris-EDTA 10 mM, pH 7.5 and dialysed in the same buffer.

The sample was than loaded on a DEAE-Sephacel column, equilibrated in Tris-EDTA 10 mM, pH 7.5 buffer and eluted with a 0.01- 0.5 M Tris-EDTA linear buffer. The next steps were two gel filtrations: the first on a Sephacryl S 300 column equilibrated and eluted with Tris-EDTA 250 mM, pH 8.3 buffer, the second on a Superose 6 equilibrated and eluted with Tris-EDTA 150 mM, pH 7.5 buffer.

The figure. 48 refers the SDS electrophoresis results of the Superose 6 eluted fraction, exhibiting the higher chemotropism-like activity.

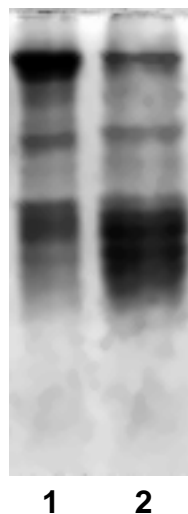


*Fig. 49: 12% (PAGE) polyacrilamide gel electrophoresis, in denaturing conditions, before (lane1) and after (lane 2) the Superose 6 chromatography. The electrophoresis was carried out according to the Laemmly [61] procedure, as referred in Materials and Methods.*

Tab. 26 sows the data of the immunoproteasome purification steps, while Tab.27 shows the specific activities of the five proteolytic components of the enzyme.

<b>Purification steps</b>	<b>Volume (ml)</b>	<b>Protein (mg/ml)</b>	<b>Total activity</b>	<b>Spec. Act. (U/mg)</b>	<b>Recovery %</b>	<b>Purific. index</b>
homogenate	1040	7	655	0.09	100	1
supernatant	740	1.3	510	0.53	77.9	5.9
(NH <sub>4</sub> ) <sub>2</sub> SO <sub>4</sub> precipitation	69	2.62	257	1.42	39.2	15.8
Sephacryl S200	222	0.50	231	2.08	35.3	23.1
DEAE-Sephacel	61	0.90	132	2.4	20.1	26.6
Superose 6	46	0.90	95.2	2.3	14.5	25.5

Tab. 26– Bovine thymus MPC purification scheme

The protein concentration has been measured with the Lowry method [209] for the first 3 steps, and with the Bradford method for the following steps. The proteolytic activities have been measured according to Materials and Methods.

<b>Component</b>	<b>Substrate conc. (mM)</b>	<b>Specific activity (μmol/mg/h)</b>
<b>BrAAP</b>	Z-GPALG-pAB (1.0)	40.23
<b>PGPH</b>	Z-LLE-2NA (0.64)	0.80
<b>ChT-L</b>	Z-GGL-pNA (0.4)	1.04
<b>T-L</b>	Z-(D)ALR-2NA (0.4)	1.07
<b>SNAAP</b>	Z-GPAGG-pAB (1.0)	0.75

Tab. 27: Thymus MPC proteolytic activities

### 3.9.3 20S proteasome inhibition activities of polyphenolic compounds.

Literature data show many ester-bond containing tea polyphenols inhibit the ChT-L activity of the 20S purified proteasome (*Methanosarcina thermophila*, Recombinant, *Escherichia Coli*). Our study shows the effect of some polyphenols on proteolytic activities of constitutive and  $\gamma$ -interferon inducible 20s proteasomes isolated respectively from bovine brain and thymus. Tab 28 show the IC<sub>50</sub> values of tested antioxidants calculated from the ChT-L (Z-GGL-pNA), PGPH (Z-LLE-2NA) BrAAP (Z-GPALG-pAB) e T-L (Z-GGR-2NA) activities: the data have been obtained from the fitting of the residual activity experimental data in

function of the antioxidant concentration, according to the equation quoted in Materials and Methods.

	<b>IC<sub>50</sub> (mM) for XYZ-proteasome</b>			
	<b>ChT-L</b>	<b>BrAAP</b>	<b>PGPH</b>	<b>T-L</b>
<b>Gallic Acid</b>	0.72 ± 0.10	13.55 ± 4.34	4.90 ± 1.09	0.27 ± 0.17
<b>EGCG</b>	0.22 ± 0.06	4.3	3.4	0.06 ± 0.02
<b>(-)epicatechin</b>	14.29 ± 1.98	5.37 ± 1.66	NI	38.44 ± 7.01
<b>Luteolin</b>	17.88 ± 8.67	2.87 ± 0.41	15.67 ± 12.00	13.62 ± 3.35
<b>Quercetin</b>	3.11 ± 0.32	5.38 ± 0.84	NI	0.96 ± 0.19
<b>Iperoside</b>	9.57 ± 0.88	24.97 ± 11.73	NI	NI
<b>Rutin</b>	7.16 ± 1.42	14.60 ± 0.43	NI	6.58 ± 0.97
<b>Resveratrol</b>	1.61 ± 0.49	9.24 ± 2.15	NI	10.07 ± 1.65
<b>Ellagic Acid</b>	2.32 ± 0.67	14.55 ± 12.49	2.54 ± 0.30	3.26 ± 0.20

	<b>IC<sub>50</sub> (mM) for LMP-proteasome</b>			
	<b>ChT-L</b>	<b>BrAAP</b>	<b>PGPH</b>	<b>T-L</b>
<b>Gallic Acid</b>	0.71 ± 0.09	6.63 ± 0.39	5.78 ± 0.64	3.04 ± 0.37
<b>EGCG</b>	0.46 ± 0.10	0.24 ± 0.07	2.07 ± 0.31	0.24 ± 0.06
<b>(-)epicatechin</b>	12.61 ± 2.14	11.56 ± 4.20	NI	13.69 ± 2.12
<b>Luteolin</b>	7.26 ± 1.54	4.41 ± 0.26	7.93 ± 1.05	NI
<b>Quercetin</b>	2.42 ± 0.28	1.17 ± 0.72	2.41 ± 0.60	3.60 ± 0.62
<b>Iperoside</b>	6.18 ± 0.36	15.19 ± 6.91	NI	NI
<b>Rutin</b>	7.25 ± 0.63	35.81 ± 21.99	NI	2.65 ± 0.27
<b>Resveratrol</b>	1.88 ± 0.57	9.07 ± 0.83	45.32 ± 7.04	15.79 ± 2.51
<b>Ellagic Acid</b>	2.63 ± 0.24	7.20 ± 4.69	1.34 ± 0.45	NI

Tab. 28; IC<sub>50</sub> values obtained with the tested polyphenolic compounds and related to the ChT-L, BrAAP, PGPH and T-L proteasomal proteolytic components expressed from constitutive and  $\gamma$ -interferon inducible type 20S proteasomes. NI (Non Inhibition) abbreviation means lack of activation or efficacy on the proteasomal activities of the tested compound. The activity and IC<sub>50</sub> tests have been carried out according to Materials and methods.

Table 28 shows the gallic acid and primarily the EGCG, in comparison with the other tested compounds, induce the higher inhibition of the ChT-L e T-L components of both the proteasome complexes. The immunoproteasomal BrAAP activity is more inhibited than the constitutive proteasome, while the PGPH activity is generally less affected by the tested compounds. The IC<sub>50</sub> values we have obtained with EGCG result not in agreement with the literature data referred to the ChT-L component, expressed from the archeobacterium *Methanosarcina thermophile* 20S proteasome and tested with the fluorescent substrate Suc-LLVY-AMC.

Thereafter, with the aim to confront our data with the literature data [210-213], the activity tests have been carried out using fluorogenic peptides with increasing EGCG concentrations and with the enzymes in basal conditions or activated with SDS 0.02%. Tabs 29 show the IC<sub>50</sub> calculates for the two proteasomes.

	<b>IC<sub>50</sub> (mM) for XYZ-proteasome</b>		
	<b>ChT-L</b>	<b>BrAAP</b>	<b>PGPH</b>
<b>EGCG + SDS (0.02%)</b>	0.038 ± 0.004	0.017 ± 0.003	NI
<b>EGCG - SDS</b>	0.14 ± 0.03	0.06 ± 0.01	0.75 ± 0.35

	<b>IC<sub>50</sub> (mM) for LMP-proteasome</b>		
	<b>ChT-L</b>	<b>BrAAP</b>	<b>PGPH</b>
<b>EGCG + SDS (0.02%)</b>	0.09 ± 0.03	0.031 ± 0.006	0.105 ± 0.008
<b>EGCG - SDS</b>	0.06 ± 0.01	0.018 ± 0.003	0.033 ± 0.002

Tab. 29: IC<sub>50</sub> values obtained with EGCG and related to the ChT-L proteolytic component expressed from constitutive and  $\gamma$ -interferon inducible type 20S proteasomes. The test has been carried out with the Suc-LLVY-AMC substrate in the presence or not of SDS. NI (Non Inhibition) abbreviation means lack of activation or efficacy on the proteasomal activities of the tested compound. The activity and IC<sub>50</sub> tests have been carried out according to Materials and methods.

The ChT-L activity tested with the Suc-LLVY-AMC substrate shows that the EGCG - IC<sub>50</sub> are lower than those obtained with the Z-GGL-pNA substrate, especially at elevated SDS activating concentrations. These inhibition level differences could be due to different subunits

composition between archeobacteria and mammal proteasomes. Furthermore, the data show the immunoproteasome more affected from the polyphenolic inhibiting action, with the lowest IC50 for the BrAAP component.

### 3.9.4 Grape seed extract effect on the 20S proteasome functionality.

On the basis of the observed inhibiting effect of single polyphenolic compounds on the isolated 20S proteasome catalytic components, we have verified the action of increasing grape seed extract concentrations on proteasomal functionality. The following figure shows the plot of the constitutive 20S proteasome ChT-L (■) and inducible  $\gamma$  interferon (○) activity vs. the grape seed extract concentration, expressed as gallic acid  $\mu\text{g}$  equivalents per reaction mixture reaction / ml.

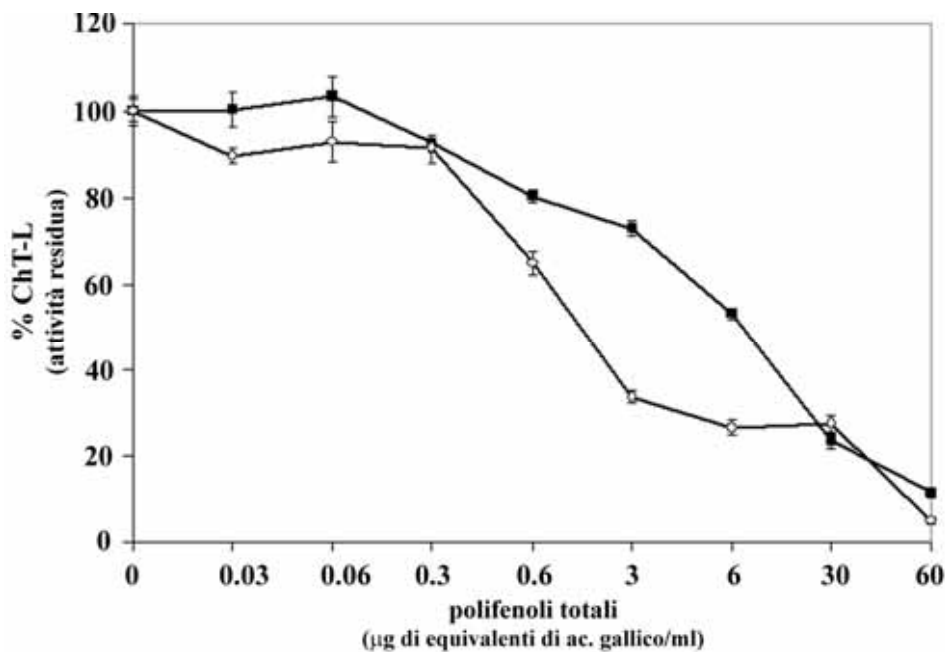


Fig. 50: Constitutive 20S proteasome ChT-L (■) and inducible  $\square$  interferon (○) activity vs. the grape seed extract concentration. The activity is expressed as % of the control (without extract)

With the aim to take in account the fluorescence produced from the extract components, each experimental point has been determined in parallel with a control sample. Both the enzymatic complexes show an extract concentration related inhibition. This behaviour does not seem directly related to the monomeric polyphenolic species, because the extract is particularly rich in polymeric species.

## **4 Conclusions**

### ***4.1 Characterization of Biophenolix Grape Seed Extract***

The product obtained maintains the characteristics of low monomeric content compared to other commercially available grape seed extracts and the data for purity and antioxidant activity is comparable. The product obtained has the possibility of obtaining an organic certification since no organic solvents are used and the production coadiuvant used are included in organic legislation (EU, NOP,). The indicated process is usable also for industrial purpose and it's ready for a scale-up process.

### ***4.2 Evolution of catechins in grape seeds during ripening***

The evolution of catechins during ripening follows a second order kinetic, for total polyphenols and single polyphenols, after reaching the maturation state. At the end of maturation there is a rising of polyphenols maybe due to degradation process of the fruit. The antioxidant activity follows the same pattern of total polyphenols.

### ***4.3 Lipidic peroxidation inhibition by GSE in oil***

The GSE added to olive oil is capable to inhibit peroxides formation even after 20 days, but with less activity respect to BHT and BHA mixture. This may be due also to low dissolution of GSE in lipidic matrix, due to the extraction conditions used for this product. GSE at 500 ppm doesn't have protection activity due to the possibility of acting as pro-oxidant. This results indicate that GSE may have a role as natural antioxidant in food applications, acting as protector of lipidic peroxidation by avoiding the formation of rancidity phenomenon and improving shelf life of food.

This can also suggest the utilization of GSE as natural antioxidant for example in organic oils, where no synthetic antioxidants can be used.

### ***4.4 Characterization of polyphenols alternative sources***

For the vegetals evaluated for possible industrial utilization for the production of extract, pomegranate and rosemary are the most favourable for this purpose. While pomegranate requires a complicated pre-extraction process, rosemary is a product ready to be used in

industrial applications. Its high antioxidant activity and elevated quantity of polyphenols makes it a valid solution for nutraceutical applications.

#### ***4.5 Polyphenols-Flavonoid interactions***

Our results clearly suggest that some flavonoids in addition to their antioxidant activity, essentially due to their chemical structure, may also exhibit a function in the regulation of some proteolytic processes, like those thrombin mediate. Furthermore the thrombinic activity has been inhibited from the Biophenolix grape seed extract, with inhibition constant similar to those of the monomeric species. A more detailed characterization of the molecular components of the extract and of their interaction mechanisms would be necessary for a better explanation of this phenomenon.

The peculiarity of this study has been the effort to understand the molecular mechanisms of the polyphenols activities. Our integrated approach allows for the first time to describe the flavonoid-thrombin interaction in a detailed model. We have clarified not only the kinetic and thermodynamic parameters but also the conformational parameters derived from structural bioinformatic methods (docking analysis and QSAR). It is important to point out the reliability of the results obtained with different experimental approaches, in accordance with each other. This verification suggests the possibility to use the derived information for the design of a mechanistic/structural model able to describe the interaction.

In our opinion this is perhaps the most important result derived from the present study. Effectively, the thermodynamic, kinetic and conformational information we have obtained might be used either for the study the interaction of flavonoids (used in our study or others) with proteolytic enzymes different from thrombin, or primarily for the design of new molecules, derived from flavonoids, possibly more efficient modulators of the thrombin mediated proteolytic processes (or mediated from other proteases), involved in many important physiopathologic processes.

#### ***4.6 Polyphenols-Plasmin interactions***

We have characterised the thermodynamic and kinetic aspects of the interactions between the human plasmin and the tested flavonoids. The 1:1 reversible complexes show dissociation equilibrium constant in the  $\mu\text{M}$  range, in particular quercetin possesses the higher affinity. The

complexes stability (in terms of  $K_d$ ) is comparable with other plasmin complexes with recently studied small ligands [214].

The biosensor tests have shown that the differences between the two tested flavonoids are primarily due to the  $k_{ass}$ , while the  $k_{diss}$  are essentially similar. This fact is due to the structural difference between the quercetin and rutin, the last one has a rutinosidic substitute in position 3, having a larger steric hindrance. This hypothesis is confirmed from the molecular docking analysis: quercetin is able to place more easily itself in the catalytic sac of the enzyme, forming a higher number of hydrogen bonds and therefore a more stable complex. These flavonoids have shown a large affinity for the plasmin/plasminogen system, thus we can suppose their possible use in the regulation in the activities involving this system.

Furthermore, the plasmin activity has been inhibited by the grape seed extract, perhaps because the monomeric polyphenols species, as confirmed from the comparable values of the inhibition constants. In any case it would be necessary a more detailed characterization of the molecular components of the extract and of their action mechanisms. Also the explanation of the physiological and clinic aspects related to the modulation process would require specific analysis.

#### **4.7 Polyphenols-DHFR interaction**

We have studied the wt-DHFR / epigallocatechin-gallate interaction. The results show the EGCG behave like a mixed competitive “*slow-binding inhibitor*” [206] . with  $K_{ic}$  e  $K_{iu}$  inhibition constants respectively equal to  $4.9 \pm 1.9 \mu\text{M}$  e  $25.0 \pm 1.9 \mu\text{M}$ ; while the  $K_{ic}$  is comparable with that one of the DHFR –Metratoxate interaction [141]. Furthermore, the EGCG soft character let speculate its use in the cancer prevention and treatment, showing highly reduced secondary effects compared to others presently used DHFR inhibitors, like Metratoxate. Other *in vivo* studies have shown a further EGCG advantage: a different effect on normal and cancer cells. In effect, at physiological concentrations, the EGCG eliminates the cancer cells inducing apoptosis with reduced or absent effect on normal cells [141].

Such different EGCG inhibition on DHFR is explained considering the higher antifolate compounds activity on cancer cells, generally showing an higher DNA turnover. Apoptosis induction can produce effective anticancer chemotherapeutic and chemiopreventive strategies. Many chemiopreventive agents exhibit their action for the carcinogenesis suppression by apoptosis induction, which eliminates specific type of cells: genetically damaged, activated or



advancing to carcinogenesis. Therefore, the soft EGCG characteristics, joint to its power to induce apoptosis, produce a convincing explanation of the epidemiological data showing the protective effect of polyphenolgallates rich diets on specific cancer types. It is possible to conclude that the EGCG, polyphenolgallates and their derivatives show noticeable potential clinic applications as anticancer agent and as antibiotic agent in the psoriasis treatment [135, 137, 215].

#### ***4.8 Polyphenols-Proteasome 20S interactions***

Epidemiological studies have demonstrated that a rich in fruit and vegetables diet and a large use of tea and red wine result an effective prevention of some neoplastic forms. The anticancer effect has been ascribed to the large amount and variety of polyphenols present in such a kind of food. Furthermore, recent publications have shown the inhibitory effect on proteolytic systems of some polyphenols present in vegetarian food and drinks like tea and red wine. In particular, it has been demonstrated that EGCG effectively and selectively inhibits the proteasome trypsin-like component, thanks to the presence of an ester bond highly susceptible to nucleophilic attack. In fact, the EGCG may form an acyclic bond with the proteasome catalytic site at level of N-terminal threonine of the  $\beta 5$  subunit.

Our results confirm the EGCG inhibitory power on the ChT-L component on isolated proteasomal systems either from animal organs like bovine brain and thymus, or from cellular lysates. Furthermore, we have demonstrated that the BrAAP is susceptible to the EGCG action, primarily at immunoproteasome level, normally expressing such activity in a preferential mode. We have also tested other polyphenolic compounds, with and without ester bonds, but the inhibitory activity was lower than EGCG and essentially dependent on the size and hydrophobicity of the compound.

Small polyphenols like the gallic acid or the Resveratrol are actually more effective, due to the easier penetration in the proteasomal hydrophobic channel and to the direct action on the catalytic site. Compounds with a larger steric hindrance and more polar, like rutin and iperoside, or with rigid bonds, like the ellagic acid, have a lower inhibiting activity. The proteasomal component more affected by the polyphenols inhibitory effect is the ChT-L for the constitutive proteasome and the BrAAP for the immunoproteasome.

The constitutive proteasomal BrAAP activity exhibit a similar  $IC_{50}$  to the ChT-L activity. With respect to the immunoproteasome some compounds result ineffective, while others show an higher activity than on the ChT-L component. A few polyphenolic compounds are able to inhibit significantly the PGPH activity.

The EGCG inhibit the T-L component both in the immuno and in the XYZ-proteasome. Furthermore, the ChT-L component of the two proteasomal complexes show an inhibition directly related to the grape seed extract concentration, although it is not possibile to relate it directly to the polyphenolic components of the extract. It is necessary a more detailed characterization of the molecular components of the grape seed extract and of the their interaction mechanisms with the proteasomal complexes.

The major interest of our study is the effort to understand the basic molecular mechanisms of the polyphenols effects. The scientific literature shows the possibility to prevent the cancer onset by the use of food with an high polyphenols content; furthermore, it has been evidentiated their pro-apoptotic effect selective on cancer cells and their potential use in the cancer therapy synergic with chemotherapeutic drugs

## 5 Bibliography

1. Iwashina, T., *The structure and Distribution of the Flavonoids in Plants*. J. Plant Res., 2000. **113**: p. 287-299.
2. Markham, K.R. and L.J. Porter, *Flavonoids in the green algae*. Phytochemistry, 1969. **14**: p. 199-201.
3. del Bano, M.J., et al., *Flavonoid distribution during the development of leaves, flowers, stems, and roots of Rosmarinus officinalis. postulation of a biosynthetic pathway*. J Agric Food Chem, 2004. **52**(16): p. 4987-92.
4. Jaakola, L., et al., *Activation of flavonoid biosynthesis by solar radiation in bilberry ( Vaccinium myrtillus L) leaves*. Planta, 2004. **218**(5): p. 721-8.
5. Routaboul, J.M., et al., *Flavonoid diversity and biosynthesis in seed of Arabidopsis thaliana*. Planta, 2006. **224**(1): p. 96-107.
6. Castellarin, S.D., et al., *Colour variation in red grapevines (Vitis vinifera L.): genomic organisation, expression of flavonoid 3'-hydroxylase, flavonoid 3',5'-hydroxylase genes and related metabolite profiling of red cyanidin-/blue delphinidin-based anthocyanins in berry skin*. BMC Genomics, 2006. **7**: p. 12.
7. Luck, G., et al., *Polyphenols, astringency and proline-rich proteins*. Phytochemistry, 1994. **37**(2): p. 357-71.
8. Lesschaeve, I. and A.C. Noble, *Polyphenols: factors influencing their sensory properties and their effects on food and beverage preferences*. Am J Clin Nutr, 2005. **81**(1 Suppl): p. 330S-335S.
9. Nicolas, J.J., et al., *Enzymatic browning reactions in apple and apple products*. Crit Rev Food Sci Nutr, 1994. **34**(2): p. 109-57.
10. Jovanovic, S.V. and S. Steenken, *Flavonoids as Antioxidants*. J. Am. Chem. Soc., 1994. **116**: p. 4846-4851.
11. Gonzalez-Paramas, A.M., et al., *Flavanol content and antioxidant activity in winery byproducts*. J Agric Food Chem, 2004. **52**(2): p. 234-8.
12. Kammerer, D., et al., *Polyphenol screening of pomace from red and white grape varieties (Vitis vinifera L.) by HPLC-DAD-MS/MS*. J Agric Food Chem, 2004. **52**(14): p. 4360-7.
13. Revilla, E., E. Alonso, and E. Kovac, *The content of catechins and procyanidins in Grapes and Wines as affected by agroecological factors and technological practices*, ed. A.C. Society. 1997, Washington, DC: American Chemical Society. 69-80.
14. Kushi L., L.E., Willet WC, *Health implications of Mediterranean diets in light of contemporary knowledge. 1. Plant foods and dairy products*. Am J Clin Nutr, 1995. **61** (Suppl): p. 1407S-1415S.
15. Sato, M., et al., *Cardioprotective effects of grape seed proanthocyanidin against ischemic reperfusion injury*. J Mol Cell Cardiol, 1999. **31**(6): p. 1289-97.
16. Sato, M., et al., *Grape seed proanthocyanidin reduces cardiomyocyte apoptosis by inhibiting ischemia/reperfusion-induced activation of JNK-1 and C-JUN*. Free Radic Biol Med, 2001. **31**(6): p. 729-37.
17. Shanmuganayagam, D., et al., *Grape seed and grape skin extracts elicit a greater antiplatelet effect when used in combination than when used individually in dogs and humans*. J Nutr, 2002. **132**(12): p. 3592-8.
18. Maffei Facino, R.e.a., *Free radical scavenging action and anti-enzyme activities of procyanidines from Vitis Vinifera*. Arzneim-Forsch/Drug Research, 1994. **44**: p. 592-601.

19. Chang, W.C. and F.L. Hsu, *Inhibition of platelet aggregation and arachidonate metabolism in platelets by procyanidins*. Prostaglandins Leukot Essent Fatty Acids, 1989. **38**(3): p. 181-8.
20. Robert, L., et al., [*The effect of procyanidolic oligomers on vascular permeability. A study using quantitative morphology*]. Pathol Biol (Paris), 1990. **38**(6): p. 608-16.
21. Dartenuc J.Y., M.P., Choussat H., *Capillary resistance in geriatry. A study of a microangioprotector- Endotelon*. Bord Med, 1980. **13**: p. 903-907.
22. Delacroix, P., *Etude en double aveugle de l'endotelon dans l'insuffisance veineuse chronique*. La Revue de Medecine, 1981. **27-28**: p. 1793-1802.
23. Talpur, N.e.a., *Effect of Chromium and Grape Seed Extract on the Lipid Profile of Hypercholesterolemic Patients*. The FASEB Journal, 2000. **14**: p. A727.
24. Troyer, J.R., *The Distribution of Rutin and Other Flavonoid Substances in Buckwheat Seedlings*. Plant Physiol, 1955. **30**(2): p. 168-73.
25. Joshi, S.S., et al., *Amelioration of the cytotoxic effects of chemotherapeutic agents by grape seed proanthocyanidin extract*. Antioxid Redox Signal, 1999. **1**(4): p. 563-70.
26. Chen, G., et al., *Ability of m-chloroperoxybenzoic acid to induce the ornithine decarboxylase marker of skin tumor promotion and inhibition of this response by gallotannins, oligomeric proanthocyanidins, and their monomeric units in mouse epidermis in vivo*. Anticancer Res, 1995. **15**(4): p. 1183-9.
27. Amella, A.L., *Inhibition of mast cell histamine release by flavonoid and bioflavonoids*. Planta Med, 1985. **51**: p. 16-21.
28. Middleton, E., Jr. and G. Drzewiecki, *Flavonoid inhibition of human basophil histamine release stimulated by various agents*. Biochem Pharmacol, 1984. **33**(21): p. 3333-8.
29. Pearce, F.L., A.D. Befus, and J. Bienenstock, *Mucosal mast cells. III. Effect of quercetin and other flavonoids on antigen-induced histamine secretion from rat intestinal mast cells*. J Allergy Clin Immunol, 1984. **73**(6): p. 819-23.
30. Hansen, C., *Grape Seed Extract: Procyanidolic Oligomers (PCO)*. 1995, New York: Healing Wisdom Publications.
31. Li, W.G., et al., *Anti-inflammatory effect and mechanism of proanthocyanidins from grape seeds*. Acta Pharmacol Sin, 2001. **22**(12): p. 1117-20.
32. Lotito, S.B., et al., *Influence of oligomer chain length on the antioxidant activity of procyanidins*. Biochem Biophys Res Commun, 2000. **276**(3): p. 945-51.
33. Bagchi, D., et al., *Oxygen free radical scavenging abilities of vitamins C and E, and a grape seed proanthocyanidin extract in vitro*. Res Commun Mol Pathol Pharmacol, 1997. **95**(2): p. 179-89.
34. Uchida, S., *Condensed tannins scavenging active oxigen radicals*. Med Sci Res, 1980. **15**: p. 831-832.
35. Rice-Evans, C.e.a. *Free radical and oxidative stress: environment, drugs and food additivies*. in *Biochemical Society Symposium*. 1994. University of Sussex.
36. Meunier, M.e.a., *Plant Medicin et Phytoterar*, 1989. **23**: p. 267.
37. Bagchi, M., et al., *Smokeless tobacco, oxidative stress, apoptosis, and antioxidants in human oral keratinocytes*. Free Radic Biol Med, 1999. **26**(7-8): p. 992-1000.
38. Maffei Facino, R., et al., *Sparing effect of procyanidins from Vitis vinifera on vitamin E: in vitro studies*. Planta Med, 1998. **64**(4): p. 343-7.
39. Simonetti, P., et al., *Procyanidins from Vitis vinifera seeds: in vivo effects on oxidative stress*. J Agric Food Chem, 2002. **50**(21): p. 6217-21.
40. Vinson, J.A., *Beneficial Effect of a Novel Grape Proanthocyanidin Extract in Atherosclerosis Models*. Free Radic Biol Med, 1999. **27 (Suppl.1)**: p. S45.

41. Vinson, J.A. *The synergism between grape seed extract and vitamins C and E*. in *219th American Chemical Society National Meeting*. 2000. San Francisco.
42. Bombardelli, E., Morazzoni, P., *Vitis Vinifera L.* Fitoterapia, 1995. **LXVI**: p. 291-317.
43. Yamakoshi, J., et al., *Safety evaluation of proanthocyanidin-rich extract from grape seeds*, in *Food and Chemical Toxicology*. 2002, Elsevier Science. p. 599-607.
44. Bagchi, D., et al., *Free radicals and grape seed proanthocyanidin extract: importance in human health and disease prevention*. Toxicology, 2000. **148**(2-3): p. 187-97.
45. Hornyak, T.J., P.D. Bishop, and J.A. Shafer, *Alpha-thrombin-catalyzed activation of human platelet factor XIII: relationship between proteolysis and factor XIIIa activity*. Biochemistry, 1989. **28**(18): p. 7326-32.
46. Ganguly, P., *Interaction of thrombin with human platelets*. Br J Haematol, 1975. **29**(4): p. 617-26.
47. Butkowski, R.J., et al., *Primary structure of human prethrombin 2 and alpha-thrombin*. J Biol Chem, 1977. **252**(14): p. 4942-57.
48. Bode, W., et al., *The refined 1.9 Å crystal structure of human alpha-thrombin: interaction with D-Phe-Pro-Arg chloromethylketone and significance of the Tyr-Pro-Pro-Trp insertion segment*. Embo J, 1989. **8**(11): p. 3467-75.
49. Bode, W., D. Turk, and A. Karshikov, *The refined 1.9-Å X-ray crystal structure of D-Phe-Pro-Arg chloromethylketone-inhibited human alpha-thrombin: structure analysis, overall structure, electrostatic properties, detailed active-site geometry, and structure-function relationships*. Protein Sci, 1992. **1**(4): p. 426-71.
50. Stubbs, M.T., et al., *The interaction of thrombin with fibrinogen. A structural basis for its specificity*. Eur J Biochem, 1992. **206**(1): p. 187-95.
51. Di Cera, E., et al., *Linkage at steady state: allosteric transitions of thrombin*. Methods Enzymol, 1995. **259**: p. 127-44.
52. Di Cera, E., et al., *The Na<sup>+</sup> binding site of thrombin*. J Biol Chem, 1995. **270**(38): p. 22089-92.
53. Engh, R.A., et al., *Divining the serpin inhibition mechanism: a suicide substrate 'springe'?* Trends Biotechnol, 1995. **13**(12): p. 503-10.
54. Maynard, J.R., et al., *Association of tissue factor activity with the surface of cultured cells*. J Clin Invest, 1975. **55**(4): p. 814-24.
55. Tracy, P.B., M.E. Nesheim, and K.G. Mann, *Coordinate binding of factor Va and factor Xa to the unstimulated platelet*. J Biol Chem, 1981. **256**(2): p. 743-51.
56. Magnusson, S., *On the primary structure of bovine thrombin*. Folia Haematol Int Mag Klin Morphol Blutforsch, 1972. **98**(4): p. 385-90.
57. Folk, J.E. and J.S. Finlayson, *The epsilon-(gamma-glutamyl)lysine crosslink and the catalytic role of transglutaminases*. Adv Protein Chem, 1977. **31**: p. 1-133.
58. Liu, C.Y., H.L. Nossel, and K.L. Kaplan, *The binding of thrombin by fibrin*. J Biol Chem, 1979. **254**(20): p. 10421-5.
59. Rosenberg, R.D. and P.S. Damus, *The purification and mechanism of action of human antithrombin-heparin cofactor*. J Biol Chem, 1973. **248**(18): p. 6490-505.
60. Valeri, A.M., S.M. Wilson, and R.D. Feinman, *Reaction of antithrombin with proteases. Evidence for a specific reaction with papain*. Biochim Biophys Acta, 1980. **614**(2): p. 526-33.
61. Kaplan, K.L., *Direct thrombin inhibitors*. Expert Opin Pharmacother, 2003. **4**(5): p. 653-66.
62. Weitz, J.I. and M. Crowther, *Direct thrombin inhibitors*. Thromb Res, 2002. **106**(3): p. V275-84.
63. Berger, D.H., *Plasmin/plasminogen system in colorectal cancer*. World J Surg, 2002. **26**(7): p. 767-71.

64. Robbins, K.C., *Fibrinolytic therapy: biochemical mechanisms*. Semin Thromb Hemost, 1991. **17**(1): p. 1-6.
65. Collen, D. and H.R. Lijnen, *The fibrinolytic system in man*. Crit Rev Oncol Hematol, 1986. **4**(3): p. 249-301.
66. Robbins, K.C., L. Summaria, and R.C. Wohl, *Human plasmin*. Methods Enzymol, 1981. **80 Pt C**: p. 379-87.
67. Barlow, G.H., L. Summaria, and K.C. Robbins, *Hydrodynamic studies on the streptokinase complexes of human plasminogen, Val442-plasminogen, plasmin, and the plasmin-derived light (B) chain*. Biochemistry, 1984. **23**(11): p. 2384-7.
68. Collen, D., *The plasminogen (fibrinolytic) system*. Thromb Haemost, 1999. **82**(2): p. 259-70.
69. Andreasen, P.A., R. Egelund, and H.H. Petersen, *The plasminogen activation system in tumor growth, invasion, and metastasis*. Cell Mol Life Sci, 2000. **57**(1): p. 25-40.
70. Mignatti, P. and D.B. Rifkin, *Plasminogen activators and matrix metalloproteinases in angiogenesis*. Enzyme Protein, 1996. **49**(1-3): p. 117-37.
71. Cavallaro, U., et al., *Response of bovine endothelial cells to FGF-2 and VEGF is dependent on their site of origin: Relevance to the regulation of angiogenesis*. J Cell Biochem, 2001. **82**(4): p. 619-33.
72. Pepper, M.S., et al., *Synergistic induction of t-PA by vascular endothelial growth factor and basic fibroblast growth factor and localization of t-PA to Weibel-Palade bodies in bovine microvascular endothelial cells*. Thromb Haemost, 2001. **86**(2): p. 702-9.
73. Kroon, M.E., et al., *Urokinase receptor expression on human microvascular endothelial cells is increased by hypoxia: implications for capillary-like tube formation in a fibrin matrix*. Blood, 2000. **96**(8): p. 2775-83.
74. Uchiyama, T., et al., *Hypoxia induces transcription of the plasminogen activator inhibitor-1 gene through genistein-sensitive tyrosine kinase pathways in vascular endothelial cells*. Arterioscler Thromb Vasc Biol, 2000. **20**(4): p. 1155-61.
75. Pepper, M.S., et al., *Urokinase-type plasminogen activator is induced in migrating capillary endothelial cells*. J Cell Biol, 1987. **105**(6 Pt 1): p. 2535-41.
76. Leak, L.V., et al., *Stimulation of plasminogen activator and inhibitor in the lymphatic endothelium*. Microvasc Res, 2000. **60**(3): p. 201-11.
77. Liu, N.F. and Q.L. He, *The regulatory effects of cytokines on lymphatic angiogenesis*. Lymphology, 1997. **30**(1): p. 3-12.
78. Pepper, M.S., et al., *Vascular endothelial growth factor (VEGF)-C synergizes with basic fibroblast growth factor and VEGF in the induction of angiogenesis in vitro and alters endothelial cell extracellular proteolytic activity*. J Cell Physiol, 1998. **177**(3): p. 439-52.
79. Pepper, M.S., et al., *In vitro angiogenic and proteolytic properties of bovine lymphatic endothelial cells*. Exp Cell Res, 1994. **210**(2): p. 298-305.
80. Romer, J., et al., *Impaired wound healing in mice with a disrupted plasminogen gene*. Nat Med, 1996. **2**(3): p. 287-92.
81. Soff, G.A., et al., *Expression of plasminogen activator inhibitor type 1 by human prostate carcinoma cells inhibits primary tumor growth, tumor-associated angiogenesis, and metastasis to lung and liver in an athymic mouse model*. J Clin Invest, 1995. **96**(6): p. 2593-600.
82. Heymans, S., et al., *Inhibition of plasminogen activators or matrix metalloproteinases prevents cardiac rupture but impairs therapeutic angiogenesis and causes cardiac failure*. Nat Med, 1999. **5**(10): p. 1135-42.

83. Berman, M., et al., *Plasminogen activator (urokinase) causes vascularization of the cornea*. Invest Ophthalmol Vis Sci, 1982. **22**(2): p. 191-9.
84. Goldfarb, R.H., et al., *Plasminogen activators (urokinase) mediate neovascularization: possible role in tumor angiogenesis*. Semin Thromb Hemost, 1986. **12**(4): p. 337-8.
85. Ribatti, D., et al., *In vivo angiogenic activity of urokinase: role of endogenous fibroblast growth factor-2*. J Cell Sci, 1999. **112** ( Pt **23**): p. 4213-21.
86. Min, H.Y., et al., *Urokinase receptor antagonists inhibit angiogenesis and primary tumor growth in syngeneic mice*. Cancer Res, 1996. **56**(10): p. 2428-33.
87. Li, H., et al., *Adenovirus-mediated delivery of a uPA/uPAR antagonist suppresses angiogenesis-dependent tumor growth and dissemination in mice*. Gene Ther, 1998. **5**(8): p. 1105-13.
88. Evans, C.P., et al., *Inhibition of prostate cancer neovascularization and growth by urokinase-plasminogen activator receptor blockade*. Cancer Res, 1997. **57**(16): p. 3594-9.
89. Guo, Y., et al., *A peptide derived from the nonreceptor binding region of urokinase plasminogen activator (uPA) inhibits tumor progression and angiogenesis and induces tumor cell death in vivo*. Faseb J, 2000. **14**(10): p. 1400-10.
90. Mishima, K., et al., *A peptide derived from the non-receptor-binding region of urokinase plasminogen activator inhibits glioblastoma growth and angiogenesis in vivo in combination with cisplatin*. Proc Natl Acad Sci U S A, 2000. **97**(15): p. 8484-9.
91. Bajou, K., et al., *The plasminogen activator inhibitor PAI-1 controls in vivo tumor vascularization by interaction with proteases, not vitronectin. Implications for antiangiogenic strategies*. J Cell Biol, 2001. **152**(4): p. 777-84.
92. Bajou, K., et al., *Absence of host plasminogen activator inhibitor 1 prevents cancer invasion and vascularization*. Nat Med, 1998. **4**(8): p. 923-8.
93. Gutierrez, L.S., et al., *Tumor development is retarded in mice lacking the gene for urokinase-type plasminogen activator or its inhibitor, plasminogen activator inhibitor-1*. Cancer Res, 2000. **60**(20): p. 5839-47.
94. Pepper, M.S. and R. Montesano, *Proteolytic balance and capillary morphogenesis*. Cell Differ Dev, 1990. **32**(3): p. 319-27.
95. Loskutoff, D.J., et al., *Regulation of cell adhesion by PAI-1*. Apmis, 1999. **107**(1): p. 54-61.
96. Ossowski, L. and J.A. Aguirre-Ghiso, *Urokinase receptor and integrin partnership: coordination of signaling for cell adhesion, migration and growth*. Curr Opin Cell Biol, 2000. **12**(5): p. 613-20.
97. Preissner, K.T., S.M. Kanse, and A.E. May, *Urokinase receptor: a molecular organizer in cellular communication*. Curr Opin Cell Biol, 2000. **12**(5): p. 621-8.
98. Stefansson, S., et al., *Inhibition of angiogenesis in vivo by plasminogen activator inhibitor-1*. J Biol Chem, 2001. **276**(11): p. 8135-41.
99. Levin, E.G. and G.J. del Zoppo, *Localization of tissue plasminogen activator in the endothelium of a limited number of vessels*. Am J Pathol, 1994. **144**(5): p. 855-61.
100. Ito, K., et al., *Expression of tissue-type plasminogen activator and its inhibitor couples with development of capillary network by human microvascular endothelial cells on Matrigel*. J Cell Physiol, 1995. **162**(2): p. 213-24.
101. Mignatti, P., et al., *In vitro angiogenesis on the human amniotic membrane: requirement for basic fibroblast growth factor-induced proteinases*. J Cell Biol, 1989. **108**(2): p. 671-82.

102. Sato, Y., et al., *Indispensable role of tissue-type plasminogen activator in growth factor-dependent tube formation of human microvascular endothelial cells in vitro*. *Exp Cell Res*, 1993. **204**(2): p. 223-9.
103. Schnaper, H.W., et al., *Plasminogen activators augment endothelial cell organization in vitro by two distinct pathways*. *J Cell Physiol*, 1995. **165**(1): p. 107-18.
104. Yasunaga, C., Y. Nakashima, and K. Sueishi, *A role of fibrinolytic activity in angiogenesis. Quantitative assay using in vitro method*. *Lab Invest*, 1989. **61**(6): p. 698-704.
105. Mawatari, M., et al., *Tumor necrosis factor and epidermal growth factor modulate migration of human microvascular endothelial cells and production of tissue-type plasminogen activator and its inhibitor*. *Exp Cell Res*, 1991. **192**(2): p. 574-80.
106. Zablocki, D.K., J.J. Rade, and B.R. Alevriadou, *Adenovirus-mediated expression of tissue plasminogen activator does not alter endothelial cell proliferation and invasion*. *In Vitro Cell Dev Biol Anim*, 2000. **36**(10): p. 625-8.
107. Stack, M.S., et al., *Angiostatin inhibits endothelial and melanoma cellular invasion by blocking matrix-enhanced plasminogen activation*. *Biochem J*, 1999. **340** ( Pt 1): p. 77-84.
108. Datta, Y.H., et al., *Targeting of a heterologous protein to a regulated secretion pathway in cultured endothelial cells*. *Blood*, 1999. **94**(8): p. 2696-703.
109. Rosnoble, C., et al., *Storage of tissue-type plasminogen activator in Weibel-Palade bodies of human endothelial cells*. *Arterioscler Thromb Vasc Biol*, 1999. **19**(7): p. 1796-803.
110. Taraboletti, G., et al., *Posttranscriptional stimulation of endothelial cell matrix metalloproteinases 2 and 1 by endothelioma cells*. *Exp Cell Res*, 2000. **258**(2): p. 384-94.
111. Nguyen, M., J. Arkell, and C.J. Jackson, *Three-dimensional collagen matrices induce delayed but sustained activation of gelatinase A in human endothelial cells via MT1-MMP*. *Int J Biochem Cell Biol*, 2000. **32**(6): p. 621-31.
112. Hertog, M.G., et al., *Dietary antioxidant flavonoids and risk of coronary heart disease: the Zutphen Elderly Study*. *Lancet*, 1993. **342**(8878): p. 1007-11.
113. Deschner, E.E., et al., *Quercetin and rutin as inhibitors of azoxymethanol-induced colonic neoplasia*. *Carcinogenesis*, 1991. **12**(7): p. 1193-6.
114. Elangovan, V., N. Sekar, and S. Govindasamy, *Chemopreventive potential of dietary bioflavonoids against 20-methylcholanthrene-induced tumorigenesis*. *Cancer Lett*, 1994. **87**(1): p. 107-13.
115. Sahu, S.C. and M.C. Washington, *Quercetin-induced lipid peroxidation and DNA damage in isolated rat-liver nuclei*. *Cancer Lett*, 1991. **58**(1-2): p. 75-9.
116. Macdonald, I.A., J.A. Mader, and R.G. Bussard, *The role of rutin and quercitrin in stimulating flavonol glycosidase activity by cultured cell-free microbial preparations of human feces and saliva*. *Mutat Res*, 1983. **122**(2): p. 95-102.
117. Paganga, G., N. Miller, and C.A. Rice-Evans, *The polyphenolic content of fruit and vegetables and their antioxidant activities. What does a serving constitute?* *Free Radic Res*, 1999. **30**(2): p. 153-62.
118. Skrzydlewska, E., et al., *Green tea as a potent antioxidant in alcohol intoxication*. *Addict Biol*, 2002. **7**(3): p. 307-14.
119. Nie, G., et al., *Polyphenol protection of DNA against damage*. *Methods Enzymol*, 2001. **335**: p. 232-44.
120. Nakagawa, T., et al., *Protective activity of green tea against free radical- and glucose-mediated protein damage*. *J Agric Food Chem*, 2002. **50**(8): p. 2418-22.



121. Dangles, O., et al., *Binding of flavonoids to plasma proteins*. Methods Enzymol, 2001. **335**: p. 319-33.
122. Gutzeit, H.O., et al., *Specific interactions of quercetin and other flavonoids with target proteins are revealed by elicited fluorescence*. Biochem Biophys Res Commun, 2004. **318**(2): p. 490-5.
123. Shanmuganayagam, D. and J. Folts, *Effect of polyphenolic flavonoid compounds on platelets*. Methods Enzymol, 2001. **335**: p. 369-80.
124. Melzig, M.F., B. Loser, and S. Ciesielski, *Inhibition of neutrophil elastase activity by phenolic compounds from plants*. Pharmazie, 2001. **56**(12): p. 967-70.
125. Sawaya, M.R. and J. Kraut, *Loop and subdomain movements in the mechanism of Escherichia coli dihydrofolate reductase: crystallographic evidence*. Biochemistry, 1997. **36**(3): p. 586-603.
126. Miller, G.P. and S.J. Benkovic, *Stretching exercises--flexibility in dihydrofolate reductase catalysis*. Chem Biol, 1998. **5**(5): p. R105-13.
127. Bystroff, C., S.J. Oatley, and J. Kraut, *Crystal structures of Escherichia coli dihydrofolate reductase: the NADP<sup>+</sup> holoenzyme and the folate.NADP<sup>+</sup> ternary complex. Substrate binding and a model for the transition state*. Biochemistry, 1990. **29**(13): p. 3263-77.
128. Adams, J.A., C.A. Fierke, and S.J. Benkovic, *The function of amino acid residues contacting the nicotinamide ring of NADPH in dihydrofolate reductase from Escherichia coli*. Biochemistry, 1991. **30**(46): p. 11046-54.
129. Appleman, J.R., et al., *Unusual transient- and steady-state kinetic behavior is predicted by the kinetic scheme operational for recombinant human dihydrofolate reductase*. J Biol Chem, 1990. **265**(5): p. 2740-8.
130. Chen, J.T., et al., *Probing the functional role of phenylalanine-31 of Escherichia coli dihydrofolate reductase by site-directed mutagenesis*. Biochemistry, 1987. **26**(13): p. 4093-100.
131. Smith, L.J., et al., *The concept of a random coil. Residual structure in peptides and denatured proteins*. Fold Des, 1996. **1**(5): p. R95-106.
132. Murphy, D.J. and S.J. Benkovic, *Hydrophobic interactions via mutants of Escherichia coli dihydrofolate reductase: separation of binding and catalysis*. Biochemistry, 1989. **28**(7): p. 3025-31.
133. Bystroff, C. and J. Kraut, *Crystal structure of unliganded Escherichia coli dihydrofolate reductase. Ligand-induced conformational changes and cooperativity in binding*. Biochemistry, 1991. **30**(8): p. 2227-39.
134. Hamilton-Miller, J.M., *Anti-cariogenic properties of tea (Camellia sinensis)*. J Med Microbiol, 2001. **50**(4): p. 299-302.
135. Mabe, K., et al., *In vitro and in vivo activities of tea catechins against Helicobacter pylori*. Antimicrob Agents Chemother, 1999. **43**(7): p. 1788-91.
136. Yam, T.S., J.M. Hamilton-Miller, and S. Shah, *The effect of a component of tea (Camellia sinensis) on methicillin resistance, PBP2' synthesis, and beta-lactamase production in Staphylococcus aureus*. J Antimicrob Chemother, 1998. **42**(2): p. 211-6.
137. Mukhtar, H. and N. Ahmad, *Tea polyphenols: prevention of cancer and optimizing health*. Am J Clin Nutr, 2000. **71**(6 Suppl): p. 1698S-702S; discussion 1703S-4S.
138. Gupta, S., T. Hussain, and H. Mukhtar, *Molecular pathway for (-)-epigallocatechin-3-gallate-induced cell cycle arrest and apoptosis of human prostate carcinoma cells*. Arch Biochem Biophys, 2003. **410**(1): p. 177-85.
139. Jung, Y.D. and L.M. Ellis, *Inhibition of tumour invasion and angiogenesis by epigallocatechin gallate (EGCG), a major component of green tea*. Int J Exp Pathol, 2001. **82**(6): p. 309-16.

140. Yang, G.Y., et al., *Inhibition of growth and induction of apoptosis in human cancer cell lines by tea polyphenols*. Carcinogenesis, 1998. **19**(4): p. 611-6.
141. Navarro-Peran, E., et al., *The antifolate activity of tea catechins*. Cancer Res, 2005. **65**(6): p. 2059-64.
142. Baumeister, W., et al., *The proteasome: paradigm of a self-compartmentalizing protease*. Cell, 1998. **92**(3): p. 367-80.
143. Bochtler, M., et al., *The proteasome*. Annu Rev Biophys Biomol Struct, 1999. **28**: p. 295-317.
144. DeMartino, G.N. and C.A. Slaughter, *The proteasome, a novel protease regulated by multiple mechanisms*. J Biol Chem, 1999. **274**(32): p. 22123-6.
145. Groll, M., et al., *Structure of 20S proteasome from yeast at 2.4 Å resolution*. Nature, 1997. **386**(6624): p. 463-71.
146. Lowe, J., et al., *Crystal structure of the 20S proteasome from the archaeon T. acidophilum at 3.4 Å resolution*. Science, 1995. **268**(5210): p. 533-9.
147. Dick, T.P., et al., *Contribution of proteasomal beta-subunits to the cleavage of peptide substrates analyzed with yeast mutants*. J Biol Chem, 1998. **273**(40): p. 25637-46.
148. Orłowski, M. and S. Wilk, *Catalytic activities of the 20 S proteasome, a multicatalytic proteinase complex*. Arch Biochem Biophys, 2000. **383**(1): p. 1-16.
149. Coux, O., K. Tanaka, and A.L. Goldberg, *Structure and functions of the 20S and 26S proteasomes*. Annu Rev Biochem, 1996. **65**: p. 801-47.
150. Lehner, P.J. and P. Cresswell, *Processing and delivery of peptides presented by MHC class I molecules*. Curr Opin Immunol, 1996. **8**(1): p. 59-67.
151. Ortiz-Navarrete, V., et al., *Subunit of the '20S' proteasome (multicatalytic proteinase) encoded by the major histocompatibility complex*. Nature, 1991. **353**(6345): p. 662-4.
152. Tanaka, K., *Role of proteasomes modified by interferon-gamma in antigen processing*. J Leukoc Biol, 1994. **56**(5): p. 571-5.
153. Grune, T., *Oxidative stress, aging and the proteasomal system*. Biogerontology, 2000. **1**(1): p. 31-40.
154. Smith, M.A., et al., *Oxidative stress in Alzheimer's disease*. Biochim Biophys Acta, 2000. **1502**(1): p. 139-44.
155. Szweda, P.A., B. Friguet, and L.I. Szweda, *Proteolysis, free radicals, and aging*. Free Radic Biol Med, 2002. **33**(1): p. 29-36.
156. Carrard, G., et al., *Impairment of proteasome structure and function in aging*. Int J Biochem Cell Biol, 2002. **34**(11): p. 1461-74.
157. Davies, K.J., *Degradation of oxidized proteins by the 20S proteasome*. Biochimie, 2001. **83**(3-4): p. 301-10.
158. Grune, T., T. Reinheckel, and K.J. Davies, *Degradation of oxidized proteins in mammalian cells*. Faseb J, 1997. **11**(7): p. 526-34.
159. Merker, K., N. Sitte, and T. Grune, *Hydrogen peroxide-mediated protein oxidation in young and old human MRC-5 fibroblasts*. Arch Biochem Biophys, 2000. **375**(1): p. 50-4.
160. Petropoulos, I., et al., *Increase of oxidatively modified protein is associated with a decrease of proteasome activity and content in aging epidermal cells*. J Gerontol A Biol Sci Med Sci, 2000. **55**(5): p. B220-7.
161. Reinheckel, T., et al., *Comparative resistance of the 20S and 26S proteasome to oxidative stress*. Biochem J, 1998. **335** ( Pt 3): p. 637-42.
162. Conconi, M., et al., *Age-related decline of rat liver multicatalytic proteinase activity and protection from oxidative inactivation by heat-shock protein 90*. Arch Biochem Biophys, 1996. **331**(2): p. 232-40.

163. Friguet, B. and L.I. Szweda, *Inhibition of the multicatalytic proteinase (proteasome) by 4-hydroxy-2-nonenal cross-linked protein*. FEBS Lett, 1997. **405**(1): p. 21-5.
164. Keller, J.N., F.F. Huang, and W.R. Markesbery, *Decreased levels of proteasome activity and proteasome expression in aging spinal cord*. Neuroscience, 2000. **98**(1): p. 149-56.
165. Almenoff, J. and M. Orłowski, *Membrane-bound kidney neutral metalloendopeptidase: interaction with synthetic substrates, natural peptides, and inhibitors*. Biochemistry, 1983. **22**(3): p. 590-9.
166. Singleton, V.L. and J.A.J. Rossi, *Colorimetry of total phenolics with phosphomolybdic-phosphotungstic acid reagents*. Amer. J. Enol. Viticult., 1965. **16**: p. 144-58.
167. Gabetta, B., et al., *Characterization of proanthocyanidins from grape seeds*. Fitoterapia, 2000. **71**(2): p. 162-75.
168. Atoui, A.K., *Tea and herbal infusions: Their antioxidant activity and phenolic profile*. Food Chemistry, 2005. **89**(1): p. 27-36.
169. Guendez, R., *Determination of low molecular weight polyphenolic constituents in grape (Vitis vinifera sp.) seed extracts: Correlation with antiradical activity*. Food Chemistry, 2005. **89**(1): p. 1-9.
170. Cao, G. and H. Alessio, *Oxygen-radical absorbance capacity assay for antioxidants*. Free Radical Biol. Med., 1993. **14**: p. 303-311.
171. Ou, B., M. Hampsch-Woodill, and R.L. Prior, *Development and validation of an improved oxygen radical absorbance capacity assay using fluorescein as the fluorescent probe*. J. Agric. Food Chem., 2001. **49**: p. 4619-4626.
172. Adema, E. and U. Gebert, *Thrombin Time Reagent with Improved Dynamic Range for Heparin*: Roche Diagnostics, Tutzing, Germany.
173. Bieth, J.G., *Some Kinetic Consequences of the Tight Binding of Protein-Proteinase-Inhibitors to Proteolytic Enzymes and Their Application to the Determination of Dissociation Constants*, in *Bayer-Symposium V "Proteinase Inhibitors"*, H. Fritz, Tschesche, H., Greene, L.J., and Truscheit, E., Editor. 1974, Springer-Verlag: Berlin. p. 463-469.
174. Jim, R.T., *A study of the plasma thrombin time*. J Lab Clin Med, 1957. **50**(1): p. 45-60.
175. Triplett, D.A., *Coagulation and bleeding disorders: review and update*. Clin Chem, 2000. **46**(8 Pt 2): p. 1260-9.
176. Krumrine, J., et al., *Principles and methods of docking and ligand design*, in *Structural Bioinformatics*, E.P. Bourne and H. Wessig, Editors. 2003, Wiley-Liss. p. 443-476.
177. MOE, *Molecular Operating Environment*. 2001, Chemical Computing Group Inc.: Canada.
178. Metropolis, N., Rosenbluth, A.W., Rosenbluth, M.N., Teller, A.H., *Equation of State Calculations by Fast Computing Machines*. Journal of Chem. Phys., 1953. **21**: p. 1087-1092.
179. Halgren, T.A., *The Merck Force Field*. J. Comp. Chem., 1996. **17**(5&6): p. 490.
180. Bohm, M., J. St rzebecher, and G. Klebe, *Three-dimensional quantitative structure-activity relationship analyses using comparative molecular field analysis and comparative molecular similarity indices analysis to elucidate selectivity differences of inhibitors binding to trypsin, thrombin, and factor Xa*. J Med Chem, 1999. **42**(3): p. 458-77.
181. Hall, L.H. and L.B. Kier, *The Molecular Connectivity Chi Indices and Kappa Shape Indices in Structure-Property Modeling*. Reviews of Computational Chemistry, 1991. **2**.

182. Richards, F.M., *Areas, volumes, packing and protein structure*. Annu Rev Biophys Bioeng, 1977. **6**: p. 151-76.
183. Shrake, A. and J.A. Rupley, *Environment and exposure to solvent of protein atoms. Lysozyme and insulin*. J Mol Biol, 1973. **79**(2): p. 351-71.
184. Filizola, M., et al., *Global Physicochemical Properties as Activity Discriminants for the mGluR1 Subtype of Metabotropic Glutamate Receptors*. Journal of Computational Chemistry, 2001. **22**(16): p. 2018-2027.
185. Moss, D.E. and D. Fahrney, *Kinetic analysis of differences in brain acetylcholinesterase from fish or mammalian sources*. Biochem Pharmacol, 1978. **27**(23): p. 2693-8.
186. Lupidi, G., et al., *Peroxynitrite-mediated oxidation of fibrinogen inhibits clot formation*. FEBS Lett, 1999. **462**(3): p. 236-40.
187. Davies, R.J., et al. Crabb, J.W. Ed. ed. 1994, San Diego: Academic Press. 285-292.
188. Hall, D.R. and D.J. Winzor, *Use of a resonant mirror biosensor to characterize the interaction of carboxypeptidase A with an elicited monoclonal antibody*. Anal Biochem, 1997. **244**(1): p. 152-60.
189. Bevington, P.R., *Data reduction and error analysis for the physical sciences*: McGraw-Hill book company. 195-203.
190. De Crescenzo, G., et al., *Real-time monitoring of the interactions of transforming growth factor-beta (TGF-beta ) isoforms with latency-associated protein and the ectodomains of the TGF-beta type II and III receptors reveals different kinetic models and stoichiometries of binding*. J Biol Chem, 2001. **276**(32): p. 29632-43.
191. Roden, L.D. and D.G. Myszka, *Global analysis of a macromolecular interaction measured on BIAcore*. Biochem Biophys Res Commun, 1996. **225**(3): p. 1073-7.
192. Wang, X., et al., *Human plasminogen catalytic domain undergoes an unusual conformational change upon activation*. J Mol Biol, 2000. **295**(4): p. 903-14.
193. Berman, H.M., et al., *The Protein Data Bank*. Nucleic Acids Res, 2000. **28**(1): p. 235-42.
194. Eleuteri, A.M., et al., *Isolation and characterization of bovine thymus multicatalytic proteinase complex*. Protein Expr Purif, 2000. **18**(2): p. 160-8.
195. Bradford, M.M., *A rapid and sensitive method for the quantitation of microgram quantities of protein utilizing the principle of protein-dye binding*. Anal Biochem, 1976. **72**: p. 248-54.
196. Ray, S., et al., *Acute and long-term safety evaluation of a novel IH636 grape seed proanthocyanidin extract*. Res Commun Mol Pathol Pharmacol, 2001. **109**(3-4): p. 165-97.
197. Yamakoshi, J., et al., *Safety evaluation of proanthocyanidin-rich extract from grape seeds*. Food Chem Toxicol, 2002. **40**(5): p. 599-607.
198. Ferguson, L.R., *Role of plant polyphenols in genomic stability*. Mutat Res, 2001. **475**(1-2): p. 89-111.
199. Scalbert, A. and G. Williamson, *Dietary intake and bioavailability of polyphenols*. J Nutr, 2000. **130**(8S Suppl): p. 2073S-85S.
200. Sonder, S.A. and J.W. Fenton, 2nd, *Thrombin specificity with tripeptide chromogenic substrates: comparison of human and bovine thrombins with and without fibrinogen clotting activities*. Clin Chem, 1986. **32**(6): p. 934-7.
201. Maffei Facino, R., et al., *Free radicals scavenging action and anti-enzyme activities of procyanidines from Vitis vinifera. A mechanism for their capillary protective action*. Arzneimittelforschung, 1994. **44**(5): p. 592-601.

202. Banner, D.W. and P. Hadvary, *Crystallographic analysis at 3.0-Å resolution of the binding to human thrombin of four active site-directed inhibitors*. J Biol Chem, 1991. **266**(30): p. 20085-93.
203. Wyman, J. and S.J. Gill, *Binding and linkage*. 1990: University Science Books.
204. Segel, I.H., *Enzyme kinetics : behavior and analysis of rapid equilibrium and steady-state enzyme systems*. Wiley Classics Library. 1993: John Wiley & sons, Inc. 109-111.
205. Lottenberg, R., et al., *Assay of coagulation proteases using peptide chromogenic and fluorogenic substrates*. Methods Enzymol, 1981. **80 Pt C**: p. 341-61.
206. Morrison, J.F. and C.T. Walsh, *The behavior and significance of slow-binding enzyme inhibitors*. Adv Enzymol Relat Areas Mol Biol, 1988. **61**: p. 201-301.
207. Nakano, T., et al., *Critical role of phenylalanine 34 of human dihydrofolate reductase in substrate and inhibitor binding and in catalysis*. Biochemistry, 1994. **33**(33): p. 9945-52.
208. Cortes, A., et al., *Relationships between inhibition constants, inhibitor concentrations for 50% inhibition and types of inhibition: new ways of analysing data*. Biochem J, 2001. **357**(Pt 1): p. 263-8.
209. Lowry, O.H., et al., *Protein measurement with the Folin phenol reagent*. J Biol Chem, 1951. **193**(1): p. 265-75.
210. Nam, S., D.M. Smith, and Q.P. Dou, *Tannic acid potently inhibits tumor cell proteasome activity, increases p27 and Bax expression, and induces G1 arrest and apoptosis*. Cancer Epidemiol Biomarkers Prev, 2001. **10**(10): p. 1083-8.
211. Nam, S., D.M. Smith, and Q.P. Dou, *Ester bond-containing tea polyphenols potently inhibit proteasome activity in vitro and in vivo*. J Biol Chem, 2001. **276**(16): p. 13322-30.
212. Smith, D.M., et al., *Docking studies and model development of tea polyphenol proteasome inhibitors: applications to rational drug design*. Proteins, 2004. **54**(1): p. 58-70.
213. Smith, D.M., et al., *Synthetic analogs of green tea polyphenols as proteasome inhibitors*. Mol Med, 2002. **8**(7): p. 382-92.
214. Okada, Y., et al., *Development of plasmin-selective inhibitors and studies of their structure-activity relationship*. Chem Pharm Bull (Tokyo), 2000. **48**(2): p. 184-93.
215. Heydendael, V.M., et al., *Methotrexate versus cyclosporine in moderate-to-severe chronic plaque psoriasis*. N Engl J Med, 2003. **349**(7): p. 658-65.

## 6 Summary

1	Introduction .....	1
1.1	Polyphenols .....	1
1.2	GSE and health.....	3
1.2.1	Effects on myocardium and the cardiovascular system .....	3
1.2.2	Cytotoxicity.....	5
1.2.3	Protection against inflammation and allergy.....	6
1.2.4	Antioxidant activity.....	7
1.2.5	Antioxidant effect on vitamin E .....	8
1.2.6	Toxicity studies on grape seeds extracts (GSE).....	9
1.2.7	Use as food preservative .....	10
1.3	Interaction polyphenols-thrombin .....	11
1.3.1	Thrombin.....	11
1.3.2	Molecular structure .....	11
1.3.3	Reaction mechanism. ....	13
1.3.4	The coagulatory process.....	14
1.3.5	Thrombin inhibitors.....	15
1.4	Interaction Polyphenols-Plasmin/Plasminogen.....	16
1.4.1	The system Plasmin/Plasminogen.....	16
1.5	Interactiun polyphenols-DHFR.....	24
1.5.1	The dihydrofolate reductase: function and structure.....	24
1.6	Interaction polyphenols- proteasome 20S.....	29
1.6.1	The complex of the multicatalitic protease and the degradation of oxidized proteins. 29	
1.6.2	Proteasome 20S: the functionality.....	34
2	Materials and methods .....	40
2.1	Materials.....	40
2.1.1	Thrombin-polyphenol, Plasmin-polyphenol, DHFR-polyphenol, Proteasome 20S-polyphenol interactions.....	40
2.1.2	Proteasome 20S-polyphenol interactions.....	40
2.1.3	RP-HPLC, Folin-Ciocalteau, DPPH Assay, ORAC Assay.....	41
2.1.4	Lipidic peroxides inhibition .....	41

2.2	Methods.....	41
2.2.1	Accelerated Solvent Extraction:.....	41
2.2.2	Folin-Ciocalteu assay:.....	42
2.2.3	RP-HPLC assay:.....	42
2.2.4	DPPH Assay.....	42
2.2.5	Lipidic peroxidation inhibition.....	43
2.2.6	ORAC.....	44
2.2.7	Spectrophotometric assay of enzymatic activity.....	46
2.2.8	Ligand immobilization.....	47
2.2.9	Studies of coagulation.....	49
2.2.10	Molecular docking of the interaction thrombin-flavonoid.....	49
2.2.11	QSAR Analysis.....	50
2.2.12	Plasminogen purification.....	50
2.2.13	Spectrophotometric assay of enzymatic activity:.....	51
2.2.14	Optical biosensor assay.....	51
2.2.15	Fluorometric determination.....	52
2.2.16	Molecular docking of the interaction plasmin-flavonoid.....	52
2.2.17	Spectrophotometric determinations of DHFR activity.....	53
2.2.18	Inhibition assay.....	53
2.2.19	Purification of 20S proteasome from thymus and from bovine brain.....	53
2.2.20	Determination of the proteasomal activities.....	54
2.2.21	Determination of IC <sub>50</sub> .....	55
2.2.22	Determination of the proteic concentration through Bradford method.....	56
3	Experimental.....	57
3.1	Characterization of Biophenolix grape seeds extract.....	57
3.2	Purification of grape seed extract on polystyrenic resins.....	58
3.3	Characterization of catechins in grape seeds during ripening.....	61
3.4	Determination of peroxidation inhibition activity in lipidic matrix.....	65
3.5	Characterization of possible alternative sources of polyphenols.....	66
3.5.1	Pomegranate.....	66
3.5.2	Prunus Spinosa.....	67
3.5.3	Rosemary.....	69
3.6	Interaction Polyphenols-Thrombin.....	73
3.6.1	Spectrophotometric tests.....	73

3.6.2	SPR analysis .....	74
3.6.3	Coagulation studies .....	77
3.6.4	Extracts effect on thrombin .....	78
3.6.5	Molecular docking.....	79
3.6.6	QSAR analysis .....	81
3.7	Polyphenols-Plasmin interactions .....	83
3.7.1	Spectrophotometric test of the enzymatic activity .....	83
3.7.2	SPR studies: equilibrium analysis.....	84
3.7.3	SPR studies: kinetic analysis.....	85
3.7.4	Fluorimetric tests.....	86
3.7.5	Grape seed extract effect on plasmin .....	86
3.7.6	Molecular docking of the plasmin-flavonoid interaction.....	87
3.8	Polyphenols-DHFR interactions .....	89
3.8.1	Wt-DHFR inhibition by monomeric catechins .....	89
3.8.2	$K_m$ determination at different EGCG concentrations.....	90
3.8.3	Inhibition constants determination .....	92
3.8.4	Grape seed extract effect on DHFR .....	92
3.9	Polyphenols-Proteasome 20S interactions .....	93
3.9.1	Isolation and purification of the bovine brain multicatalytic protease.....	93
3.9.2	Isolation and purification of the bovine thymus multicatalytic protease.....	95
3.9.3	20S proteasome inhibition activities of polyphenolic compounds.....	97
3.9.4	Grape seed extract effect on the 20S proteasome functionality.....	100
4	Conclusions .....	101
4.1	Characterization of Biophenolix Grape Seed Extract .....	101
4.2	Evolution of catechins in grape seeds during ripening .....	101
4.3	Lipidic peroxidation inhibition by GSE in oil.....	101
4.4	Characterization of polyphenols alternative sources.....	101
4.5	Polyphenols-Flavonoid interactions .....	102
4.6	Polyphenols-Plasmin interactions .....	102
4.7	Polyphenols-DHFR interaction .....	103
4.8	Polyphenols-Proteasome 20S interactions .....	104
5	Bibliography.....	106
6	Summary .....	117